MOLECULAR PROFILING OF ACUTE CHORIOAMNIONITIS-AFFECTED PLACENTAS: INSIGHTS INTO GENOMIC VARIATION UNDERLYING A COMMON PRETERM BIRTH CONDITION

by

Chaini Konwar

M.Sc., Dalhousie University, 2014

A THESIS SUBMITTED IN PARTIAL FULFILLMENT OF

THE REQUIREMENTS FOR THE DEGREE OF

DOCTOR OF PHILOSOPHY

in

THE FACULTY OF GRADUATE AND POSTDOCTORAL STUDIES

(Medical Genetics)

THE UNIVERSITY OF BRITISH COLUMBIA

(Vancouver)

May 2019

The following individuals certify that they have read, and recommend to the Faculty of Graduate and Postdoctoral Studies for acceptance, the dissertation entitled:

Molecular profiling of acute chorioamnionitis-affected placentas: insights into genomic variation underlying a common preterm birth condition

submitted by Chaini Konwar in partial fulfillment of the requirements for

the degree of Doctor of Philosophy

in Medical Genetics

Examining Committee:

Dr. Wendy P Robinson
Supervisor

Dr. Michael Kobor
Supervisory Committee Member

Supervisory Committee Member

Dr. Louis Lefebvre
University Examiner

Dr. Laura Sly
University Examiner

Additional Supervisory Committee Members:

Dr. Alex Beristain
Supervisory Committee Member

Dr. Inanc Birol
Supervisory Committee Member

Dr. Jefferson Terry
Supervisory Committee Member

Abstract

Acute chorioamnionitis (aCA), a preterm birth (PTB) associated inflammatory condition, can have adverse effects on the health of the baby. This condition is characterized by inflammatory lesions in the fetal membranes and can also involve the chorionic plate in the placenta. Histologic examination of the placenta is the gold standard for diagnosing aCA, but is only possible after delivery; thus, this method is not suitable for prenatal diagnosis of aCA. This necessitates the development of non-invasive biomarkers to allow effective management of the disease and hence, reduce the incidence of PTB. Additionally, genetic variation in immune-system genes may contribute to the placenta's inflammatory responses, thus influencing susceptibility to aCA.

The overarching objective of this dissertation is to understand how genetic, epigenetic, and miRNA variation in the placenta is associated with the disruption of immune balance in aCA. To achieve this, I first examined the association of single nucleotide polymorphisms (SNPs) in innate immune system genes and aCA status. I observed that differences in *IL6* (rs1800796) placental allele frequencies were associated with the presence of aCA. Further, I showed the *IL6* SNP may regulate *IL6* gene expression and DNA methylation (DNAme) in the placenta, and alter disease risk to aCA. Secondly, using the Illumina HumanMethylation850 BeadChip, I characterized epigenetic variation associated with aCA in placenta and fetal membranes. Specifically, I observed that aCA-affected placentas showed a unique DNAme profile that may reflect an increase in immune cell number as a response to inflammation and/or represent activation of the innate immune response in the placenta. Lastly, I investigated whether altered miRNA profiles were associated with aCA-affected placentas. Expression was quantified for six inflammation-related miRNAs using quantitative real-time PCR. I observed that

expression of miR-518b and miR-338-3p were differentially expressed in aCA-affected placentas. I also showed that miR-518b expression in placenta was associated with *IL6* (rs1800796) genotype, where carriers of the C allele exhibited decreased miR-518b expression compared to the carriers of the G allele. In summary, this research uniquely investigated genetic alterations, DNAme, and miRNA expression patterns in aCA-affected placentas, adding insights into the processes likely impacting immune function during aCA.

Lay Summary

Globally, 1 in 10 babies are born before 37 weeks of gestation and are classified as "preterm births". Babies born too early are at an increased risk of life-long health complications, and long term developmental delay. One of the major causes of preterm birth is inflammation of the placenta and associated membranes known as acute chorioamnionitis, estimated to be present in 25-40% of preterm cases. The etiology of chorioamnionitis is rarely identified and diagnosis of inflammation is generally not made prior to delivery. The goal of my dissertation is to improve our understanding of inflammation related changes that occur during acute chorioamnionitis. I compared the genetic, epigenetic and miRNA profiles in placentas from preterm births with and without inflammation to identify characteristic changes. This information may be used to identify candidate biomarkers that could be detected in maternal blood when the inflammation is present for rapid prenatal detection of aCA.

Preface

Data chapters in this dissertation (Chapters 3-5) are presented in manuscript format, as they are published (Chapter 3 and Chapter 4) or under submission (Chapters 5). Studies in Chapter 3-5 were approved by the University of British Columbia Children's & Women's Research Ethics Board (H04-70488).

Parts of Chapter 1, Introduction have been previously published (Section 1.6.5) or under submission (Section 1.5.2 and Section 1.6.4):

- Peñaherrera MS, **Konwar C**, Yuan V, Wilson SL, Robinson WP. (2019). Epigenetic modifications in the human placenta. In *Human Reproductive* and *Prenatal Genetics* (pp. 293-311). Academic Press. An imprint of Elsevier. Elsevier Inc. Reprinted with permission from Elsevier Inc (License Number: 4512120475008).
  I authored sections covering altered placental DNA methylation in spontaneous preterm birth and maternal exposures, and contributed one figure (Fig 13.2). Dr. Maria Peñaherrera wrote the section on monallelic gene inactivation and critically edited the manuscript. Victor Yuan wrote the section on epigenetic profiles of placental cell types and contributed one figure (Fig 13.1). Dr. Samantha L Wilson wrote the section on altered DNA methylation in preeclampsia and contributed to Figure 13.2. Dr. Wendy P Robinson prepared the overall outline of the book chapter and authored the sections on epigenetic features of the placenta.

- Del Gobbo GF*, **Konwar C***, Robinson WP. (2019). The significance of placental genome and epigenome in maternal and fetal health. (submitted)
  *Authors contributed equally to the content development of this review article.

A version of Chapter 3 has been published:

- **Konwar C**, Del Gobbo GF, Terry J, Robinson WP. (2019). Association of a placental Interleukin-6 genetic variant (rs1800796) with DNA methylation, gene expression and risk of acute chorioamnionitis. *BMC Medical Genetics*, 20(1), pp.36 © 2019 Konwar et

al. under the Creative Commons Attribution 4.0 International License (http://creativecommons.org/licenses/by/4.0/).

I developed the study design and research questions for this study alongside Dr. Wendy P Robinson. I performed DNA extractions for chorionic villus samples, prepared samples for genotyping, conducted all statistical analyses, interpreted results, wrote the draft of the manuscript and prepared all the publication figures. Gulia F Del Gobbo performed the ancestry analysis, assisted in sample preparation for genotyping, statistical analyses and results interpretation. Dr. Jefferson Terry performed the recruitment and ascertainment of a subset of the study cohort. All the authors critically edited the manuscript.

A version of Chapter 4 has been published:

- **Konwar C**, Price EM, Wang LQ, Wilson SL, Terry J, Robinson WP. (2018). DNA methylation profiling of acute chorioamnionitis-associated placentas and fetal membranes: insights into epigenetic variation in spontaneous preterm births. *Epigenetics & Chromatin*, 11(1), pp.63. © 2018 Konwar et al. under the Creative Commons Attribution 4.0 International License (http://creativecommons.org/licenses/by/4.0/).

  Dr. Wendy P Robinson conceived of the study and contributed to study design alongside Dr. E Magda Price, and myself. I performed DNA extractions for fetal membranes, ran the microarrays, conducted all statistical analyses, interpreted results, designed and analyzed pyrosequencing assays, drafted the manuscript, and prepared all the publication figures. Dr. E Magda Price assisted in statistical analyses and results interpretation, and Liqing Q Wang participated in the pyrosequencing assay design and collected the pyrosequencing data. Dr. Samantha LWilson aided in sample preparation and ran the 850K arrays. Dr. Jefferson Terry performed the recruitment and ascertainment of validation cohort patients. All authors critically edited the manuscript.

A version of Chapter 5 has been published:

- **Konwar C**, Manokhina I, Terry J, Inkster A, Robinson WP. Altered expression levels of miR-338-3p and miR-518b is associated with acute chorioamnionitis and Interleukin-6 genotype. *Placenta*. Technical Note. © 2019 Konwar et al.
  Dr. Irina Manokhina and I developed the experimental design and research questions for this study with input from Dr. Wendy P Robinson and Dr. Jefferson Terry. I assisted in RNA extractions, conducted all statistical analyses, interpreted results, wrote the draft of the short communication, and generated all the figures. Dr. Irina Manokhina performed RNA extractions and the RT-qPCR runs, participated in the study design, and results interpretation. Amy Inkster assisted in RNA extractions, and statistical analysis, and performed the target prediction analysis. All authors critically edited the manuscript.

Chapter 2 (Study cohort, sampling and methods) and Chapter 6 (Discussion) is original and unpublished.

As Chapter 3-5 have remained largely unchanged from their published versions, I have preserved the use of plural first-person pronouns in these chapter. In the remainder of the dissertation, I use singular first-person pronouns.

Table of Contents

List of Tables

List of Figures

List of Symbols

$\Delta\beta$	Difference in DNA methylation

List of Abbreviations

450K	Illumina Infinium HumanMethylation450K Beadchip Array
850K	Illumina Infinium HumanMethylationEPIC Beadchip Array
5hmC	5-hydroxymethylcytosine
5mC	5-methylcytosine
aCA	acute chorioamnionitis
AIM	ancestry informative marker
cCA	chronic chorioamnionitis
cDNA	complementary DNA
cfp-DNA	cell free placental DNA
CGIs	CpG islands
CpG	cytosine-phosphate-guanosine
CRP	C-reactive protein
CTB	cytotrophoblasts
DM	differentially methylated
DMR	differentially methylated regions
DNAme	DNA methylation
EPIC	epigenetics in pregnancy study
EWAS	epigenome-wide association study
FIRS	fetal inflammatory response syndrome
GA	gestational age
GR	glucocorticoid receptor

GWAS	genome-wide association studies
HPA	hypothalamic pituitary adrenal
HWE	hardy-weinberg equilibrium
ICM	inner cell mass
IL6	interleukin -6
IUGR	intrauterine growth restriction
KS	kolmogorov-smirnov
LD	linkage disequilibrium
MDS	multidimensional scaling
MeCP2	methyl-CpG-binding protein
MeDIP	methylated DNA immunoprecipitation
mQTL	methylation quantitative trait loci
ns	not significant
PAT	placental atlas tool
PCA	principal component analysis
PCR	polymerase chain reaction
PE	preeclampsia
PMD	partially methylated domains
PPROM	preterm premature rupture of membranes
PTB	preterm birth
QC	quality control
qPCR	quantitative real-time PCR

R	R programming language and software environment
rs	reference SNP
RT	Reverse transcription
SD	standard deviation
SES	socioeconomic status
SNP	single nucleotide polymorphism
SOGC	society of obstetricians and gynecologists of Canada
sPTB	spontaneous PTB
TF	transcription factor
TLR	toll-like receptor
TSS	transcription start site
UCSC	University of California Santa Cruz
VUE	villitis of unknown etiology
WBC	white blood cells

Acknowledgements

This dissertation would not have been possible without the support of a number of people. First, I would like to thank my graduate supervisor, Dr. Wendy Robinson for being the phenomenal supervisor I could hope for. Thank you for your guidance, mentorship, motivation, critical feedback, and support throughout my PhD. I have learned so much from you. I would also like to acknowledge my committee members: Dr. Michael Kobor, Dr. Terry Jefferson, Dr. Alex Beristain, and Dr. Inanc Birol for your insightful inputs and guidance. My special thanks to Cheryl Bishop, Medical Genetics Graduate Program Assistant who have been a constant help throughout my PhD.

Many thanks to former and current members of the Robinson lab (Maria, Ruby, Johanna, Magda, Samantha, Giulia, Victor, Amy, Olivia, Irina, Desmond, and Li Qing) who have truly made my PhD experience memorable. Specifically, thank you Magda for your mentorship at the beginning of my PhD journey. Thank you Giulia and Samantha for the stimulating discussions, continued support and encouragement. I am so glad you both were a part of my crazy Indian wedding celebrations. I would also like to acknowledge Sumaiya for your constant motivation, warmth, and academic advice that have helped me to make progress throughout my PhD.

To my best friends Basanti and Lakshana, thank you girls for being there to celebrate every little victory in my PhD and providing a shoulder to cry on whenever I needed. I would not have survived without those ranting sessions, lunch meet-ups, and cocktail nights. My loving annoying little brother Suraj, thank you for believing in me. To my supportive husband, Ronak I could not have done any of this without you. Thank you for your patience, your calmness has been my strength that helped me get through a lot during this journey. Finally, I would like to

express my gratitude and love to my Mom and Dad, thank you for your selfless love and sacrifices. I Love You.

Dedication

To my loving family (my husband, my brother, and my parents

Chapter 1: Introduction

1.1 Preterm Birth

1.1.1 Definition, prevalence, and classification

Preterm birth (PTB), as defined by the World Health Organization, refers to all births occurring prior to 37 weeks gestational age (GA) (1). PTB occurs 1 in 10 pregnancies worldwide, although there is significant variability in the incidence of PTB on a per-country basis. For example, in 2010, the PTB rate in Sub-Saharan Africa exceeded 12%, while several European countries had PTB rates close to 5% (2). While these PTB rates were highest in low-income countries, high PTB rates were also observed in countries such as U.S. (12%), which alone accounted for 42% of all PTBs in the developed nations.

Based on GA at delivery, PTB is classified as: i) extreme preterm (delivery <28 weeks); ii) very/severe preterm (delivery 28-<32 weeks); iii) moderate preterm (delivery 32-33 weeks); iv) late preterm (delivery at 34-<37 weeks) (1-3). Late PTB accounts for approximately 60-70% of all preterm deliveries. Clinically, PTB is categorized into spontaneous PTB (sPTB) or medically-indicated/provider-initiated PTB (iatrogenic) (1). Iatrogenic PTB includes induced labor or elective cesarean births indicated by maternal and/or fetal complications. Making up 40% of PTBs, sPTB is etiologically heterogeneous but is typically associated with infections and dysregulation of inflammatory pathways (4-8). This often presents as acute chorioamnionitis (aCA), defined by an infiltration of maternal neutrophils into the extraplacental fetal membranes, the amnion and chorion (9, 10). The studies described in this dissertation focus on aCA; therefore, this pregnancy complication is discussed in detail in sections 1.3-1.7.

1.1.2 Health outcomes associated with preterm birth

PTB is the leading cause of neonatal mortality, and accounts for approximately 28% of all neonatal deaths within the first seven days of life (11). As the immune system of newborns is underdeveloped, one of the major complications affecting preterm newborns is infection, accounting for 40% of all neonatal deaths (12). *Group B Streptococcus* and *Escherichia coli* are responsible for the majority of infection cases in preterm newborns (13). Children born preterm are also more likely to suffer from life-long health complications, including cerebral palsy, sensory deficits, attention-deficit hyperactivity disorder, language and learning disabilities and respiratory complications like asthma (14-17). However, attention has been given to interventions for improving health, survival and long-term outcomes for preterm newborns. For example, administration of antenatal corticosteroids have significantly reduced incidence of respiratory distress syndrome, cerebral hemorrhage, and mortality among preterm infants (18).

1.2 Role of placental inflammation in preterm birth

1.2.1 Placental development and structure

Development of the placenta begins as soon as the human embryo reaches the blastocyst stage and implants into the uterine wall (19). The blastocyst is composed of an inner cell mass (ICM) and an outer trophectoderm layer. This outer trophectoderm layer differentiates into the trophoblast lineage of the human placenta, whereas the fetal and remaining extraembryonic tissues are ICM-derived. Specifically, the amniotic epithelium is likely derived primarily from the epiblast just before primitive streak formation, while amniotic mesoderm is derived from mesodermal cells of the primitive streak (20, 21). Origin of the chorion is less clear, but likely includes trophoblast and/or extraembryonic mesoderm.

The human placenta is made up of 60-70 chorionic villus trees that grow throughout development in a clonal manner (20). These tree-like structures consist of an outer layer of stem-like cytotrophoblasts (CTB), which fuse together to form the multi-nucleated syncytial trophoblasts (STB). The outer STB layer, the syncytium, is in direct contact with the maternal blood, a typical feature of a hemochorial placenta (22). The syncytium secretes placental-associated hormones such as human chorionic gonadotropin, human placental lactogen, and placental growth factor to support a successful pregnancy. In addition, a subset of the CTBs differentiate into the extravillous trophoblasts that invade the maternal endometrium and remodel the uterine spiral arteries to increase blood flow to the placenta. The inner mesenchymal core of the chorionic villi is a mixture of immune cells such as Hofbauer cells (placental macrophages), endothelial cells (fetal blood vessels), and fibroblast cells. Although the etiologies of many pregnancy complications are associated with alteration of cell-specific placental processes, there are significant gaps in our current understanding of placental cell populations. For example, altered numbers of Hofbauer cells are found at sites of increased placental inflammation in chorioamnionitis, but their developmental origin and their exact function in pregnancy pathologies is unclear (23, 24).

1.2.2 Acute chorioamnionitis

Inflammation of the extraplacental membranes, often presenting as aCA, is typically associated with PTB. aCA is characterized by an infiltration of maternal neutrophils through the extraembryonic fetal membranes and into the amniotic space, often as a response to an ascending microbial infection from the lower genital tract (10, 25). Apart from the female genital tract, microorganisms can reach the amniotic cavity by other routes (26, 27) including across the

placental disc, as shown in Figure 1.1. Irrespective of the route, microbial invasion of the amniotic cavity elicits a strong inflammatory response both in the mother and the fetus. Although aCA is frequently associated with microbial invasion of the amniotic space, it can also occur in the absence of detectable microorganisms and may be triggered by non-microbial "danger signals" including cellular stress and cell death (28-30). Therefore, it can be concluded that aCA is representative of intra-amniotic inflammation and may not necessarily always reflect intra-amniotic infection.

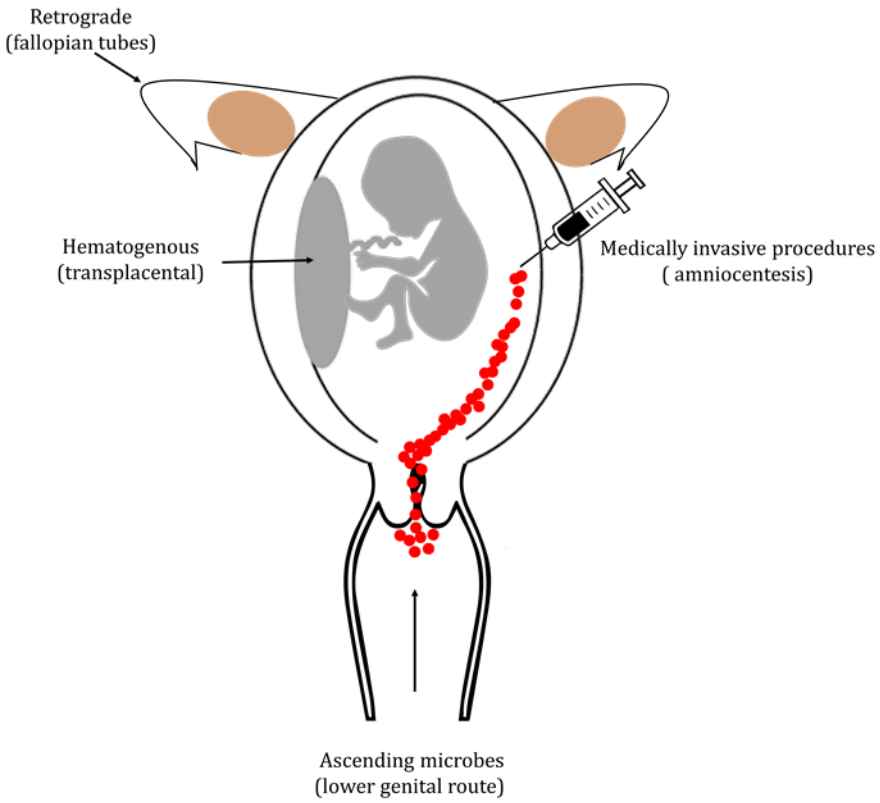

Figure 1.1. Routes of microbial entry into the amniotic space (Adapted from Zhou et al. (31)).

Although microbes commonly enter the amniotic space via the lower genital tract, alternate routes of microbial entry have been identified: i) hematogenous dissemination through the placenta; ii) accidental introduction during a medically invasive procedure such as amniocentesis; iii) retrograde seeding from the peritoneal cavity through the fallopian tubes.

Inflammatory processes during aCA are not only limited to the chorioamniotic membranes, but may also affect the chorionic villous trees (32), presenting as acute intervillositis and villitis, which are seen with maternal sepsis (33) and fetal bacterial sepsis, respectively. Further, acute inflammation is associated with an increased risk of fetal inflammatory response syndrome (FIRS), mainly involving the umbilical cord (acute funisitis) and chorionic vessels (chorionic vasculitis). Progression and severity of inflammatory processes in aCA will be discussed in detail in section 1.3.1.

1.2.3 Other inflammatory lesions

Aside from aCA, other commonly occurring inflammatory lesions of the placenta include chronic chorioamnionitis (cCA), chronic villitis, and villitis of unknown etiology (VUE). cCA is characterized by an influx of lymphocytes into the chorioamniotic membranes. Unlike aCA, which is most common in extreme PTB deliveries (<28 weeks), cCA is frequent in late PTB (34-<37 weeks) (34). It is possible that cCA may be associated with microbial infection; however careful examination for pathogens has shown no evidence of infectious agents in cCA cases (35). In addition, cCA cases commonly occur with villitis of unknown etiology (VUE) (35, 36) and studies have shown that VUE is a placental manifestation of maternal graft vs host-type response to fetal antigens (37-40). Further, the concentration of intra-amniotic T-cell chemokines (CXCL9, CXCL10 and CXCL11) is significantly elevated in cCA cases and in VUE cases (41). Therefore, the frequent coexistence of cCA and VUE and their similar chemokine profile suggest that these two pathological lesions likely have a similar non-infectious immunologic origin.

Chronic villitis, including VUE, is a histologic diagnosis. VUE encompasses all cases of chronic villitis not associated with an identified pathogen and absence of any clinical signs of

infection in either the mother or neonate (40, 42). Histologically, VUE is identified by the presence of lymphohistiocytic infiltrate affecting the distal villous tree of the placenta. Lymphocytes in VUE are predominantly CD8+ T-cells, and maternal in origin (43, 44). Interestingly, VUE is observed frequently in term or late third trimester placentas, and is much more common (50-150/1000 live births) than infectious chronic villitis (1-4/1000 live births). VUE is also associated with intrauterine growth restriction (IUGR) (45), small for gestational age (SGA) (46, 47), recurrent reproductive failure (47), and long-term neurodisability (48).

1.3 Acute chorioamnionitis: disease overview

1.3.1 Histologic staging of acute chorioamnionitis

A commonly used staging system to describe the severity of aCA-associated inflammatory processes is recommended by the Amniotic Fluid Infection Nosology Committee of the Perinatal Section of the Society for Pediatric Pathology in 2003 (9, 10). Placental inflammatory lesions associated with aCA are classified as: maternal inflammatory responses and fetal inflammatory responses. Stage 1 of the maternal inflammatory response is characterized by the presence of neutrophils in the subchorionic plate fibrin and at the membranous choriodecidual interface; Stage 2 is identified by the influx of neutrophils into the chorionic plate or chorionic connective tissue and/or the amnion, and Stage 3/necrotizing chorioamnionitis involves necrosis of the amniotic epithelium. On the other hand, fetal inflammatory responses begins in the chorionic vessels and umbilical vein (Stage 1- chorionic vasculitis/umbilical phlebitis), spreads to the umbilical arteries (Stage 2-umbilical vasculitis), and, if prolonged results in localized tissue necrosis (Stage 3- necrotizing funisitis).

1.3.2 Diagnosis of acute chorioamnionitis

Currently, histologic examination of the placenta is the gold standard for diagnosing aCA; however it is only possible after delivery; thus, this method is not suitable for rapid prenatal diagnosis of aCA. Clinically, aCA is diagnosed by assessment of non-specific clinical signs of inflammation such as maternal fever, fetal tachycardia, maternal tachycardia, maternal leukocytosis, uterine fundal tenderness, or abnormal vaginal discharge (49). However, studies have reported that only a small percentage of women with aCA exhibit these clinical signs of inflammation (50). Alternatively, amniotic fluid analysis by amniocentesis has been attempted to diagnose intra-amniotic inflammation/infection associated with aCA. Amniotic fluid analysis includes microbiologic culture tests for aerobic and anaerobic bacteria, Gram staining examinations (51), measurement of glucose (52), cytokines (53, 54) and white blood cell (WBC) counts (55). Although amniotic fluid cultures have been successful in diagnosing infection associated with aCA, certain limitations might account for some of the discrepancies between amniotic fluid culture results and histological findings, such as: the time needed for culture, inadequate amniotic fluid culture conditions, microorganisms escaping detection with standard microbiologic techniques, and amniotic fluid cultures failing to detect intra-amniotic inflammation unrelated to microbial invasion of the amniotic cavity (56). As amniocentesis is an invasive procedure with many accompanying risks, quantification of components in maternal blood may be a useful less invasive approach for rapid diagnosis of aCA. However, to date, maternal serum markers have not consistently been shown to have predictive value in aCA. Thus, a more accurate test is needed for earlier detection of aCA, which in turn may improve PTB associated outcomes.

1.4 Biomarkers for acute chorioamnionitis

1.4.1 Amniotic fluid markers

Early diagnosis of aCA is important; however it is limited by the fact that histological examination of the placenta is only possible after delivery, and therefore cannot be used for rapid prenatal diagnosis of aCA. Measuring biomarkers of placental inflammation, such as levels of amniotic fluid interleukin -6 (IL6), offer another potential diagnostic approach for detection of aCA. Such an approach can show improved sensitivities compared to amniotic fluid culture and often positively correlate with histologic evidence of chorioamnionitis (53, 57, 58). However, if intrauterine infection has occurred recently, the host may not have yet mounted a strong cytokine response and IL6 abundance may not reach detectable levels, whereas histologic changes of inflammation in the placenta could occur during the time interval between amniocentesis and delivery. Another study demonstrated that amniotic fluid MMP-8 levels correlate with the histopathologic staging and grading of aCA-affected placentas (59); however the diagnostic measures of accuracy including sensitivity, specificity, and likelihood ratios were not evaluated. Supplementary Table 1.1 provides a summary of the studies assessing amniotic fluid biomarkers for predicting aCA.

1.4.2 Maternal serum markers

There has been some promise in utilizing maternal serum biomarkers to predict aCA including C-reactive protein (CRP) (60, 61), cytokines such as IL6 (62-64), and neutrophil to lymphocyte ratio (65). Although studies in maternal serum suggested increased CRP levels as a good predictor of aCA, there is no clear evidence from systematic reviews to support the utility of CRP as a biomarker for aCA (66, 67). The authors of these reviews pointed out that studies

often vary widely in the reported optimal cut-off thresholds of CRP. This variability may be attributable to different laboratory techniques used to measure CRP. It is important to note that the studies often reported low diagnostic accuracy with sensitivity of 50%-80% and a false positive rate of 10-30%. Further, CRP is a non-specific marker, produced by the liver as an acute phase protein (68), in response to inflammatory conditions that may be unrelated to intra-amniotic inflammation and/or aCA. To my knowledge, no maternal serum marker has high enough sensitivity or specificity to be utilized in the clinic for aCA prediction, as of the publication of this dissertation. An overview of studies assessing maternal serum markers for predicting aCA maternal serum markers is presented in Supplementary Table 1.1.
Overall, it is not clear i) whether these biomarkers apply to all cases of aCA and in all populations, ii) whether the biomarkers can be used to predict the associated inflammatory responses in the newborns as well, and iii) whether these biomarkers can be used for predicting aCA in routine clinical settings as test performance metrics are not always and uniformly assessed.

1.4.3 Placenta as a source of biomarkers

During pregnancy, placenta-derived nucleic acids can enter maternal circulation in a number of ways: as a part of normal extravillous trophoblast invasion, release of deported trophoblasts derived from syncytial trophoblast knots, breakdown of apoptotic/necrotic cells at the placental surface, blebbing of microvesicles from trophoblast membrane, or through mechanisms of active cell communication (69, 70). Because invasion of the maternal uterine vasculature is a normal property of the extravillous trophoblasts, it would be expected to find them in maternal circulation; however they are only found in low rates, typically a ratio of less

than 1 fetal/placental cell to 100,000 maternal cells (71). Deported trophoblast structures are found in the uterine vein blood of normal pregnancies (72), with higher levels in preeclamptic women. These structures may be transcriptionally active in maternal blood and synthesize a substantial proportion of placental mRNA and proteins (73). As a response to apoptotic and activating signals, different types of syncytiotrophoblast microvesicles are released from the placenta and circulate in the plasma of normal pregnant women. The amount of syncytiotrophoblast microvesicles is known to increase during preeclampsia (PE), a condition associated with increased trophoblast apoptosis (74). Active cell communication involves exosomes, microvesicles and complexes of subcellular components. The concentration of placental-derived exosomes is 50-fold greater in the plasma of pregnant women compared with healthy non-pregnant women (75), and is significantly increased during pregnancy complications such as gestational diabetes mellitus (76) Moreover, the specific syncytiotrophoblast protein, syncytin-2, is markedly down-regulated in exosomes derived from preeclamptic placentas compared to placentas from healthy control pregnancies (77). Although the roles of placenta-derived extracellular vesicles remain to be fully elucidated, their profiles may be of diagnostic utility for screening placental pathologies such as aCA prior to the onset of clinical symptoms.

In addition, subcellular fragments including cell free placental DNA (cfp-DNA) and RNA have also been found in maternal circulation. cfp-DNA originates mainly from STBs (78, 79) and represents approximately 10% of total cell-free DNA relative to total maternal cell-free DNA (80). Currently, cfp-DNA is used in clinical settings for screening of fetal aneuploidy (81, 82); however, the placental origin of this DNA suggests that false positive results can occur due to confined placental mosaicism. While cfp-DNA may be increased in sPTB in the second trimester (83-86), most studies have found no associations between first trimester cfp-DNA

levels and sPTB (86-88). Similar to cfp-DNA, placental-specific transcripts are detectable in maternal blood during pregnancy, and are rapidly cleared from plasma within a few hours post-delivery (89, 90). Although Tsui et al. (2000) identified a large panel of placenta-specific transcripts in maternal plasma (91), few studies have investigated placental mRNAs for the prediction of PTB (92-94). The main limitations to the use of placental mRNAs as biomarkers are that mRNAs can degrade rapidly, they require stricter handling guidelines, and their expression profiles are more likely to change with sample processing time. Trophoblast miRNAs are attractive candidates for biomarkers as they are stable and relatively abundant in maternal plasma (95). Studies investigating placental miRNAs associated with PTB are discussed in detail in section 1.7.2.

1.5 Genetic predisposition to acute chorioamnionitis

While placental-derived biomarkers might be used for the diagnosis and early detection of aCA, genetic variants in innate immune system genes may contribute to the placenta's inflammatory response, thus predisposing some pregnancies to aCA. Genetic susceptibility to aCA can be hypothesized based on: i) evidence supporting familial segregation of PTB, ii) association studies supporting genetic variation in immune-system genes related to PTB, iii) association of placental histopathological inflammatory lesions with recurrent PTB, and iv) ethnic disparities in PTB and aCA rates (discussed further below).

1.5.1 Familial nature of preterm birth

Twin studies have estimated high heritability for PTB, ranging from 15-30% (96, 97). Women who have previously delivered a preterm baby (98), have sisters who had a preterm

delivery (99), or were themselves born before 37 weeks of GA (100), are at an increased risk of experiencing a PTB. Several mechanisms have been proposed to explain the recurrence risk of PTB through the maternal line. For example, physical characteristics of mothers such as body size and height alter their PTB risk, and can be inherited by daughters (101). Additionally, mothers and their daughters are more likely to share lifestyle factors such as smoking (102), which may themselves be the risk factors for PTB. Another possibility is that shared exposures or genetics can influence susceptibility to microbial infections (103, 104), which is a well-known cause of PTB, particularly aCA. Further, variation in mitochondrial genes may likely explain some of the maternal lineage PTB effects as the mitochondrial genome is almost exclusively transmitted by mothers (105, 106). While the importance of maternal genetic effects in PTB is well-established (99, 107), significance of fetal-placental genetic factors cannot be ignored (108, 109), in fact fetal genetic effects explained 20% of the variation in PTB-related conditions such as PE (110).

1.5.2 Candidate and genome-wide association studies in preterm birth

The placenta is genetically identical to the fetus and thus risk-conferring genetic variants may influence the placenta and the fetus similarly during various pregnancy complications including PTB. Furthermore, the placenta protects the developing fetus from inflammation and/or infection in various ways (Figure 1.2). Risk for aCA may be increased if the placenta is less effective at preventing and fighting infection due to structural or genetic variation altering the mechanisms for response to inflammation or infection.

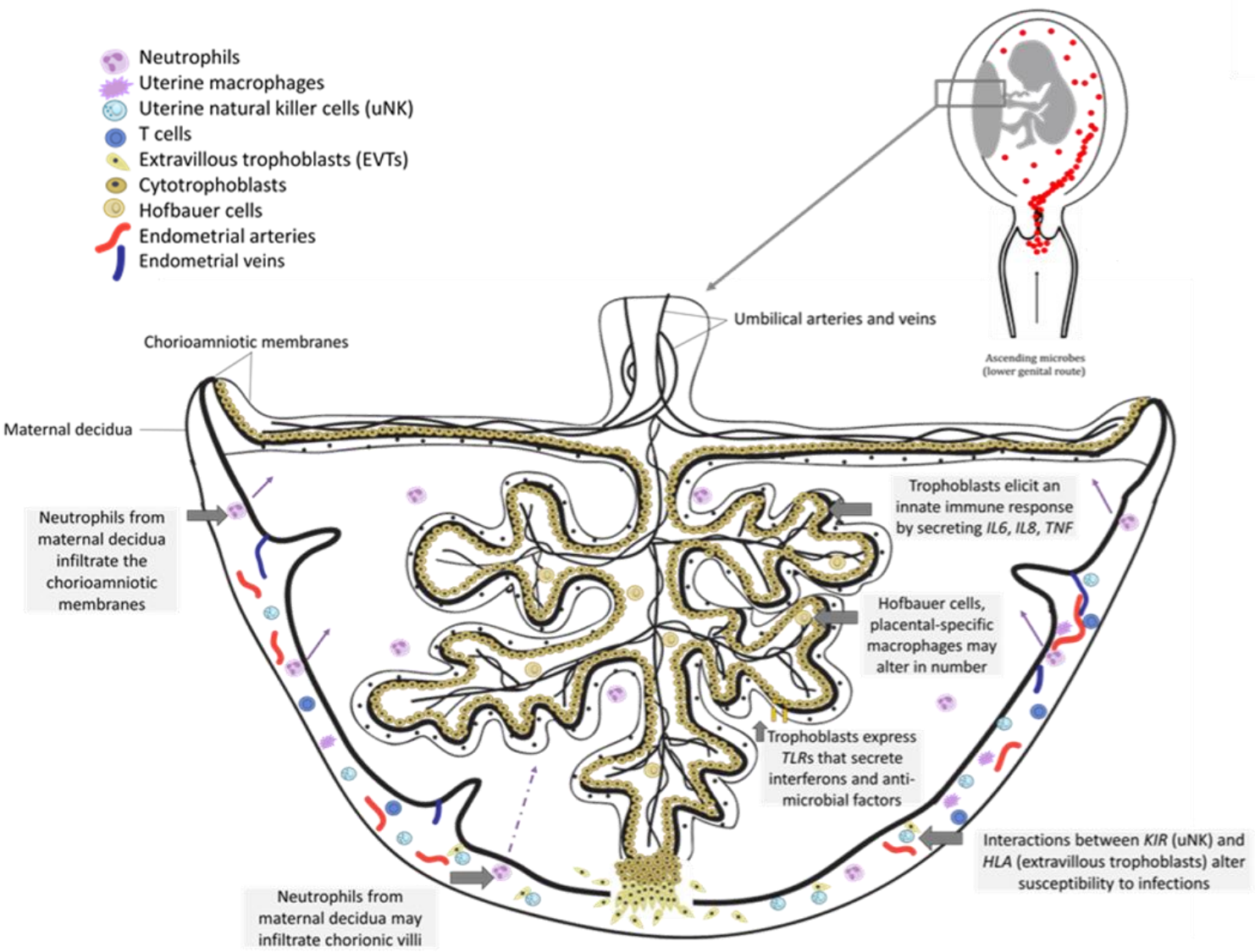

Figure 1.2 Placental response against microbial infection.

Placenta employs various mechanisms to fight against the ascending microbes from the lower genital tract. Placental trophoblasts, for example, express Toll-like receptors (*TLRs*) that behave as "sensors" of the immediate surrounding environment, and respond to a wide range of microbial pathogens by activating multiple inflammatory pathway (111, 112). Further, placental trophoblasts are capable of mounting an innate immune response by secreting anti-microbial factors including human beta defensins, secretory leukocyte protease inhibitors and cytokines such as *IL6* and *IL8*. Hofbauer cells are another class of resident immune cells that protect the fetus from inflammation by preventing the crossing of pathogens between mother and fetus. The *KIR* receptors on uterine NK cells bind directly to the *HLA-C* molecules expressed on the trophoblasts and these interactions have been shown to alter susceptibility towards infections and play an important role in allocating resources between the fetus and the mother.

Candidate gene studies have reported maternal and fetal (placental) genetic variation in *TLRs* and cytokine genes associated with PTB (113-116). Allelic variation in *TLR*s, *IL6* and *TNF-α* has been associated with placental inflammation in aCA (116-119). A small number of studies have examined the interaction between maternal and fetal genotypes (120, 121), and have identified a compounded risk of PTB when the mother and the infant carried a specific combination of SNPs. For example, presence of the *IL1β* "GG" genotype (rs16944) in mothers and the *IL6* "GC" genotype (rs1800795) in newborns in a South American population is associated with increased PTB risk (OR 12.3, $p<0.01$); however no significant association with PTB was observed when the SNPs were analyzed independently likely because both alleles were only predisposing in individuals with European ancestry (121). Further, it has been shown that the maternal *KIR* "AA" genotype in combination with a fetal *HLA-C* "C2" allele is associated with an increased risk of adverse pregnancy outcomes including PE and recurrent miscarriage (122, 123). The *KIR* receptors on uterine Natural Killer cells bind directly to the *HLA-C* molecules expressed on placental trophoblasts and these interactions likely play an important role in regulating the degree of invasion and allocating resources between the fetus and the mother.

Genome-wide association studies (GWAS) have identified several genetic variants in relation with sPTB (124-126), but there is little reproducibility across these studies. Recently, a GWAS study investigating 43,568 women of European ancestry identified multiple genetic variants associated with sPTB (127). Although they replicated three of the maternal genomic loci (*EBF1*, *EEFSEC*, and *AGTR2*) in an independent cohort, none of the identified genetic variants had been previously implicated in sPTB. The aforementioned work as well as other studies have mainly focused on maternal genetic effects, but the contribution of fetal (placental) genetic

variants remain significantly understudied. A risk variant in the fetal genome near *FLT1* is one of the few validated single gene variants found to be associated with increased susceptibility to PE (128).

Many efforts have been made to identify specific risk variants in sPTB, and though the scientific community has not been successful at identifying reproducible SNP associations through genome-wide screens, common biological pathways underlying sPTB have been recognized (16, 129). The infection-inflammation response network is the most consistent pathway shown to be associated with sPTB (130, 131). Microbial invasion of the amniotic cavity is a frequent pathological finding in sPTB cases. In fact, approximately 25% of sPTB cases with intact membranes are associated with infection (6), which is also a well-known cause of aCA. Microbial invasion of the amniotic cavity elicits a strong inflammatory response in the mother and fetus, accompanied by an increase in the concentrations of proinflammatory cytokines detected in the amniotic fluid (132, 133). In response to this chemotactic gradient, maternal neutrophils and/or other immune cells normally residing in the maternal decidua and intervillous space migrate towards the chorionic plate of the placenta. Neutrophil chemotaxis stimulates the synthesis of metalloproteases, which in turn facilitates cervical ripening, and degrades the chorioamniotic membranes, causing them to rupture prematurely. Placental trophoblasts respond to microbial products by mounting a specific innate immune response (134-136). Simultaneously, the fetal membranes also synthesize various inflammatory cytokines (137), which, in turn, stimulate the release of prostaglandins, leading to premature uterine contractions, and preterm delivery.

The maternal-fetal hypothalamic pituitary adrenal (HPA) axis activation is a second pathway commonly occurring with sPTB (128). It has been proposed that increased production

of placental corticotropin-releasing hormone (CRH), driven by the maternal HPA axis in response to stress, stimulates the fetal secretion of cortisol (138), and thereby leads to preterm delivery. Other mechanisms such as glucocorticoid receptor (GR) signaling have also been implicated in PTB. Impairments in the GR signaling pathway due to stress and/or infection may alter the inflammatory environment during pregnancy, and may lead to premature activation of labor-initiating signals resulting in PTB (139). Recently, whole exome sequencing identified the GR signaling pathway as the most significantly enriched pathway associated with recurrent preterm deliveries (140). Specifically, within the GR pathway, damaging missense variants in heat shock protein family A member 1 like (*HSPA1L*) were identified as risk factors for sPTB. This gene was previously implicated in pregnancy complications including aCA (141), intra-amniotic infection (141), and PE (142).

1.5.3 Recurrent placental inflammatory lesions in preterm birth

Regardless of the causative factor or the underlying pathway, histologic evidence of inflammation in the placenta, fetal membranes, or umbilical cord is commonly observed in sPTB cases (34, 143-148). Placental inflammatory lesions were frequently observed in pregnancies complicated by sPTB, in fact a high recurrence risk for these lesions has been well-demonstrated (149-151). While sPTB-associated placentas exhibited more acute inflammatory lesions such as aCA compared to placentas from medically-indicated PTBs, chronic inflammatory lesions, particularly diffuse decidual leukocytoclastic necrosis, were frequently detected in placentas from medically-indicated PTBs (151). The incidence of acute infectious inflammatory lesions is common in PTBs across GA, whereas placental maternal vascular malperfusion lesions are most common in sPTBs and medically-indicated PTBs >28 weeks GA (152).

1.5.4 Ancestry differences in preterm birth rates

Substantial differences in PTB rates were noticed among different ethnic subgroups within a country (153) For example, in U.S., the PTB rates among "African Americans" were as high as 17.8%, whereas rates for "white women" were 11.5% (16). Further, recurrent PTBs in "black women" also occur at substantially higher rates than in "white women" (154). Several studies have confirmed that rates of infections during pregnancy are significantly higher in "black/African American women" including bacterial vaginosis, and lower genital tract infections. (155-157). Accordingly, cases of aCA, and preterm premature rupture of membranes (PPROM) are more common in "black women" (158, 159). In sPTBs before 35 weeks, 55% of placentas from "black women" showed maternal inflammatory responses, whereas only 12% of placentas from other ethnic origins exhibited histologic evidence of inflammatory response (144). Similar findings in other studies confirm such ethnic disparities in the prevalence of aCA (158, 160, 161). While factors that underpin these ethnic disparities are poorly understood, socioeconomic status (SES), commonly measured in terms of occupational status, household income, and parental educational attainment, can likely explain some of these ethnic discrepancies in PTB (162). Lower SES is also independently associated with increased PTB (163); however it is important to note that even after accounting for SES, ethnic disparities in PTB have been observed (159, 164, 165). Some of these disparities may be attributed to differences in frequencies of genetic variants associated with inflammatory responses, vaginal microbiome, infections during pregnancy, stress, nutrition, and prenatal care (166, 167).

Extraplacental membranes exhibit ethnicity-specific cytokine profiles in response to an infectious stimulus. Menon et al. (2006) observed higher concentrations of IL6 and IL10 after lipopolysaccharide (LPS) stimulation in extraplacental membranes derived from "Caucasians" as

compared to “African-Americans”, whereas IL1 concentration was increased in the “African-American derived samples (168). Notably, *IL10* has been shown to inhibit preterm uterine contractions induced by *IL1* (169). The same group also reported increased MMP9 concentration in membranes from “African-Americans” after LPS stimulation (170), and MMP9 is involved in premature rupturing of the membranes (171). In addition, multiple studies have confirmed ethnic differences in amniotic fluid concentrations of inflammatory cytokines (172-174), suggesting that pathophysiological processes related to sPTB vary across ethnicities. However, the underlying cause of these differing physiologic responses to infection/inflammation remains substantially undetermined, and maybe dependent on genetic and/or epigenetic factors, or interactions of exposures with ethnicity.

For example, genetic variants in *IL6* (rs1800796 and rs1800795) influence IL6 concentrations in sPTB (175). These SNPs have been shown to alter disease risk of various inflammatory disorders including aCA (176-178), and are strongly correlated with ancestry. Based on 1000 Genomes Project data, the C allele of rs1800795 is frequent in European ancestry individuals (40-50%), and almost absent in individuals of East Asians. On the contrary, the C allele of rs1800796 is common in individuals of East Asian (70-80%), and rare in individuals of European ancestry (3-5%). (www.ncbi.nlm.nih.gov/variation/tools/1000genomes/)

Pathway enrichment analysis of genetic variants related to PTB suggested unique biological pathways associated with ethnicity (179). Although PTB-associated genetic variants were enriched in inflammatory processes in both self-reported “African-Americans” and “Caucasians”, hematological diseases such as decidual hemorrhage and thrombosis were prominent among the “Caucasian” group, and processes related to connective tissue disorders

involving PTB-related genes such as *MMP9, MMP2, MMP3* were identified in “African American” mothers (179).

1.6 Epigenetic alterations associated with acute chorioamnionitis

1.6.1 Definition of epigenetics

The evolution of the term “epigenetics” has been previously reviewed in multiple publications (180-183). The word “Epigenetics” stems from the word “epigenesis”, first used by Aristotle to elucidate the development of specialized tissue structures from an undifferentiated egg. Conrad Waddington described the phrase “epigenetic landscape” (184, 185), as a concept to illustrate how genes regulate cell differentiation during development. Waddington portrayed the “epigenetic landscape” as a hillside with numerous bifurcating canals. This can be compared to a ball, which represents a pluripotent cell, rolling down from the top of a hill comprising of ridges and valleys. As the ball rolls down the hill, it encounters different branching points or paths, which represent a series of cell differentiation fates or “choices” made by the pluripotent cell before reaching its final differentiated state. Further, he proposed that on this landscape, "the presence or absence of particular genes acts by determining which path shall be followed from a certain point of divergence” (184), signifying the role of genes in regulating regulate cellular differentiation.

Recently, Lappalainen and Greally (2017) have attempted to define “epigenetics” based on cellular properties including cellular reprogramming and polycreodism (183). Typically, cellular reprogramming events may lead to the emergence of a small, mosaic population of altered cells from a canonical cell type, but this minor subset of cells will likely retain the original identity of the canonical cell population. Alternatively, perturbations during

development may affect cell fate decisions, resulting in variation in proportion of cell types within a tissue and may be associated with potential phenotypic effects. Taken together, epigenetic processes are defined as mitotically heritable chemical modifications to the DNA molecule or its regulatory components that potentially influence cellular states (cellular reprogramming) or fates (polycreodism), and occur in the absence of a change to the nucleotide sequence (182, 183, 186, 187).

1.6.2 DNA methylation

DNA methylation (DNAme) is the most commonly interrogated epigenetic mark in human population studies, as recent technological advancements have permitted for the inexpensive high-throughput measurement of DNAme across the genome and the relationship between DNAme and gene expression is relatively well demonstrated. DNAme is the addition of a methyl group to the 5'carbon of the cytosine base, most typically at cytosine-phosphate-guanosine (CpG) dinucleotides (188). Apart from methyl groups, other cytosine modifications have been identified and thought to play a role in DNA demethylation. For example, 5-hydroxymethylcytosine (5-hmC), an oxidized derivative of 5-methylcytosine (5-mC) may inhibit the maintenance methylation reaction catalyzed by DNMT1 (189), resulting in passive demethylation. Alternatively, 5-hmC may be involved in active demethylation through DNA repair-associated mechanisms. Generally, 5-hmC tend to be low in most tissues including placenta (190); however, 5-hmC is abundant in the human brain (191).

CpG dinucleotides are generally depleted in the genome, due to the tendency for methylated cytosines to be spontaneously deaminated to thymines. Exceptions to this are CpG islands (CGIs), which are high CpG density regions often associated with gene promoters (192).

The University of California Santa Cruz (UCSC) Genome Browser defines a CpG island as a region with length >200 bps, CG content >50%, obs/exp CpG ratio >0.60. Non-CpG DNAme (CpH, where H includes A, C, and T) occurs primarily in mammalian pluripotent stem cells and non-dividing cells such as neurons (193, 194). The term "DNAme" has been used in this dissertation to refer to DNAme at CpG dinucleotides.

DNAme is a commonly interrogated epigenetic mark in human population studies, as it is relatively easy to measure, and its relationship with gene expression has been extensively studied. The relationship between DNAme and gene expression regulation is complex and tends to be dependent on genomic context. For example, DNAme at gene promoters is generally associated with transcriptional repression of the related gene; however, the relationship between levels of gene-body DNAme and gene expression is highly variable (195). Further, other epigenetic mechanisms such as histone modifications may work in tandem with DNAme to influence gene expression (196, 197).

While DNAme may reflect changes to gene expression patterns in specific cell types, it may also reflect altered cell composition. DNAme signatures differ strikingly between different cell lineages, in fact, samples originating from the same tissue cluster together over samples originating from the same individual (198, 199). This pattern highlights the role of DNAme in tissue identity. DNAme is involved in hematopoietic cell lineage commitment (200-202), and differences in DNAme between blood cell types is often located at sites of binding of transcription factors involved in lineage specification (202). Not only is DNAme involved in cell lineage commitment, it is also involved in immune cell activation. Infection of human dendritic cells with a live virulent strain of *Mycobacterium tuberculosis* is associated with rapid demethylation at several CpGs, and a majority of these loci were located in distal enhancer

elements, including those that modulate the activation of key immune transcription factors (203). The rapid loss in DNAme was accompanied by extensive epigenetic remodeling, including gain of histone activation marks, and increased chromatin accessibility.

1.6.3 Methods for measuring DNA methylation

In a single diploid cell, at a single CpG site, DNAme can be denoted by one of three numeric conditions: absent on both alleles (0), present on both alleles (1), or present on one of the alleles (0.5). In a tissue sample of mixed cell population such as chorionic villi or blood, DNAme measured is an average across a pool of cells (0-1), and a change in DNAme could either reflect an average change in DNAme across all cell types in the sample, or an alteration in the composition of different cell types.

Numerous techniques have been developed to assay DNAme. A widely-used method for measuring genome-wide DNAme is the Illumina Infinium HumanMethylationEPIC BeadChip (850K array), which interrogates DNAme at 866,895 CpGs across the genome (204). Illumina microarrays will be discussed in more detail in Chapter 2. Although the 850K array provides a somewhat genome-wide perspective of the methylome, such bisulfite conversion-dependent methods cannot distinguish been the canonical 5-methylcytosine mark from its oxidized derivative 5-hmc. However, additional bisulfite treatments such as oxidative bisulfite sequencing have been developed to overcome this challenge. Studies, however suggest that 5-hmC values tend to be low in most tissues, including the placenta (190). Alternative genome-wide techniques like methylated DNA immunoprecipitation (MeDIP) can be utilized to immunoprecipitate DNA with methylated CpG sites, and can be a cost-effective approach when single-base resolution is not desired. However, MeDIP tends to exhibit biases associated with CpG density (205).

Sequencing techniques such as whole genome bisulfite sequencing and reduced representation bisulfite sequencing have also been used to assess DNAme. The major advantage of whole genome bisulfite sequencing is its ability to quantify the DNAme levels of nearly every CpG site in the genome, including low-CpG-density regions. On the other hand, reduced representation bisulfite sequencing may exhibit a lack of coverage at intergenic and distal regulatory elements. The selection of a method for quantifying DNAme mainly depends on the cost, amount of input DNA required, and the experimental question. A summary of the existing techniques available for profiling genome-wide DNAme is reviewed in Yong et al. (2016) (206).

1.6.4 Placental methylome

The DNAme profile of the placenta is unique as compared to somatic tissues. The major component that makes up placental chorionic villi, the trophoblast, has a unique DNAme landscape compared with maternal decidua, fetal membranes (chorion and amnion), and embryonic tissues (brain, kidney, muscle, spinal cord) (207). Approximately 40% of the placental genome comprises of large blocks (>100kb) of low to intermediate methylation, termed "partially methylated domains" (PMDs) (208). PMDs are relatively gene-poor and are associated with a relative increase in H3K9me3 and H3K27me3 marks. As opposed to the bimodal distribution DNAme in somatic tissues (209), where most CpGs typically are either on average 0% methylated or 100% methylated, the presence of PMDs and imprinted genes in the placenta results in a unique trimodal distribution of DNAme measures. Also contributing to the unique landscape of placental DNAme are several families of retrotransposable elements that are reported to be hypomethylated in the placenta (210). However, within these families, the DNAme levels can be highly variable. The lower level of DNAme at several retrotransposable

elements may contribute to placental-specific gene expression of endogenous retrovirus envelope proteins including syncytin, which is involved in the fusion of pluripotent CTBs into differentiated syncytiotrophoblasts (211).

1.6.5 Altered DNA methylation in placenta and preterm birth

DNAme signatures vary vastly between different cell lineages and change with i) GA (212) and ii) placental pathology (207). In the context of sPTB, only a limited number of studies have investigated differential DNAme in the placenta and extraplacental fetal membranes (213-217). Using the Illumina Infinium HumanMethylation450 BeadChip (450K array), Tilley et al. (2018) identified 250 differentially methylated CpG sites between sPTBs and medically-indicated preterm deliveries from extreme PTBs (<28 weeks GA) (215). Although they found that many genes associated with these CpGs were ontologically involved in neural development processes, the 450K array is enriched for developmental pathways and cell differentiation gene ontology terms (218). Further, Tilley et al. showed that placental DNAme levels at 17 of these 250 CpG sites were able to predict childhood cognitive impairment at ten years of age. Using methylation-sensitive, restriction-enzyme-based Methyl PCR assays, another group focused on autism spectrum disorder-specific genes found that hypermethylation of the *OXTR* promoter was specific to sPTB-associated extraplacental membranes; however no difference in *OXTR* expression was identified between sPTBs and uncomplicated term deliveries (216).

Identifying changes to the placenta specifically associated with sPTB is difficult as the epigenetic profile of the placenta changes with GA (212), and hence term controls are not a proper match for comparison. Furthermore, given that the etiology and presentation of sPTB is heterogeneous (219), the associated features have not typically been defined in majority of the epigenetic studies performed as yet. Additionally, iatrogenic cases (delivered because of PE or

other indication) are sometimes included. Further, DNAme is prone to batch effects, and some methodologies use to adjust for batch effects such as *ComBat* can introduce false biological signal into the data (220). Despite this, epigenetic studies often do not provide a description of the tools used to assess and adjust for batch effects. A systematic review of placental epigenetic modifications associated with sPTB also highlighted the lack of standardized procedures for tissue collection, case-control ascertainment, clinical data collection, quality control procedures, and analytical approaches amongst previous publications (221). Additional high-quality studies are needed before the extent of epigenetic changes associated with sPTB can be fully assessed.

1.7 Gene expression alterations in placenta and preterm birth

1.7.1 mRNA alterations

Transcriptomic studies investigating gene expression profiles in sPTB-associated placentas are limited, in fact only 18% of PTB research has focused on sPTB (222). Using a Benjamini-Hochberg adjusted *p*-value of <0.05 and a fold-change of >2.9, 426 differentially expressed probes were identified between sPTBs and spontaneous term births in placenta, with a panel of 36 sPTB-associated RNA transcripts potentially detectable in maternal plasma (223). Among these, *IL1RL1* showed the highest fold-change in the sPTB placentas compared with the placentas from spontaneous term deliveries. Another study compared placental expression profiles between sPTBs and term elective cesarean deliveries (94); however, this study did not address or account for the fact that mode of delivery may influence placental gene expression (224). Candidate studies have identified altered gene expression in immune-system genes such as *TLRs* and *CXCLs* in placental inflammation associated with sPTBs (225-227). Because some of these inflammation-related mRNA signatures were also observed during normal spontaneous

labor (228), mRNA profiles identified in studies may not be specific to placental inflammation in sPTB.

1.7.2 miRNA alterations

It is now well established that specific microRNAs produced by the human placenta are found in maternal plasma (95, 229). Concentrations of placental specific microRNAs increase in the maternal plasma as pregnancy progresses and return to normal levels after delivery (95, 230). Numerous studies have shown altered miRNA expression in PE-associated placentas, though there is little reproducibility across these studies (231, 232). This low reproducibility may be attributable to incomplete understanding of placental miRNAs or insufficient study power. Few studies have investigated placental-specific miRNAs in sPTBs (94, 233-235). Interestingly, placental-specific imprinted C19MC microRNAs showed increased expression in sPTBs, but decreased expression in PPROM pregnancies (233). Limited studies have investigated placental-specific microRNA changes in aCA (235, 236). Recently, expression of mir-331 was reported to be up-regulated in aCA-affected placentas and the expression of miR-331 correlated with the severity of inflammation in aCA. Montenegro et al. (2007) showed increased expression of miR-223 and miR-338 in aCA-affected chorioamniotic membranes (235); however, these miRNAs were not followed-up in matched maternal plasma samples, and thus it remains to be seen if their expression is reflected in maternal circulation.

1.8 Research Objectives and Hypothesis

Risk for aCA may be increased if the placenta or the extraplacental fetal membranes are less effective at preventing and fighting infection due to structural, functional or genetic variation. Genetic variants in innate immune genes may contribute to the placenta's

inflammatory response, thus predisposing some pregnancies to aCA. Genetic variants in inflammatory genes may also modulate epigenetic processes such as DNAme, which is involved in regulating gene expression, and in turn might affect susceptibility to aCA. In addition, changes to placental and membrane cell composition and function occur in response to infection, a common cause of aCA. Both predisposing and consequential changes to the placenta may cause changes in DNAme and miRNA levels. I thus hypothesize that aCA is associated with unique genetic, DNAme, and miRNA signatures that reflect both a susceptibility to and a response to infection/inflammation.

The overarching objective of this dissertation is to understand how genetic, epigenetic, and miRNA variation in the placenta are associated with the disruption of immune balance during inflammation in aCA. To accomplish this, I undertook the following studies:

i. Characterization of immune-system genetic variants in the placenta in association with aCA.
ii. Characterization of genome-wide DNAme signatures in aCA-associated placentas and extraplacental fetal membranes.
iii. Characterization of candidate miRNA changes in aCA-associated placentas.

Chapter 2: Study cohort, sampling and techniques

2.1 Study population

The study cohort is based on an ongoing collection of samples for our Epigenetics in Pregnancy study (EPIC). The past clinical coordinators of Robinson lab, K. Louie, and Dr. J. Schuetz were responsible for recruiting study patients. Research assistants R. Jiang and D. Hui collected placentas from pregnancies delivered at the B.C. Women's Hospital and Health Centre, Vancouver, Canada. Placentas were recruited in two main ways: 1) recruited by the Robinson lab from high-risk patients or controls with written consent; these cases include (mostly) term and preterm deliveries 2) samples obtained through the Anatomical Pathology lab at B.C. Women's Hospital and Health Centre and de-identified; these are more heavily biased to preterm deliveries. Minimal clinical information was available for majority of the preterm samples including GA at delivery, fetal sex, maternal age, mode of delivery, and birth weight. We calculated birth weight defined by its' standard deviation (SD) relative to normative values by GA and fetal sex (237).

In PTB-related cases, known conditions such as – PE (Preeclampsia), IUGR (Intrauterine Growth Restriction), PPROM (Preterm Premature Rupture of Membranes), incompetent cervix, placental abruption, and aCA were recorded. Both PE and IUGR were defined according to the Society of Obstetricians and Gynaecologists of Canada (SOGC) guidelines (237, 238). Specifically, PE was diagnosed as gestational hypertension (BP > 140/90 mmHg) with one or more of the following conditions: i) proteinuria after 20 weeks gestation (> 300 g/day), or ii) adverse maternal symptoms, maternal organ dysfunction, abnormal maternal lab findings, or fetal conditions. IUGR was defined as birth-weight <3rd percentile accounting for both fetal sex

and gestational age, or birth-weight <10th percentile with additional clinical findings such as: absent or reversed end diastolic velocity on Doppler ultrasound, uterine artery notching, or oligohydramnios. aCA was diagnosed by pathological examination of associated fetal membranes using consensus histological criteria, described in detail in section 1.3.1 (9). I reviewed pathology reports for aCA cases to confirm the presence of neutrophils in the fetal membranes, recorded evidence of placental inflammatory lesions such as intervillositis and villitis associated with the cases. While the pathology reports indicated a microbial etiology for majority of the aCA cases, this information was not available for all the cases. Further, chronic chorioamnionitis cases were specifically excluded as these conditions are primarily suspected to have a non-microbial immunologic origin, and unlike aCA, chronic cases are typically identified by presence of lymphocytes in the extraplacental membranes. A subset of aCA cases recruited from the Anatomical Pathology lab were ascertained in detail alongside Dr. Jefferson Terry, Pediatric and Perinatal Pathologist, B.C. Women's Hospital and Health Center. Figure 2.1 shows the breakdown of samples used in the data chapters (Chapter 3-5); however selection of the aCA cases and non-aCA cases is described explicitly in the data chapters.

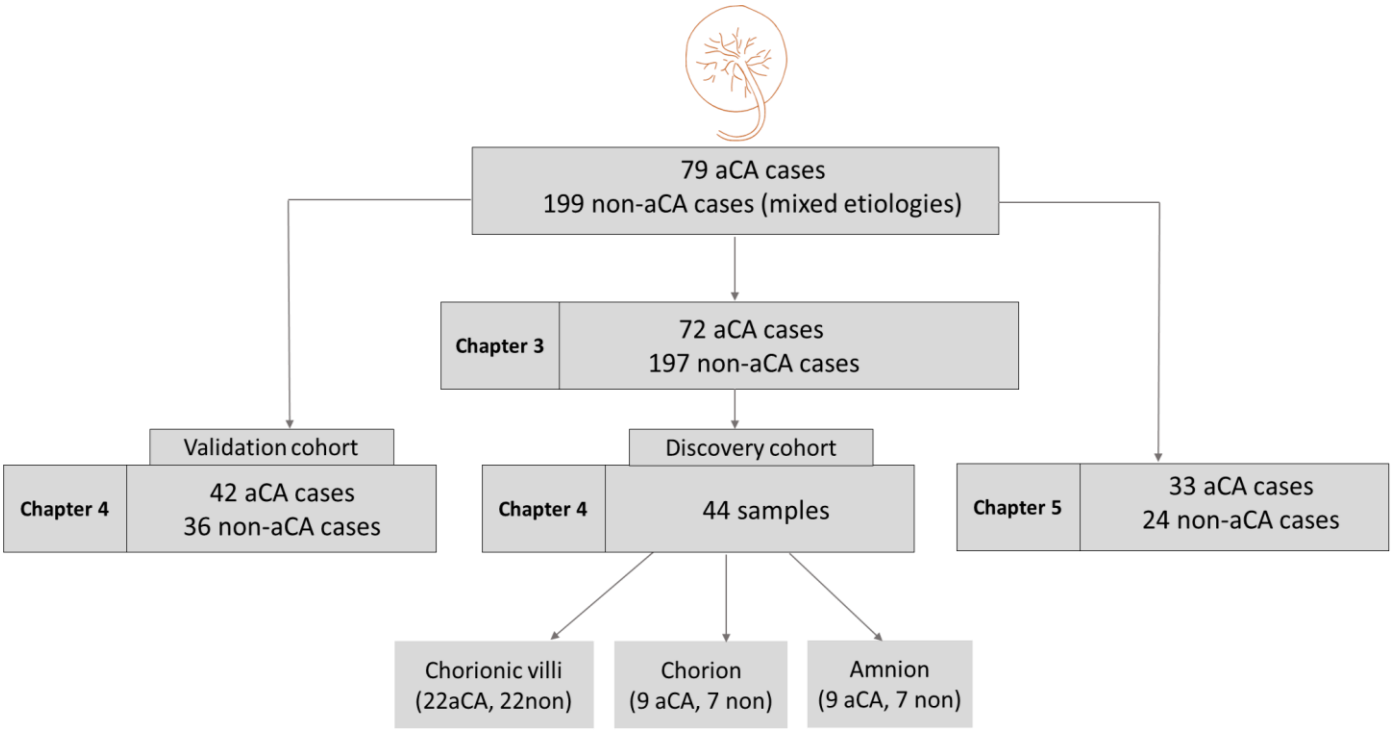

Figure 2.1 Schematic representation of the breakdown of samples utilized in the data chapters presented in this dissertation

2.2 Placental sampling

Previous publications from Robinson lab have described placental sampling in detail (20, 239). Briefly, the fetal membranes (amnion and chorion) were teased apart with tweezers, and washed thoroughly to minimize maternal blood contamination. Independent samples of chorionic villi, approximately 2 cm^3, were taken from 2-4 distinct locations from just below the fetal surface of the placenta to avoid maternal decidua. Typically, at least one site was sampled near the umbilical cord and one near the periphery of the placental disk. Other sites were sampled approximately halfway between the cord and placental edge. Samples were thoroughly washed with phosphate-buffered saline to avoid maternal blood contamination.

DNA was extracted from chorionic villus and fetal membranes by a standard salting out procedure, modified from Miller et al. (240). The salting out method involves the use of high concentration of saturated NaCl solution to precipitate cellular proteins to the bottom of the solution. The DNA within the supernatant is then extracted using ice-cold ethanol. A NanoDrop 1000 spectrophotometer (ThermoScientific, USA) was used to assess DNA purity and concentration.

2.3 DNA methylation microarray

For this dissertation, genome-wide DNAme was assessed using the 850K array, which quantifies DNAme at 866,895 CpG sites across the genome (204). The platform covers >90% of the 450K array and includes 413,745 new CpG sites which were not previously targeted by the 450K array. The additional probes substantially improved the coverage of regulatory elements, including enhancers identified by FANTOM5 (241) and the ENCODE project (242).

Illumina's DNAme microarray technology is based on "quantitative genotyping of C/T single nucleotide polymorphisms (SNPs) introduced following bisulfite conversion", which essentially converts unmodified cytosines to uracil, and leaves cytosines with DNA modifications unaffected. Placental samples used in this dissertation were bisulfite converted using the Zymo EZ DNA MethylationTM Kit (Zymo Research, USA). Bisulfite-converted samples were whole-genome amplified before being hybridized to the microarray chip as per the manufacturer's protocol (204), and the 850k array chips were scanned by a HiScan 2000 (Illumina).

The 850k array is organized as a "chip", on which eight samples can be loaded in parallel, with the bisulfite converted DNA from each sample loaded onto one of the eight

"arrays". Since the maximum number of samples that can be analyzed in a single chip is eight, this organization introduces two batch variables: chip and chip position (indicating the eight spots on the chip the sample is loaded onto). Adding batch variables into statistical models or removing batch signal using computational methods such as surrogate variable analysis (SVA) and *ComBat*, are widely used approaches used to account for unwanted technical noise. However, studies have shown that some batch-correction methods can introduce false biological signal, if applied to an unbalanced study design (220, 243-245). In this dissertation, *ComBat* (246) implemented in the R software environment, was used to correct for batch effects (Chapter 4); however, technical replicates and unadjusted p-value distributions were used as measures to carefully monitor the data processing methods. Further, we used a stratified randomization study design that distributed aCA cases and non-aCA cases equally across the chips, and thus create a balanced study design.

The 850k array targets CpG sites with 50-mer oligo "probes" adhered to "beads", which are randomly arranged on the surface of each array. Similar to the previous version (247), the 850k array contains two different probes types, with different probe chemistries. For Type I probes, methylated and unmethylated versions of the probe are designed and incorporated on different beads, and thus, presence of a fluorescent signal indicates DNAme. Type II probes, have only a single probe to measure DNAme, where the colour of fluorescence (Cy3-**Green**/Cy5-**Red)** suggests whether the CpG site was methylated or unmethylated in the template DNA. Specifically, methylation is inferred from the green signal and lack of methylation is inferred from the red signal. Further, type I probes cover more CpG-dense regions than type II probes (248). The intensity of fluorescence is translated into a level of DNAme for each targeted CpG site - either as a β value, a number between 0 and 1 (0 = no methylation, 1 = fully

methylated) or logit-transformed β values (M values), a less heteroscedastic value used for all statistical analysis purpose (209).

A variety of normalization methods including functional normalization (249), subset-within array normalization (250), noob (251), and β-mixture quantile normalization (252) have been developed to account for these probe type differences. In this dissertation, functional normalization was used to account for probe bias. This method uses control probes and out-of-band probes to act as surrogates for unwanted technical variation, and has been shown to outperform some existing normalization methods with respect to improving replication of results across experiments, reducing technical variability, and accounting for batch variation.

2.4 Sequenom® iPlex® Gold platform for genotyping

Samples in Chapter 3 were genotyped using the Sequenom® iPlex® Gold platform at the Génome Québec Innovation Centre (Montréal, Canada). This protocol is described in detail by Gabriel et al. (2009) (253). Briefly, Sequenom® iPLEX® Gold genotyping is based on a robust multiplexed polymerase chain reaction (PCR) followed by a template-directed single base extension reaction in which oligonucleotide extension primers anneal directly adjacent to each targeted SNP site, and are extended and terminated by a single complementary base into the genotyping target site with mass-modified dideoxynucleotide terminators. The products are detected by matrix-assisted laser desorption/ionization time-of-flight (MALDI-TOF MS). Incorporation of mass-modified terminators into the single base extension reaction provides sufficient mass for allele separation and detection using MALDI-TOF MS. Finally, the SpectroTYPER software automatically translates the mass of the observed extended primers into a genotype for each reaction to identify the SNP alleles (homozygous or heterozygous).

2.5 Quantitative reverse transcription PCR (RT-qPCR)

RNA was reverse transcribed using TaqMan™ miRNA Reverse Transcription Kit (Thermo Fisher Scientific, Applied Biosystems™, CA, USA) and specific stem-loop primers (Thermo Fisher Scientific, Applied Biosystems™, CA, USA), according to the manufacturer's protocol (https://assets.thermofisher.com/TFS-Assets/LSG/manuals/cms_042167.pdf). Quantification using these TaqMan™ miRNA assays is performed in two steps: a reverse-transcription (RT) step and a PCR step. In the RT step, the cDNA is reverse transcribed from total RNA using a stem-loop RT primer which is specific for the mature miRNA target. This is followed by a PCR step where PCR products are amplified from the cDNA samples using a separate specific TaqMan miRNA Assay. The TaqMan™ probes comprise of a reporter dye attached to the 5' end of the probe, a nonfluorescent quencher dye and a minor groove binder linked to the 3' end of the probe.

When the probe is intact, the close proximity of the quencher dye and the reporter dye results in little to no fluorescence, typically by Förster-type energy transfer (254). However, during the PCR step, the Taq DNA polymerase which has a 5′-exonuclease activity cleaves the probe that hybridizes/anneals to the complementary target sequence. This cleavage releases the reporter dye from the probe, which is now no longer in close proximity to the nonfluorescent quencher, and thus results in increased fluorescence by the reporter dye. Increase in fluorescence occurs only if the target sequence is complementary to the TaqMan probe.

2.6 Genetic ancestry

Association studies are prone to population stratification if case and control groups are not matched by ancestry. Because ancestry was largely unknown in the study cohort, we selected

55 ancestry informative marker (AIM) SNPs to genotype in our population. These AIM SNPs were designed to differentiate between African, European, East Asian, and South Asian ancestries (255-257). After initial quality control (removal of SNPs with call rate <90%), 50 AIM SNPs were used to infer ancestry in the placental villus DNA samples. Ancestry was described using the top three coordinates derived from a multidimensional scaling (MDS) analysis of AIM SNP genotypes of the placental villus samples and n=2,157 1000 Genomes Project samples (n=661 African, n=504 East Asian, n=504 European, n=489 South Asian) used as ancestry reference populations, as described in Del Gobbo *et al.* (2018) (258). Distributions of the three ancestry MDS coordinates are compared between aCA and non-aCA groups to identify any population stratification by ancestry.

Chapter 3: Association of a placental Interleukin-6 genetic variant (rs1800796) with DNA methylation, gene expression and risk of acute chorioamnionitis

3.1 Background

PTB occurs in approximately 11% of live births worldwide, although there is substantial variability in the incidence of PTB based on geographical regions (259). Children who are born preterm are at a higher risk for long-term developmental delays and life-long health complications (14, 260). sPTB, making up the majority of PTBs, often presents as aCA, which is characterized by an infiltration of maternal neutrophils into the chorioamniotic membranes. This acute placental inflammation can also be triggered by non-microbial "danger signals" including cellular stress and/or cell death (28, 29).

Genetic susceptibility for aCA can be hypothesized based on: i) high heritability estimates of PTB (15-30%) (97, 108), ii) evidence supporting familial segregation of PTB (99, 261), iii) association of placental histopathological inflammatory lesions with recurrent PTB (150, 262), and iv) ethnic disparities in PTB (263-265) and chorioamnionitis rates (158). Inherited differences in immune system genes also influence susceptibility to microbial infection (266-269), which is a well-known cause of aCA. In addition, a strong genetic predisposition underlies many infectious and inflammatory diseases, particularly in early childhood (270-272); this may also hold true for *in utero* susceptibility for aCA.

Studies investigating candidate genes have reported that maternal and fetal genetic variation in *TLRs* is associated with sPTB (113, 114, 273). Allelic variation in *TLR* genes has been shown to modulate immune responses during parturition, and thus confer an altered risk of preterm delivery (274). Genetic variants in cytokine genes such as *IL6* have also been associated

with intrauterine infection and/or inflammation in sPTB (115, 117, 275). Furthermore, elevated concentration of *IL6* in maternal serum, cervical secretions and amniotic fluid are associated with sPTB (276-279). Recently, a genome-wide association study investigating >40,000 women of European ancestry identified several genetic variants associated with sPTB (127). Although variants in *EBF1, EEFSEC,* and *AGTR2* genes were replicated in an independent cohort of >8,000 women, none of the identified genes had been previously identified in sPTB or known to have a direct role in inflammatory mechanisms (127). While these studies have provided some insight on genetic variation linked to sPTB, rarely are the same loci reported with sPTB risk. sPTB is heterogeneous in etiology (219), thus inconsistent phenotyping of sPTB cases and differences in population structure may likely explain the discrepancies across these studies.

Genetic variants within coding regions may directly affect protein function, while those in regulatory regions may affect molecular processes such as DNAme (280-282) that are involved in regulating gene expression (283, 284). Alternatively, genetic variants can alter the binding site of TFs and affect gene expression, which then influences DNAme levels, suggesting DNAme as a consequence of gene regulation (285). Irrespective of the underlying mechanism, these effects can in turn affect susceptibility to inflammatory diseases. For example, in rheumatoid arthritis (RA), DNAme at an *IL6*-related CpG was altered in RA affected patients, and a negative relationship between DNAme and *IL6* mRNA levels was observed (286). While increased serum levels of *IL6* have been previously reported in aCA (62, 64, 287), these studies did not take into account the genotype at the *IL6* locus and/or the DNAme status of the *IL6*-related CpGs. Furthermore, the maternal genotype is often investigated although the placental genotype may be more relevant in terms of mediating pregnancy-related inflammation.

Elucidating these complex relationships between genotype, DNAme and gene expression is important to improve our understanding of the genetic regulation of placental inflammation.

In this study, we investigated the association between 16 candidate SNPs in 12 innate immune system genes and the presence of aCA. These SNPs were chosen based on published reports of an association with chorioamnionitis (288-290), placental inflammation (116, 119) or neonatal sepsis/infection (176, 291, 292). We validated these associations in a population of 269 placentas, of which 72 were affected with aCA and 197 were unaffected (non-aCA). Further, we investigated whether aCA-associated SNPs showed also a correlation with altered DNAme of the associated gene, and determined whether DNAme levels correlated with gene expression.

3.2 Methods

3.2.1 Study cohort

The study cohort is based on an ongoing collection of samples for our EPIC study, and overlaps with samples described in previous publications related to placental DNAme (213, 258, 293). Placentas from 72 aCA cases were selected based on a diagnosis of aCA determined by pathological examination of the placenta and associated membranes using consensus histological criteria (9). Another set of 197 non-aCA cases were identified from this same collection of placentas. These consisted of 73 PTBs with no evidence of aCA and/or placental inflammation including cases of spontaneous premature preterm rupture of the membranes, placental abruption, fetal vascular malperfusion, acute hypoxic ischemic event, and preterm labor), in addition to 124 term (> 37 weeks gestation) cases from healthy, uncomplicated pregnancies. Criteria for exclusion were fetal and/or placental chromosomal abnormalities, fetal malformations, congenital abnormalities, IUGR (237), PE (238), and hypertension.

Demographic characteristics of the study cohort is presented in Table 3.1. Of the variables investigated, GA at delivery was significantly different between the aCA cases and non-aCA cases in our study cohort, as aCA cases are associated with PTB. Although male fetuses are reported to be at an increased risk of adverse pregnancy outcomes including chronic inflammation, neonatal sepsis, and and stillbirth; in our study, fetal sex was not significantly different between aCA and non-aCA groups.

Further, the aCA cases and the non-aCA cases were sampled from a single urban population (Vancouver) and delivered at a single centre, BC Children's & Women's Health Centre, which is located in a high socio-economic status neighborhood. Of the documented observations for maternal smoking status (80/269), almost all (79/80) identified themselves as non-smokers. Additionally, the most reproducible finding between maternal smoking and altered DNAme is observed at CpG sites linked with *AHRR* and *CYP1A1*. We therefore tested for differences at these sites and did not observe altered DNAme associated with our pathology at these sites in our study cohort.

Table 3.1 Identification of variables confounded with acute chorioamnionitis status

	aCA	Non-aCA	*p*-value*
N	72	197	
Maternal age (yrs); range (mean)	19.6 - 44.0 (32.0)	17.0 - 43.5 (33.0)	ns
GA at delivery (weeks); range (mean)	20.0 - 40.0 (28.0)	19.4 - 41.9 (36.0)	4.32e-15
Birth weight (SD); range (mean)	-3.10 - 3.05 (-0.14)	-3.13 - 3.23 (0.04)	ns
Sex; M/F	38/34	103/94	ns

**p*-values are calculated by comparison of aCA cases to non-aCA cases using Wilcoxon-Mann-Whitney rank sum test for continuous variables, Fisher's exact test for fetal sex. ns = $p > 0.05$.

3.2.2 Candidate Single Nucleotide Polymorphism selection

SNPs in 12 innate immune system genes were chosen based on published findings of an association with any of the following: i) chorioamnionitis (288-290), ii) placental inflammation (116, 119), or iii) neonatal sepsis/infection (176, 291, 292). The estimates of the minor allele frequency for the 16 SNPs varied between >1-48% in the general population based on 1000 Genomes Project Phase III records (294). Table 3.2 provides a detailed description of the 16 candidate SNPs investigated in the study.

Table 3.2 Candidate SNP information for 16 SNPs in innate immune system genes

Genes	Gene name	Chromosome	SNPs*	Genomic location
MBL2	Mannose binding lectin 2	10	rs1800450	Exon
TLR2	Toll-like receptor 2	4	rs3804099	Exon
TLR4	Toll-like receptor 4	9	rs1554973	3′ UTR
			rs4986790	Exon
			rs2149356	Intron
TLR5	Toll-like receptor 5	1	rs5744105	Intron
TLR9	Toll-like receptor 9	3	rs352140	Exon
CD14	Cluster of differentiation 14	5	rs2569190	5′UTR
IL6R	Interleukin-6 receptor	1	rs2228144	Exon
IL6	Interleukin-6	7	rs1800795	Promoter
			rs1800796	Promoter
IL1B	Interleukin-1 beta	2	rs1143643	Intron
IL10	Interleukin-10	1	rs1800896	Promoter
			rs2222202	Intron
IL8	Interleukin-8	4	rs4073	Promoter
MMP-16	Matrix metalloproteinase-16	8	rs2664349	Intron

*This information is obtained from dbSNP: database from short genetic variations (https://www.ncbi.nlm.nih.gov/snp/)

3.2.3 Genotyping

All samples were genotyped using the Sequenom iPlex Gold platform at the Génome Québec Innovation Centre (Montréal, Canada). Primary quality control of the genotype data comprised of the following steps i) removal of samples with call rate <90% (n=1), and ii)

removal of SNPs with call rate <90% (n=1; rs4986790). After primary quality control, each gene involving multiple SNPs was investigated for linkage disequilibrium (LD) to determine if the SNPs were independent of one another. Strong evidence for LD was observed for two SNP pairs (rs1800795–rs1800796 in *IL6* and rs1800896–rs2222202 in *IL10*) with D'=0.99. Haplotype analysis was performed for these two SNP pairs to investigate whether carriers of a specific haplotype had increased susceptibility for aCA. The 15 SNPs were also tested for Hardy-Weinberg Equilibrium (HWE) to detect genotyping error and/or population stratification.

3.2.4 Inferring ancestry of the study population

See Chapter 2, section 2.6

3.2.5 Publicly available datasets

To investigate whether candidate SNPs were associated with altered DNAme, we used our previously obtained DNAme microarray data that was available for a subset of placental (chorionic villus) samples (n=67). Some of these (GSE100197 and GSE74738; n=25) were assessed on the 450K array; 485,512 CpG sites) (295), while the remaining samples (GSE115508; n=42) were assessed on the 850K array; 866,895 CpG sites) (204). Probes for 453,093 CpG sites were present on both arrays. Probe filtering was performed as described in Wilson et al. 2018 (204). To account for type I- type II probe bias on the DNAme arrays, normalization was performed using *preprocessFunnorm* function in the R *minfi* package (249). Principal component analysis (PCA) was used to detect sources of variability in the DNAme dataset. Known technical variation associated with array type was corrected with the function *ComBat* in R *sva* package (246). DNA methylation values were reported as β values ranging from 0 to 1 (0 = no methylation, 1 = fully methylated) and were used for biological

interpretation. However, log-transformed β values, M values, were used for statistical analyses as they are less heteroscedastic (209).

Further, we took advantage of publicly available datasets to determine whether DNAme levels correlated with gene expression at the associated gene. Our group has previously published gene expression data (GSE44711) (296) on a set of 16 chorionic villus samples that were also run on the 450K array to measure DNAme (GSE44667) (296). Another set of 48 matched chorionic villus samples were also utilized to evaluate correlation between gene expression and DNAme levels (GSE98224) (297). DNAme data was already normalized and corrected for batch effects. Log2-transformed expression values were used for statistical analysis.

3.2.6 Statistical analysis

All statistical analyses were performed using R version 3.4.1. *p*-values for Table 3.1 were calculated by Wilcoxon-Mann-Whitney rank sum test for continuous variables and Fisher's exact test for categorical variables. Kolmogorov-Smirnov (KS) test was used to assess the differences in distribution of ancestry MDS coordinate values between aCA cases and non-aCA cases. Deviation from HWE in controls was assessed using an exact test for HWE. Statistical tests for differences in allele frequencies between aCA cases and non-aCA cases were conducted with Fisher's Exact tests. Haplotype analysis was performed using SNPStats (https://www.snpstats.net/start.htm) (298). Comparison of DNAme levels between genotype groups was carried out using the non-parametric Kruskal-Wallis test. Spearman's correlations were conducted to determine whether DNAme levels correlated with gene expression at the

associated gene. Power was calculated using the Online Sample Size estimator, OSSE (http://osse.bii.a-star.edu.sg/index.php)

3.3 Results

3.3.1 Characterization of population stratification in study population

It is important to determine whether pathology showed evidence of confounding with ancestry, as frequencies of genetic variants and the incidence of chorioamnionitis often vary between different ancestries (158). There were no significant differences in the distribution of the three ancestry MDS coordinates between the 72 aCA cases and 197 non-aCA cases (Bonferroni-corrected $p>0.05$, Figure 3.1). However, we observed that ancestry MDS coordinate 1, which largely separates European and East Asians, shows the greatest variability while ancestry MDS coordinate 3, which largely separates the Europeans and South East Asians, shows the least variability.

Genotype frequencies did not conform to HWE expectations in three SNPs (rs1800795, rs1800796, and rs1554973, $p<0.01$). Because rs1800796, rs1800795 and rs1554973 deviated from HWE, we next investigated whether the frequencies of these genetic variants were associated with ancestry. Significant differences in the distribution of the two ancestry MDS coordinates between the SNP genotypes was observed (Supplementary Figure 3.1), confirming that deviation from HWE at these loci was due to our heterogeneous study cohort. Additionally, both rs1800795 and rs1800796 are in LD and do not conform to HWE, thus it is unlikely it is an artefact of genotyping.

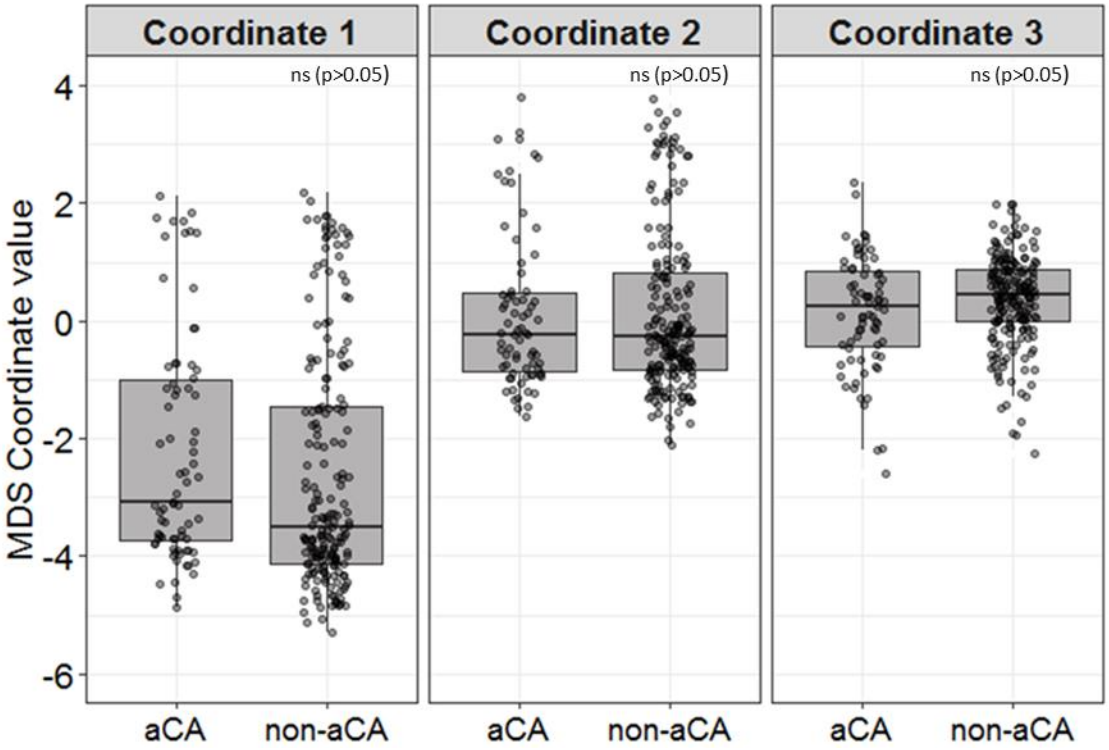

Figure 3.1 Distribution of ancestry MDS coordinates in the study cohort.

The three ancestry MDS coordinates were not significantly different between the aCA cases and non-aCA cases in the study cohort, suggesting pathology was not confounded by ancestry in our study population. *p*-values were calculated by Kolmogorov-Smirnov test.

3.3.2 Association of candidate immune SNP allele frequencies with acute chorioamnionitis

To investigate whether placental (fetal) genetic variation may lead to an increased susceptibility to developing aCA, we genotyped 16 SNPs within 12 innate immune system genes among our study cohort samples (72 aCA, 197 non-aCA). We limited our analysis to SNPs previously implicated in aCA or related phenomenon. Given our small sample size, we estimated that our study had 50% power to detect differences in allele frequencies associated with aCA, at a *p*-value <0.05, MAF >1%. Despite this limitation, we found that the minor C allele at rs1800796 in *IL6* was associated with aCA (Fisher's exact test, p=0.044). (Supplementary Table 3.1). To explore this further we looked at the genotype distributions for rs1800796 and found

that the CC genotype was associated with increased risk for aCA (Fisher's exact test, p=0.02, OR=3.1).

The *IL6* rs1800796 SNP is known to be strongly correlated with ancestry. Based on 1000 Genomes Project data, the C allele is common in individuals of East Asian (70-80%), and rare in individuals of European ancestry (3-5%) (https://www.ncbi.nlm.nih.gov/variation/tools/1000genomes/). We also found that the genotype frequencies of this SNP varied between different ancestries in our study population (Supplementary Figure 3.1). We thus sought to explore the association of rs1800796 with aCA within more genetically homogeneous subpopulations. To select homogenous ancestry groups from our placental chorionic villus samples, an unsupervised clustering method, *k*-means clustering, with k=3, was used to cluster samples into three groups of common ancestry. The CC genotype was absent in cluster 1, which was predominantly of European ancestry (Figure 3.2 and Supplementary Table 3.2). Allele frequencies of rs1800796 were significantly associated with aCA status only in cluster 3 samples (n=41) that were largely of East Asian ancestry (Fisher's exact test, p=0.041). Specifically, 8 of the 12 (67%) cases of aCA in cluster 3 had the "CC" genotype as compared to 10 of 29 (34%) non-CA cases. In our study cohort, rs1800796 was in nearly complete LD with rs1800795 (D' = 0.99); however, unlike rs1800796, rs1800795 was polymorphic in individuals of European ancestry and uninformative in the East Asian cluster 3 samples as the GG genotype was completely absent. Although allele frequencies in rs1800795 alone were not associated with aCA, there was an increased risk of aCA in carriers of the C-C haplotype (p=0.02).

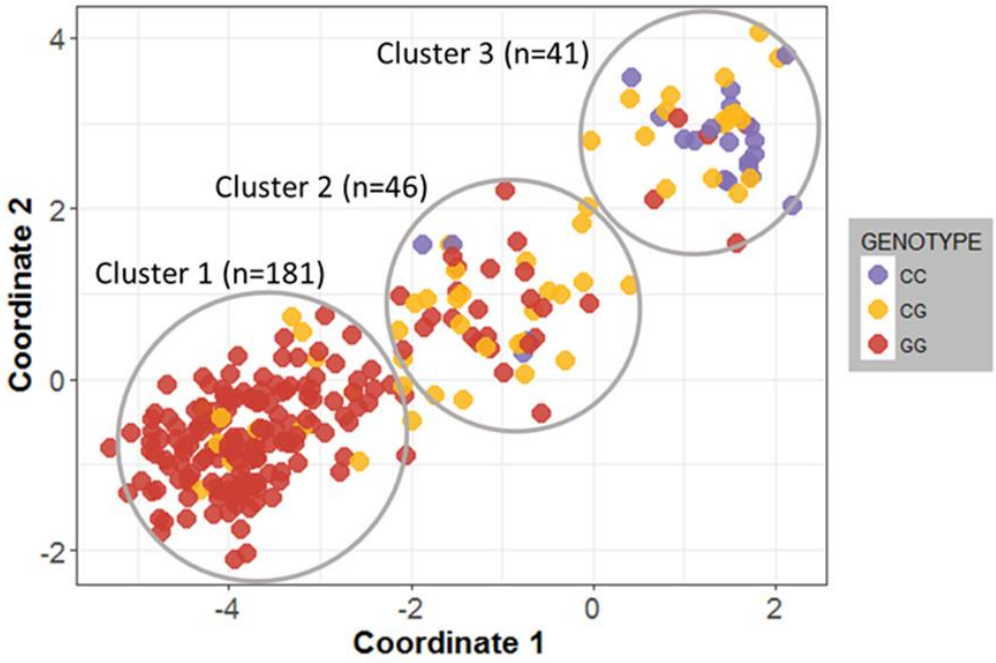

Figure 3.2 rs1800796 genotype is associated with ancestry.

Based on the ancestry MDS coordinate values, three ancestry clusters were identified by *k*-means clustering. Of the 22 cases with CC genotype, 11 (50%) were associated with aCA, while 22% (60/246) of the CG/GG genotypes were linked to aCA. Samples are colored by *IL6* rs1800796 genotype.

3.3.3 Association of *IL6* rs1800796 genotype with *IL6* DNA methylation

A few studies have investigated the relationship between genetic variants in *IL6* and DNAme of the CpGs in the promoter region of *IL6* as a mechanism by which genetic variants may modulate disease risk (299-301). As these studies had been done in blood, we sought to examine whether the *IL6* SNP rs1800796 was associated with differential DNAme in *IL6*-related CpG sites (n=8 CpGs) in a subset chorionic villus samples for which DNAme microarray data were available (n=67). Modest ($r>0.5$) to strong ($r>0.7$) correlations were observed between β values across most of the CpG sites (Supplementary Figure 3.2). DNAme was significantly associated with rs1800796 genotype at cg01770232 (upstream enhancer, Bonferonni-corrected $p<0.05$), cg02335517 (intronic, Bonferonni-corrected $p<0.05$), cg07998387 (intronic,

Bonferonni-corrected p<0.05), cg13104385 (intronic, Bonferonni-corrected p<0.05); and cg0526589 (intronic, Bonferonni-corrected p<0.05), whereby homozygous C samples showed significant hypermethylation compared to homozygous G samples (Figure 3.3). These sites have been previously identified as linked to methylation quantitative trait loci (mQTL) in blood (302), meaning CpGs where individual genotypes may result in different DNAme patterns (283). The CG genotype was present in only four samples, therefore we did not include them in statistical analysis, though as expected, the heterozygotes showed intermediate DNAme levels (Supplementary Figure 3.3). Further, altered DNAme at cg01770232, cg7998387, and cg02335517 were associated with aCA (p<0.05) (Supplementary Figure 3.4).

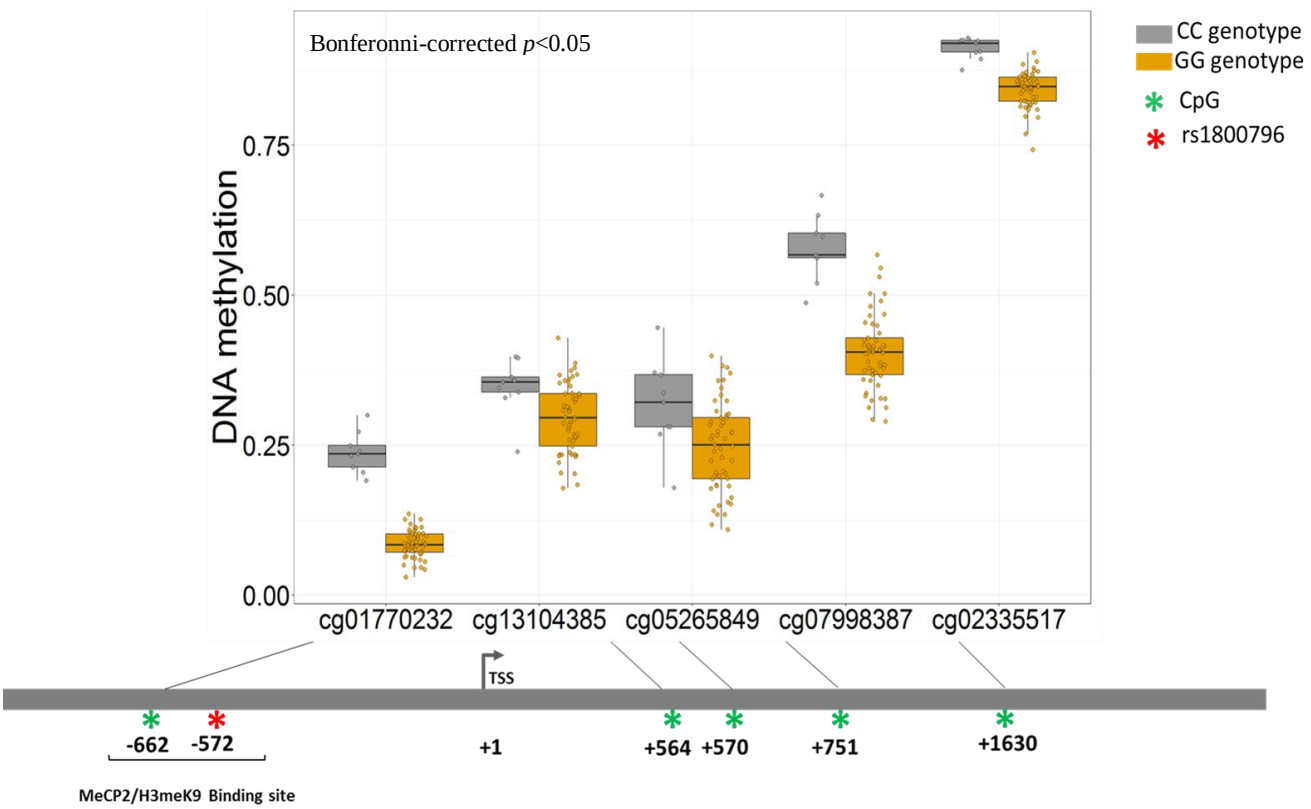

Figure 3.3 Differentially methylated *IL6* CpGs in chorionic villi associated with *IL6* rs1800786 genotype.

Unadjusted DNAme (β) values are plotted on the y-axis w.r.t the CpGs on the x-axis. Carriers of CC genotype showed increased DNAme levels compared to carriers of GG genotype, suggesting DNAme levels at these CpG sites are influenced by *IL6* genotype. Position of the CpGs are indicated below the boxplots relative to the transcription start site (TSS) (UCSC GRCh37/hg19).

3.3.4 Correlation of DNAme and gene expression for *IL6*

To evaluate whether DNAme is associated with altered gene transcription activity, we investigated whether DNAme levels of the *IL6* CpGs correlated with gene expression at the *IL6* locus in chorionic villi. Using two independent publicly available datasets, we observed that the DNAme level at cg01770232 was negatively correlated with *IL6* expression (GSE44711; GSE44667: r=-0.67, p<0.004; GSE98224: r=-0.56, p<2.937e-05) (Figure 3.4). Similar trends were observed for cg02335517, cg07998387, and cg13104385 (Supplementary Figure 3.5).

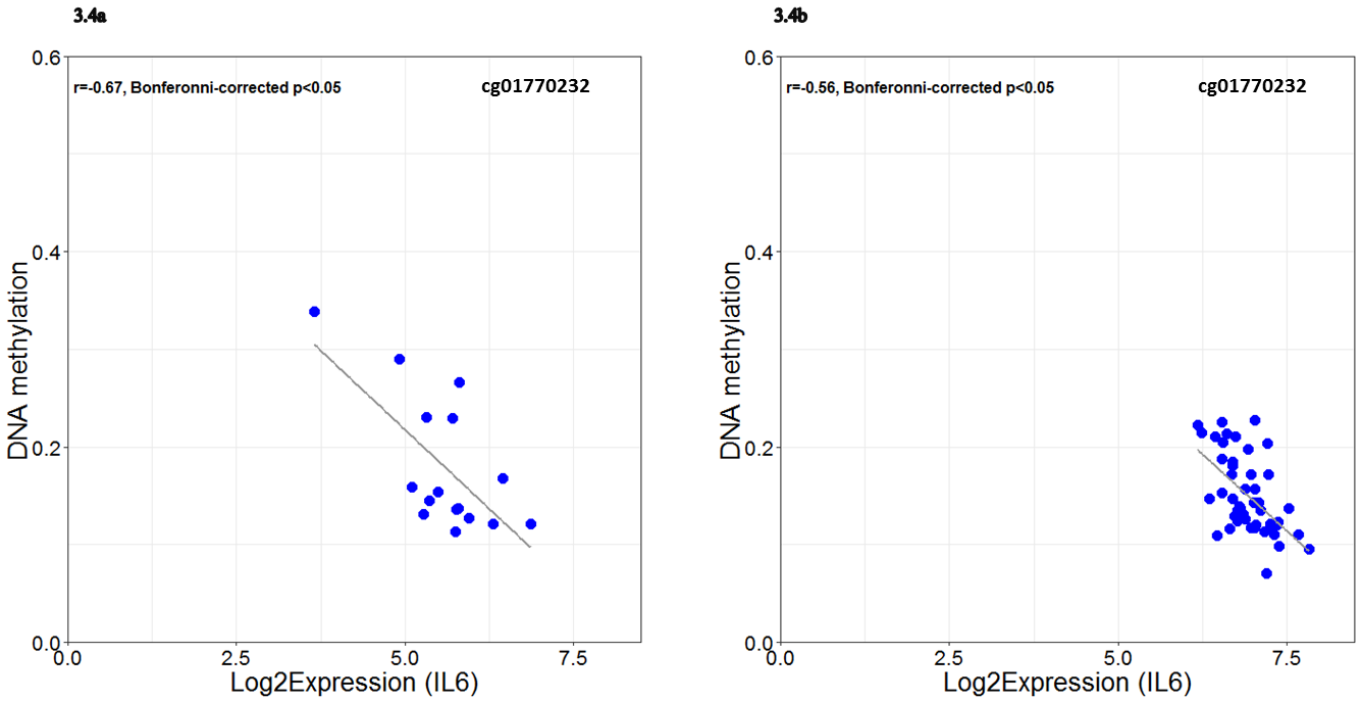

Figure 3.4. Placental DNAme at cg01770232 is associated with *IL6* gene expression.

DNAme at the *IL6* CpG site was negatively correlated with *IL6* log2 transformed gene expression in chorionic villi from a) GSE44711; GSE44667 (r=-0.67, Bonferonni-corrected $p<0.05$), and b) GSE98224 (r=-0.56, Bonferonni-corrected $p<0.05$)

3.3.5 Association of *IL6* expression and DNAme with GA, fetal sex or preeclampsia status

Using the GSE98224 dataset, we observed that *IL6* expression in chorionic villus samples was not associated with GA or fetal sex (Supplementary Figure 3.6). Although previous studies found altered *IL6* expression in placentas from preeclamptic pregnancies, there was no significant difference in *IL6* expression between PE and non-PE groups in this dataset (Supplementary Figure 3.6). Using the same dataset, we also did not observe an association between DNAme at the *IL6*-related CpGs and gestational age, fetal sex or PE status.

3.4 Discussion

In this study, we sought to validate associations of SNPs in innate immune system genes with aCA status in the placenta. As the placenta and fetus are genetically identical, risk-conferring genetic variants in innate immune-system genes may impact inflammation-response pathways in the placenta and fetus similarly. Additionally, the placenta employs a number of mechanisms to protect the developing fetus from inflammation and/or infection (111, 303). Few studies have reported an association between genetic variants in inflammatory genes, alterations in immune function and risk for aCA. The majority of these studies suggest a genetic predisposition of the mother to aCA (288, 289), but the contribution of fetal (placental) genetic variants remain significantly understudied.

In our study sample, we were able to confirm that the C allele in the *IL6* SNP rs1800796 was associated with aCA status (p=0.04). This allele was linked to increased DNAme, at both an upstream regulatory region and within the gene body, and associated with decreased expression of *IL6*. Interleukin-6 is a pleiotropic cytokine with a wide range of biological functions (304). Primarily, *IL6* facilitates neutrophil recruitment and their subsequent clearance from the sites of inflammation (305). In addition to eliciting innate immune responses, *IL6* also regulates adaptive immunity by influencing proliferation and maturation of T cells and B cells (304). As such, increased *IL6* has been shown to be protective against bacterial infection (306). Therefore, decreased expression observed in the placenta in association with rs1800796 may lead to increased risk for inflammation and aCA.

The *IL6* SNPs rs1800796 and rs1800795 were previously associated with increased incidence of aCA and development of sepsis in children in a study undertaken in Finland (117).

In the cases of rs1800796, the heterozygous "CG" genotype was found to be associated with sepsis, and in fact the "CC" genotype was absent from their study population. These same genetic variants have also been investigated in association with other inflammatory disorders including chronic periodontitis, systemic onset juvenile chronic arthritis, and distal interphalangeal osteoarthritis (177, 307-310); however, results from these studies are conflicting. Inconsistencies across these studies may be explained by ancestry differences in the study populations as the CC genotype at rs1800796 is common in East Asians and rare in individuals of European ancestry (311, 312). Though a small sample, we also found no CC genotypes in the placentas of individuals of European ancestry and the C allele was more common individuals of East Asian ancestry (Figure 3.2). Further, we found that the allele frequencies of rs1800796 were associated with aCA status only in individuals of East Asian ancestry, possibly as there was a low power to detect an effect in Europeans as the CC genotype was lacking and heterozygotes are expected to have less of an effect. Similarly, variants at the *PGR* locus, specifically the *PGR* SNP rs11224580, that significantly modulates PGR expression in the ovary has been shown to be common in East Asians compared to individuals of European and African ancestry (313), but in this case the Asian-specific variant is linked with decreased incidence of early sPTBs (313). Because polymorphisms such as rs1800796 (*IL6*) and rs11224580 (*PGR*) exhibit extreme population-specific aleleic variation, these genomic loci are likely to have undergone positive selection that is specific to Asian populations (313, 314).

In addition to genetic variation, circulating levels of IL6 in the serum and amniotic fluid may influence the risk for aCA. Although placental trophoblasts have the capacity to synthesize IL6 (315, 316), the source of elevated IL6 plasma levels observed in pregnancy complications such as PE is primarily attributed to maternal leukocytes and/or endothelial cells

(317). Elevated IL6 levels in the mother may occur as part of a pro-inflammatory response to infection. In contrast, we found that the placental genotype (rs1800796) associated with aCA is linked with decreased *IL6* expression in the placenta. As *IL6* mediated innate immune response has been shown to exhibit a protective effect against microbial infections (306, 318-321), reduced *IL6* expression observed in the placenta may predispose an individual to infection, by preventing an appropriate innate immune response to microbes.

Although the role of *IL6* in modulating innate immune response has been well-elucidated, molecular mechanisms such as DNAme underlying the genetic regulation of *IL6* transcription have rarely been investigated (322). To our knowledge, this is the first study to show the role of *IL6* genetic variants in modulating DNAme patterns in aCA-affected placentas. We identified that carriers of the rs1800796 C allele had increased placental DNAme levels at multiple *IL6*-related CpGs, most significantly at cg01770232, which is located at an upstream enhancer, compared to individuals with *IL6* G allele. Although this CpG has been described as linked to an mQTL in blood, we showed that this relationship also exists in the placenta. Further, we observed aCA cases were more methylated than the non-aCA cases at cg01770232, cg07998387, and cg02335517 (Additional file 2: Figure S4).

The DNAme patterns in the placenta may imply a primary phenomenon where increased DNAme at cg01770232 is associated with an increased risk of developing aCA in individuals carrying the *IL6* C allele. Alternatively, some of these subtle DNAme changes could be secondary to the disease itself. Although we were not able to measure circulating levels of IL6, using publicly available matched placental DNAme and gene expression data, we observed that DNAme levels at cg01770232 negatively correlated with *IL6* gene expression. Dandrea et al. (2009) (322) demonstrated that *IL6* repression in pancreatic adenocarcinoma cell lines is

facilitated by binding of methyl-CpG-binding protein (MeCP2) to the methylated CpGs spanning from positions -666 to -426 relative from the transcription start site of *IL6*. Interestingly, rs1800796 and cg01770232 is located at position 572 and 662 respectively, and it is therefore possible that rs1800796 alters the binding of MeCP2 to cg01770232, thereby affecting IL6 expression and DNAme, though this has not been tested in placental tissue. Further, the *IL6* upstream region contains several $(A/T)_{>4}$ motifs adjacent to the methylated CpGs including cg01770232, shown to mediate high-affinity MeCP2 binding (323). Understanding these mechanisms will provide insights into how genetic variation in *IL6* may contribute towards disease pathogenesis in aCA.

Overall, the present study has limitations. Our sample size was relatively small, especially among the genetically homogenous subpopulations; therefore, the findings of this study should be evaluated in larger subpopulations of different ancestries. In particular, the lack of an association between the other genetic variants we investigated and aCA might be a result of our small sample size. Although we utilized publicly available datasets to investigate functional consequences of the *IL6* rs1800796 polymorphism, and confirmed that DNAme changes correlated with changes in *IL6* gene expression, we could not examine whether IL6 protein levels in maternal blood would reflect placental DNAme and expression. Further, potential confounding factors for our study, such as socio-economic status, maternal smoking status, maternal alcohol use, and PPROM status, were not documented for all the cases in our study cohort and thus not accounted for in statistical analyses. Finally, our results only highlight the biological significance of placental (fetal) genetic variants in aCA, but this does not exclude the role of maternal genetic factors in altering disease risk to aCA, given that maternal genetic effects have been shown as important contributors to PTB (99).

Chapter 4: DNA methylation profiling of acute chorioamnionitis-associated placentas and fetal membranes: insights into epigenetic variation in spontaneous preterm births

4.1 Background

Preterm babies are at an increased risk of life-threatening infections in the first few weeks of life, as well as long-term health complications (14, 259). PTBs are commonly associated with inflammation of the placenta and fetal membranes (amnion and chorion) known as aCA (49, 324). aCA is also a risk factor for newborn complications, regardless of GA at birth (324-326).. aCA is associated with other inflammatory lesions of the placenta including acute intervillositis and villitis, which affect the chorionic villous trees (32, 326). Thus, characterizing these molecular or cellular changes in the placenta can in turn improve our current understanding of the full consequences of aCA.

Epigenetics may be a useful tool to characterize some of the molecular and cellular processes involved in placental inflammation, yet its role in the context of aCA is substantially understudied. DNAme, the addition of a methyl group to the 5'carbon of cytosine, most typically at CpG dinucleotides, is a commonly interrogated epigenetic mark in human population studies. The relationship between DNAme and gene expression regulation is complex and tends to be dependent on genomic context (327). In the context of PTB, only a limited number of studies have investigated DNAme changes in the placenta (217, 328). While these studies provided some preliminary insights on DNAme patterns associated with PTB, rarely are the same CpG candidates reported as differentially methylated (DM) between cases and controls. Additionally, the definition of PTB pathology was ambiguous, which limits the utility of these studies in

understanding the role of DNAme in aCA. A focus on a distinct pathology linked to PTB, such as aCA, is needed to further research in this area.

While DNAme may reflect changes to gene expression in specific cell types, it may also reflect altered cell composition. DNAme signatures differ strikingly between different cell lineages, including those in extra-embryonic tissue. Chorionic villi have a unique DNAme landscape compared with maternal decidua, fetal membranes (chorion and amnion), and embryonic tissues (brain, kidney, muscle, spinal cord) (207). In whole placenta samples (chorionic villi), DNAme patterns also change with GA (212), and in certain placental pathologies (207). We hypothesize that the increase in the number of immune cells that occur during placental inflammation will be reflected in changes to DNAme in whole placental samples. Specifically, we sought to address three questions: (1) Are there genome-wide DNAme changes associated with aCA in chorionic villi, chorion and amnion?; (2) Are there common aCA-associated DNAme changes between chorionic villi, chorion, and amnion? ; (3) Can we use DNAme signatures to characterize immune cell-types in aCA-associated placentas?

An overview of the study design is presented in Figure 4.1. We first compared genome-wide DNAme profiles of aCA-associated pregnancy tissues (22 placental chorionic villi, including 9 with matched chorion and amnion samples) to profiles of non-aCA preterm pregnancy tissues (22 placental chorionic villi, including 7 with matched chorion and amnion samples). Next, we identified overlapping aCA-associated DNAme changes across the three tissue types, chorionic villi, chorion, and amnion. Differentially methylated CpG sites associated with aCA in the “discovery cohort” were followed up in an independent set of samples (N= 42 aCA cases, 36 non-aCA cases) by a site-specific technique for measurement of DNAme (pyrosequencing). Finally, we used unsupervised hierarchical clustering with neutrophil-specific

CpG sites to segregate chorionic villus samples based on aCA status. Collectively, our genome-wide array analysis of aCA placentas was able to capture some immunity-related changes, which may be in part attributable to changes to immune cell type ratios and gene expression during placental inflammation in aCA.

Question: 1 Are there genome-wide DNAm changes associated with aCA in chorionic villi, chorion and amnion?
Question: 2 Are there common aCA-associated DNAm changes between chorionic villi, chorion, and amnion
Question: 3 Can we use DNAm signatures to detect immune cell infiltration in aCA-associated placentas?

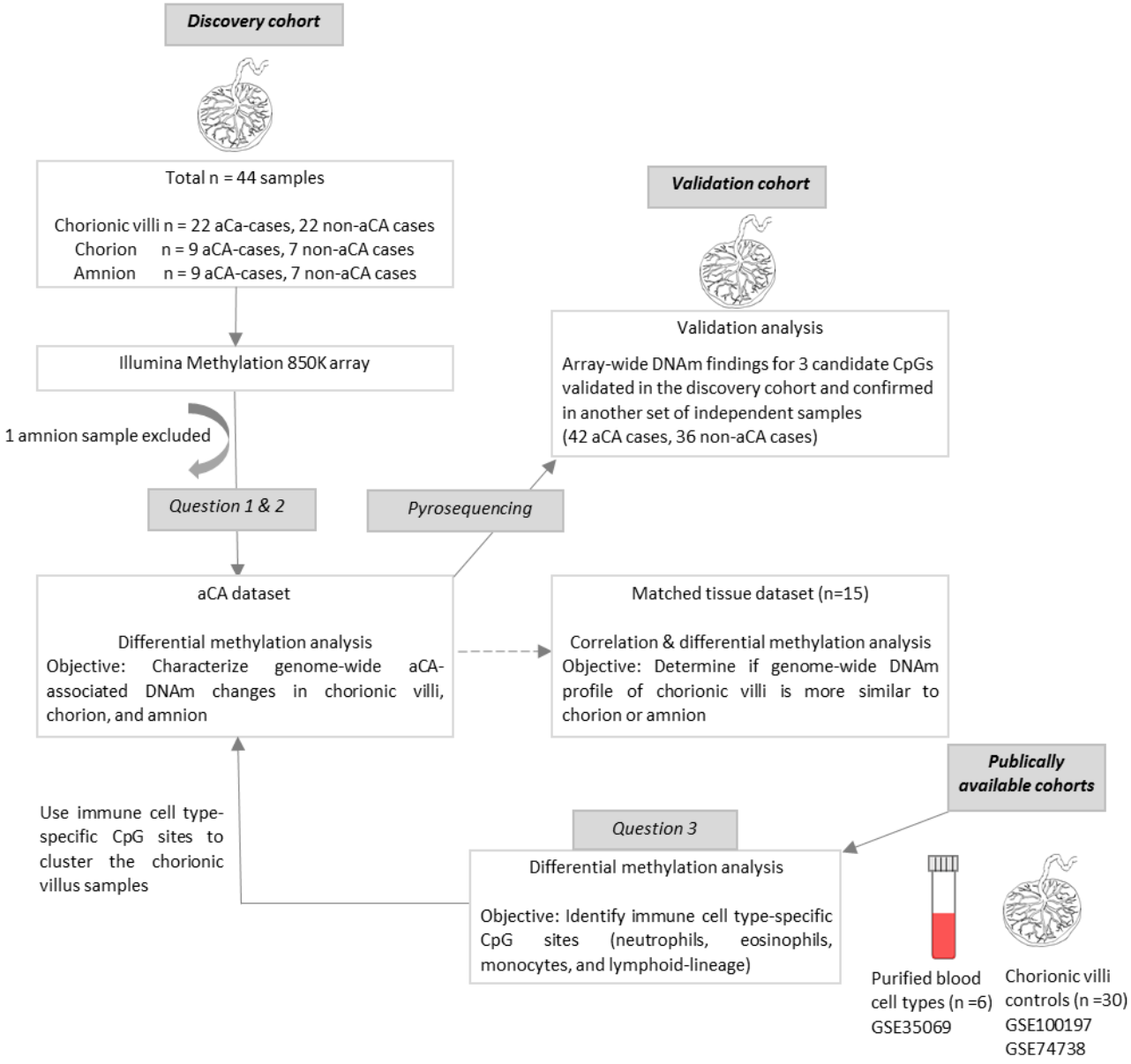

Figure 4.1 Schematic representation of the study design and workflow

4.2 Methods

4.2.1 Study cohort

Discovery cohort: Placentas from 44 PTBs, 22 with aCA and 22 without aCA were collected from the deliveries at the BC Women's Hospital. A subset of these samples have been previously described in Wilson et al. (2018) (19). Diagnosis of aCA was performed using validated histological criteria by clinical pathologists (9). Distribution of non-aCA preterm cases was chosen to be of mixed etiology based on clinical history and placental examination and is as follows: 11cases of spontaneous premature preterm rupture of the membranes, 6 cases of placental abruption, 2 cases of placental previa, 1 case of preterm labor, 1 case of PE, and 1 case of unexplained PTB. Exclusion criteria for samples were (i) chromosomal abnormalities either diagnosed prenatally by amniocentesis or on the placenta postnatally after delivery as determined by postnatal screening, (ii) fetal malformations, (iii) intrauterine growth restriction, and (iv) multi-fetal pregnancies. Demographic and clinical characteristics of the discovery cohort are presented in Table 4.1. Although the GA at delivery differed between the groups, the age range was the same and GA was accounted for in statistical analyses.

Table 4.1 Demographic and clinical characteristics of the discovery cohort

Variables	aCA (n=22)	Non-aCA (n=22)	*p* value
Maternal age, years (mean)	19.6-43.9 (33.41)	20.4-43.5 (32.08)	ns
GA at delivery, weeks (mean)	28-36 (30.74)	28-36.7 (32.28)	<0.01
Birth weight (SD)	-1.02-1.51	-1.36-0.73	ns
Fetal sex (M/total)	11/22	13/22	ns

*p-values are calculated by Wilcoxon-Mann-Whitney rank sum test for continuous variables, Fisher's exact test for fetal sex. ns = non-significant

Ancestry was inferred from AIM SNPs using MDS based on the method as described in Del Gobbo et al. (2018) (258) (See Chapter 3, section 2.6). While overall similar, there were significant differences in the distribution of ancestry MDS coordinates between aCA cases and non-aCA cases as assessed by KS tests; therefore, ancestry was accounted for in statistical analyses.

Validation cohort: Fresh frozen placental chorionic villi was obtained from the Anatomical Pathology Laboratory at BC Children's & Women's Health Centre. Clinical characteristics of the validation cohort are presented in Table 4.2. Both aCA cases and non-aCA preterm cases were chosen using the same criteria as the discovery cohort. DNA was extracted using the same protocol as described for the discovery cohort samples.

Table 4.2 Demographic and clinical characteristics of the validation cohort

Variables	aCA (n=42)	Non-aCA (n=36)	*p* value
Maternal age, years (mean)	21-44 (32)	17-43 (29.27)	<0.03
GA at delivery, weeks (mean)	20-41 (26.83)	20-39 (29.2)	<0.02
Birth weight (SD)	-2.24-1.23	-3.13-1.67	ns
Fetal sex (M/total)	24/42	21/36	ns

*p-values are calculated by Wilcoxon-Mann-Whitney rank sum test for continuous variables, Fisher's exact test for fetal sex. ns = non-significant

4.2.2 Illumina Infinium HumanMethylationEPIC BeadChip quality control and pre-processing

Chorionic villi (n=44), amnion (n=16), and chorion (n=16) from the discovery cohort samples were run on the 850K array, which quantifies DNAme at 866,895 CpG sites across the genome (204). To minimize technical effects of sample processing, all samples were run in the same batch and by the same operators, and 4 samples were run in duplicate to assess data processing. See Supplementary Figure 4.1 to view distribution of samples across chips.

The discovery cohort genomic DNA was purified using DNeasy blood and tissue kit (Qiagen, CA, USA) followed by bisulfite conversion of the purified DNA using the Zymo EZ DNA Methylation^{TM} Kit (Zymo Research, USA). Bisulfite converted DNA was then whole-genome amplified, enzymatically fragmented, and hybridized to the array as per the 850K array protocol (204). Chips were scanned using an Illumina HiScan2000 and raw intensity was read into GenomeStudio Software (Illumina). Within Genome Studio samples were background normalized, after which data was read into R statistical software (version 3.4.1) with the Bioconductor *lumi* (329) package to generate M values from the signal intensities.

An initial sample quality control (QC) check was performed in GenomeStudio using Illumina's 636 control probes to assess technical parameters including array staining, extension, hybridization, target removal, specificity, and bisulfite conversion. Clustering of samples based on all probes confirmed tissue identity except for one amnion and one chorion sample which were likely tissue label swaps as they were from the same placenta and clustered with the wrong fetal membrane tissue group. The samples were reassigned labels and were kept in for the remainder of the analysis. One amnion sample clustered further away from the amnion group as seen in hierarchical clustering and PCA (Supplementary Figure 4.2a and 4.2b) and was removed from the analysis as it is likely this is due to either poor DNA quality or a contaminated sample. Sample quality was further assessed as in Price *et al.* (2016) (330) and no other sample was excluded from the analysis.

After initial QC, 44 placental chorionic villi, 16 chorion, and 15 amnion samples were identified for the aCA analysis. Further analysis was conducted independently for the three tissues. Probe filtering was performed as shown in Table S3 in Additional file 1 (331-333). To account for type I- type II probe differences on the 850K array, functional normalization (249) was done. *ComBat* (246) was used to correct for known technical variation associated with Sentrix_row (chip position) and Sentrix_Id (chip Id). Correlation of the technical replicates in chorionic villi improved from the raw data to batch corrected cleaned data (Supplementary Figure 4.3). Because there were no technical replicates for amnion and chorion, performance metrics in R *wateRmelon* package (334) were used to monitor data preprocessing for the fetal membranes.

4.2.3 Differential methylation analysis of acute chorioamnionitis data

To identify differential methylation associated with aCA, we first used a candidate gene approach. Genes of interest (n=12) were chosen based on publications reporting a genetic association with chorioamnionitis (288-290), placental inflammation (116, 119), and neonatal sepsis/infection (176, 291, 292). CpG sites from the 850K array that mapped to these genes were then identified (195 CpG sites, Table S4 in Additional file 1). Using this set of biologically-relevant CpGs, we modelled DNAme as a function of aCA status with GA, fetal sex, and ancestry were included as additive covariates. Subsequently, an epigenome-wide association study (EWAS) was conducted using the batch corrected cleaned data (711789 CpG sites). To account for multiple tests, the resulting *p*-values were adjusted using the Benjamini and Hochberg (335) false detection rate (FDR) method. Group differences in DNAme ($\Delta\beta$) were then calculated by subtracting the average beta (β) of non-aCA cases from aCA cases on an individual CpG site basis. Differentially methylated sites associated with aCA were identified based on FDR and $\Delta\beta$ thresholds. Using similar thresholds, sites identified in the chorionic villi were also examined in the chorion and amnion samples and the overlap of the chorionic villi sites in chorion and/or amnion was confirmed by a random sampling function as described in Wilson et al. (2018) (293). Finally, *dmrFind* function in the R *charm* package was used to find differentially methylated regions (DMR) (336), as described in (330).

4.2.4 Pyrosequencing

We performed pyrosequencing (PyromarkTM Q96 MD pyrosequencer, Qiagen) for some of the CpG sites identified as DM in the 850K array comparison of aCA cases and non-aCA cases. Genomic DNA was bisulfite converted using the EZ DNA methylation Gold kit (Zymo,

USA) as per manufacturer's protocol. PyroMark Assay Design software version 2.0 was used to design the forward, reverse, and sequencing primers. Primer sequences and reaction conditions for all pyrosequencing assays are listed in Supplementary Figure 4.4. For quality control, synthetic fully methylated and unmethylated samples (standard controls) were included on each plate. PyroMark Q-CpG software (Qiagen) was used to generate quantitative methylation levels of the targeted CpG of interest. Spearman's rank order correlation was used to illustrate agreement between the 850K array findings and pyrosequencing data. A linear model was fitted for each follow up CpG site, with aCA status as main effect and GA, fetal sex, and ancestry as covariates.

4.2.5 Correlation analysis and differential methylation analysis on matched tissue dataset

To address the overlap between differential methylation for different tissues, it is useful to understand patterns of correlation across our three aCA-associated tissues (chorionic villi, chorion, amnion). To do this, we utilized the strength of our matched sample cohort of 15 individuals. Data pre-processing of the matched tissue cohort was performed as described in Supplementary Methods 4.1. Correlation of DNAme on a per CpG level was calculated between chorionic villi and the fetal membranes independently using Spearman rank-order correlation on M values. Adopting a similar approach from (333), we generated a null distribution of correlations by shuffling the order of the chorionic villus samples and ran the correlations calculations with each fetal membrane. Comparing against the null distribution allowed us to confirm whether the correlated sites between chorionic villi and fetal membranes were significantly more than what we would expect by chance.

To quantify the similarity between fetal membranes and placental chorionic villi, differential DNAme analysis on a per CpG level was also performed between the tissue pairs

(chorionic villi-chorion and chorionic villi-amnion) by applying a linear model to M values using *limma* (337). This is described in detail in Supplementary Methods 4.2, and Supplementary Table 4.1.

4.2.6 Immune cell-type analysis on the acute chorioamnionitis dataset

Because we hypothesized that altered DNAme exhibited by aCA-associated placentas might reflect an increase in the number of immune cells, we anticipated that the aCA cases and immune cell types might follow similar trends in DNAme for the DM sites identified in our EWAS analysis. To test this, we first utilized a publicly available dataset assessing DNAme in blood immune cell types isolated from six healthy adults (338). These samples had been run on the 450K array, measuring DNAme at 485,512 CpG sites across the genome (295), 93.3% of which overlap the 850K array used in the present study. Beta value distributions of DM sites were compared across aCA cases and the blood immune cell types to identify concordance in DNAme patterns.

To identify immune cell-type specific DNAme, we used the previously described publicly available dataset (338), and also included 30 chorionic villi controls from two published studies in our lab (293, 339). Similar site filtering criteria were adopted as described previously in Supplementary Table 4.2. To identify neutrophil-specific CpG sites, we first performed differential methylation analyses for the following comparisons: i) neutrophils - chorionic villi, ii) neutrophils - eosinophils, iii) neutrophils - monocytes, and iv) neutrophils - lymphoid lineage cells (T cell + B cells + Natural Killer cells), using linear modelling on filtered and normalized data (442495 CpGs). We next identified overlapping DM CpG sites between the above comparisons to determine neutrophil-specific CpG sites. This procedure was also used to identify

eosinophil-specific CpG sites, monocyte-specific CpG sites, and lymphoid lineage-specific CpG sites. Finally, these immune cell type-specific CpG sites were used to cluster the chorionic villus samples in the discovery cohort. Stability of the resulting clusters was determined using the R package *pvclust* (340) and the R *sigClust2* package (341) was used to assess if the resulting clusters were significantly different from one another, both using 1000 iterations.

4.3 Results

4.3.1 Characterization of unique aCA associated DNA methylation changes in chorionic villi and fetal membranes

To investigate differences in DNAme between aCA cases and non-aCA cases, we fitted a linear model testing for differential methylation in each of the three tissues in the discovery cohort; chorionic villi (22 aCA, 22 non-aCA), amnion (8 aCA, 7 non-aCA), and chorion (9 aCA, 7 non-aCA). We first looked at DNAme in a subset of 12 genes that might be biologically relevant to aCA (Supplementary Table 4.3). CpG sites from the DNAme array that mapped to these candidate genes were not DM between aCA cases and non-aCA cases. Next, using an epigenome-wide approach, no sites were identified as DM in amnion or chorion, but 66 sites were DM in chorionic villi (FDR <0.15 and $\Delta\beta$ >0.05) (Figure 4.2). Detailed descriptions of these sites are provided in Supplementary Table 4.4. We chose less stringent statistical cutoffs here as our small sample size may limit our ability to detect significant DNAme differences at individual CpG sites. Hierarchical clustering of chorionic villus samples using these 66 DM CpG sites completely separated the aCA cases from the non-aCA cases (Supplementary Figure 4.5). Although not significantly enriched for any gene ontology terms using ermineJ (342), some of the DM sites were located within immune-relevant genes such as *HLA-E, CXCL14, RAB27A,*

IRX2, and HSD11B2. Each of these DM CpG sites were located 200-1500 base pairs up-stream of the transcription start site.

We also tested for differences in DNAme across regions (i.e., DMRs) to integrate information across neighbouring CpGs. This reduces the number of statistical tests, potentially increasing the power to detect a DNAme change. However, none of the DMRs withstood correction for multiple tests in each of the three tissues (chorionic villi, chorion, and amnion).

Male fetuses are at an increased risk of PTB (343, 344) and are more likely to show adverse outcomes including chronic inflammation, respiratory distress syndrome, neonatal sepsis, infection, and stillbirth (345-348). To identify whether there may be sex-specific DNAme changes associated with placental inflammation, we repeated the EWAS analysis on male and female chorionic villus samples separately. We fitted a linear model testing for differential methylation in the discovery cohort of chorionic villus samples, analyzing males (11 aCA, 13 non-aCA) and females (11 aCA, 9 non-aCA) separately. None of the 711,789 CpG sites was DM between aCA cases and non-aCA cases in males or females (FDR <0.15 and $\Delta\beta$ >0.05) (Supplementary Figure 4.6). However, our ability to characterize sex-specific significant differences at individual CpGs is limited by the small sample sizes.

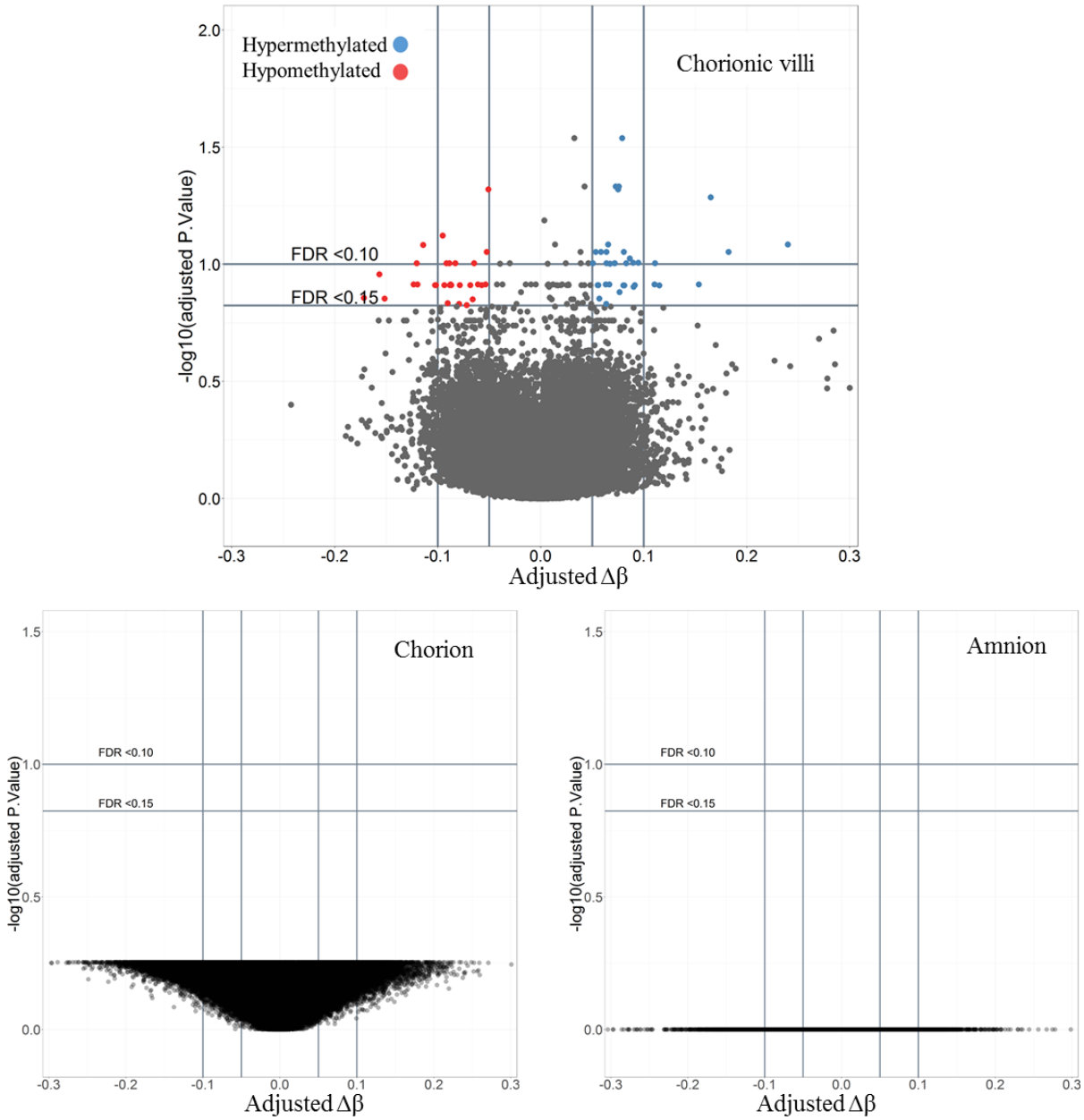

Figure 4.2 Acute chorioamnionitis array-wide volcano plots.

For each probe, FDR corrected p-values from fitted linear models were plotted against group differences in DNAme for each tissues. Sites at FDR <0.15 and adjusted Δβ >0.05 are highlighted in red and blue. Sites highlighted in red are those that are hypermethylated in aCA cases compared to non-aCA cases. Sites highlighted in blue are those that are hypomethylated aCA cases compared to non-aCA cases. The flat volcano plots demonstrate a lack of differential methylation associated with aCA in the fetal membranes after correction for multiple comparisons.

4.3.2 Pyrosequencing validation of aCA-associated differentially methylated sites

To verify our array-wide findings, we performed pyrosequencing on three of the DM CpG sites (cg01276475, cg11340524, and cg21962324) in chorionic villi in the discovery cohort (22 aCA cases, 22 non-aCA cases) and in an additional set of 42 aCA and 36 non-aCA cases (i.e., validation cohort). One CpG site, cg01276475 (*RIMS1*) was chosen as it showed highest magnitude of methylation difference ($\Delta\beta > 0.20$) between the groups in the discovery cohort. The other two sites (cg11340524, *RAB27A*; cg21962324, *IRX2*) were chosen to follow-up based on functional relevance in immune system and inflammation, which may be of interest in aCA. DNAme measured by pyrosequencing was significantly correlated with the 850K array data at all three CpG sites (cg01276475, r=0.8 (p<2.2e-16); cg21962324, r=0.8 (p<2.2e-16); cg11340524, r=0.7 (p<1.322e-07)) and was verified in the discovery cohort (p<0.003). Furthermore, the differences at these three CpG sites also replicated in the validation cohort (p<0.01) (Figure 4.3).

Next, we tested for differential methylation at the three selected CpG sites in males and females separately, as correcting for a large number of CpG sites may have limited our power to detect array-wide sex-specific DNAme differences between our study groups. The three DM CpG sites showed a DNAme trend in the same direction in both males and females as observed in the discovery cohort and validation cohort chorionic villus samples (Supplementary Figure 4.7). For these selected CpG sites, we also assessed variation in DNAme between fetal sexes over gestation. Though we failed to observe a significant difference in DNAme between the sexes, we did however, observe sex-specific trends in DNAme across gestation for cg21962324 (*IRX2)* and cg01276475 (*RIMS1*) (Supplementary Figure 4.8).

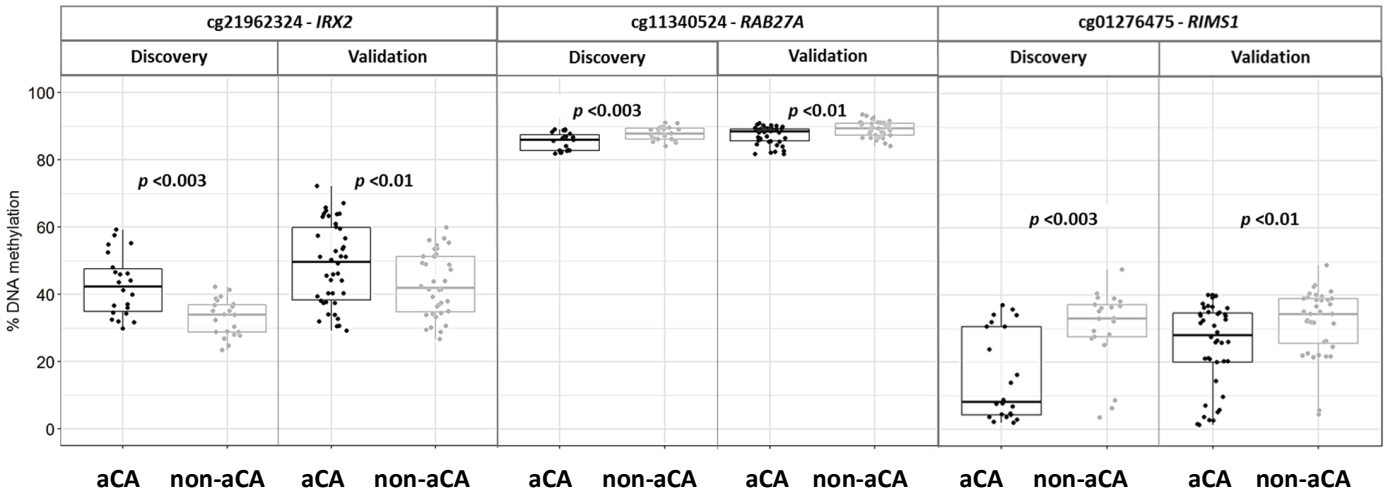

Figure 4.3 Pyrosequencing of cg11340524, cg21962324, and cg01276475 in chorionic villi.

Pyrosequencing was performed to follow up differential methylation at three CpG sites (cg11340524, cg21962324, and cg01276475), identified in the chorionic villus samples in discovery cohort. We confirmed significant differential DNAme in the discovery cohort ($p < 0.003$) and replicated in the independent set of samples (i.e, validation cohort) ($p < 0.01$).

4.3.3 Characterization of common aCA-associated DNA methylation changes between chorionic villi and fetal membranes

DNAme patterns vary widely by tissue type (198, 199). Because chorionic villi and chorion are considered to partially share a similar trophectoderm-derived cell lineage (339), we predicted that changes in response to inflammation specific to the trophoblast lineage might create more overlap in aCA-associated DNAme changes between chorionic villi and chorion than compared to amnion. We first confirmed that the genome-wide DNAme profile of chorionic villi is more correlated to chorion than amnion (Supplementary Figure 4.9). Next, we compared the DNAme landscapes of chorionic villi to the fetal membranes by a differential DNAme analysis. To enrich for tissue-specific DNAme differences, we adopted strict statistical (FDR <0.01) and biological thresholds ($\Delta\beta > 0.20$); and identified more DM sites when comparing

chorionic villi to amnion than when comparing chorionic villi to chorion (Supplementary Figure 4.10). We then used the 66 DM sites in chorionic villi, and fitted a linear model to test for similar changes in DNAme at these sites in the chorion and/or amnion. At the same thresholds (FDR <0.15 and $\Delta\beta$ >0.05), no sites were DM in amnion, while ~20% (13/66) of chorionic villi sites were also DM in chorion, higher than expected by chance (p=0.0001).

4.3.4 Characterization of immune cell-types in aCA-associated placentas

We hypothesized that some of the aCA-associated DNAme changes captured by the 850K array could be attributable to an increase in immune cell number especially neutrophils, during placental inflammation. Therefore, we expected the 66 DM sites associated with aCA in chorionic villi may trend in the same direction as immune cell types. DNAme data for neutrophils, eosinophils, monocytes, lymphoid cells and whole blood were obtained from GEO (GSE35069). As this data was run on a previous version of the Illumina array, the 450K array, only data for 36 of our 66 DM sites was available. We compared the β value distributions of 36/66 DM sites available in GSE35069 for each immune cell type to our data. Taking neutrophils as an example, 24/36 (66.6%) DM sites showed a similar trend in DNAme to the aCA cases versus non-aCA cases, which is higher than what we would expect by chance (p=0.00001). This pattern was also observed across all the other immune cell types including whole blood, suggesting that the DNAme profile of the aCA cases may be more shifted in the direction of blood immune cell type than a non-aCA associated placenta (Figure 4.4).

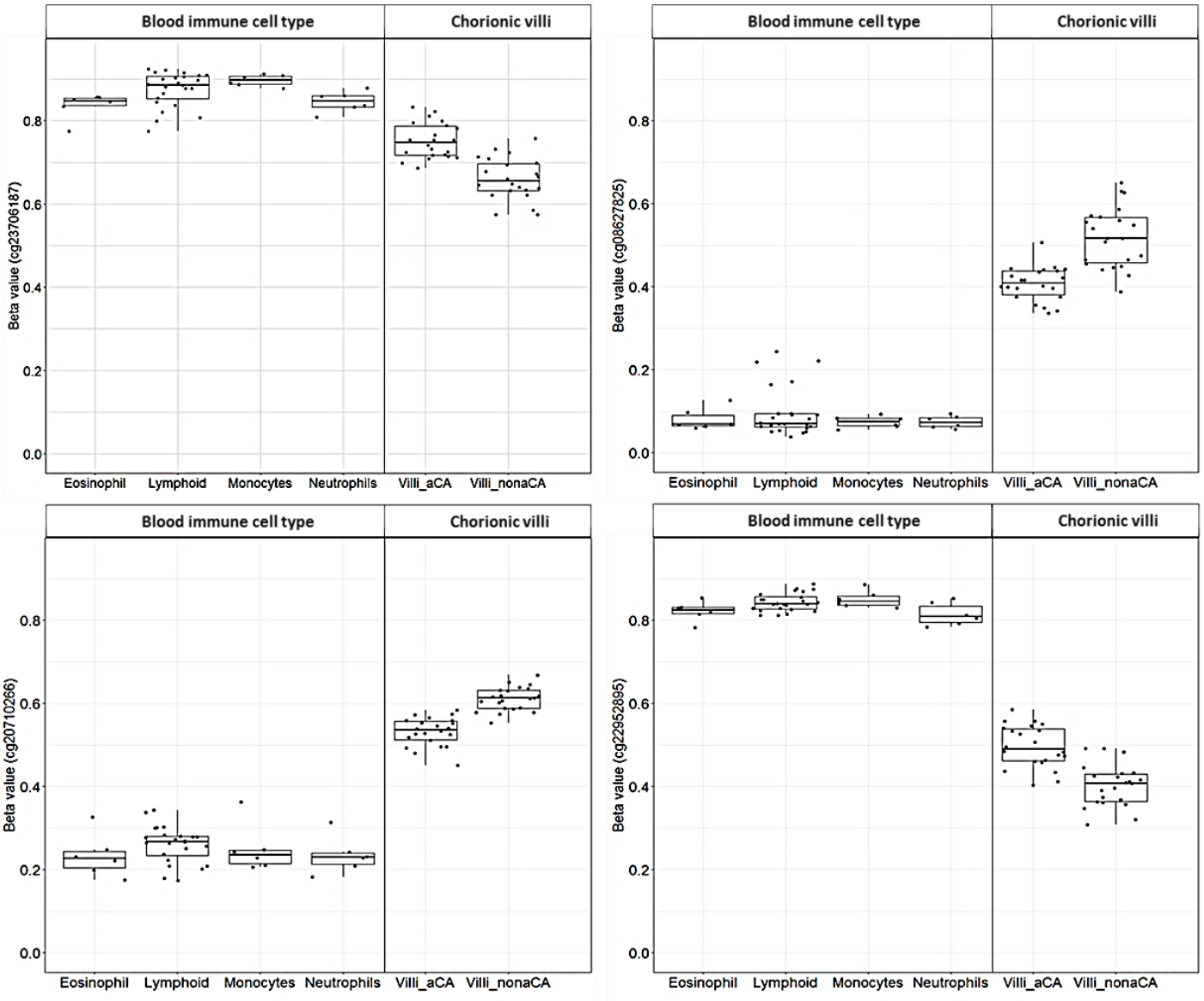

Figure 4.4. Differentially methylated CpG sites in the chorionic villi comparison of aCA cases to non-aCA cases.

Box plots of DNAme for four representative CpGs sites that are either hypermethylated or hypomethylated in the aCA cases compared to non-aCA cases in chorionic villi. These sites are among 24/36 sites that showed similar trends in DNAme for the the multiple immune cell types (eosinophil, neutrophil, monocytes, and lymphoid) as aCA chorionic villi cases. For example, when aCA cases were hypomethylated compared to non-aCA cases, immune cells were also hypomethylated compared to non-aCA.

Next, we sought to detect if there was a specific immune cell-type more likely to be linked to aCA-associated placentas. We identified immune cell type-specific CpG sites using this same data by a differential methylation analysis (see Methods). Unsupervised hierarchical clustering was performed in the discovery cohort of chorionic villus samples using these immune cell-type specific CpGs. Neutrophil-specific sites (2069 CpGs) produced two stable and significantly different clusters (Fisher's test, $p<0.005$) which separated most aCA cases from the non-aCA cases (Figure 4.5), while the same analysis using eosinophils, monocytes, lymphoid lineage specific-sites did not yield stable clusters. No other differences were observed between the two neutrophil-specific clusters based on the available clinical information (Table 4.3). Neutrophil-specific cluster 1 was significantly enriched for aCA cases ($p<0.005$), suggestive of a "placental inflammation-mediated" phenotype in this group. Neutrophil-specific cluster 2 consisted predominantly of non-aCA cases. Although two sub-clusters were observed in this latter group; the sub-clusters were not stable as determined by multi-scale bootstrap resampling (1,000 permutations).

Table 4.3. Clinical information on samples assigned to cluster 1 and cluster 2 obtained by neutrophil-specific CpGs.

Neutrophil-specific	Cluster 1 (n=22)	Cluster 2 (n=20)	*p* value*
aCA status (aCA/total)	17/22	5/20	<0.005
Fetal sex (M/total)	15/24	9/20	ns
Gestational age, weeks	28.3-36	28-36.7	ns
Maternal age, years	21.2-43.9	20.4-43.5	ns
Fetal birth weight (SD)	-1.14-1.58	-2.46-0.73	ns

**p*-values are calculated by Wilcoxon-Mann-Whitney rank sum test for continuous variables, Fisher's exact test for fetal sex and aCA status. ns = non-significant

Because we did not observe an overlap of DM CpG sites between the 66 DM aCA-associated CpGs and the neutrophil-specific CpGs, the later may manifest as subtle changes that do not meet our criteria of $\Delta\beta>0.05$. It is also likely that some of the stronger aCA-associated DNAme changes might reflect alterations in cell populations inherent to the placenta such as Hofbauer cells, trophoblasts, and/or endothelial cells or to changes in gene expression, within some of those cell types. However, it is important to note that the 66 DM CpGs were identified using the 850K array whereas the neutrophil-specific CpGs were characterized using the 450K array, and only 36/66 DM sites were common between the arrays. Additionally, different statistical and biological thresholds were used to identify the 66 DM CpGs and the neutrophil-specific CpGs, which could explain the lack of an overlap between the CpG sites.

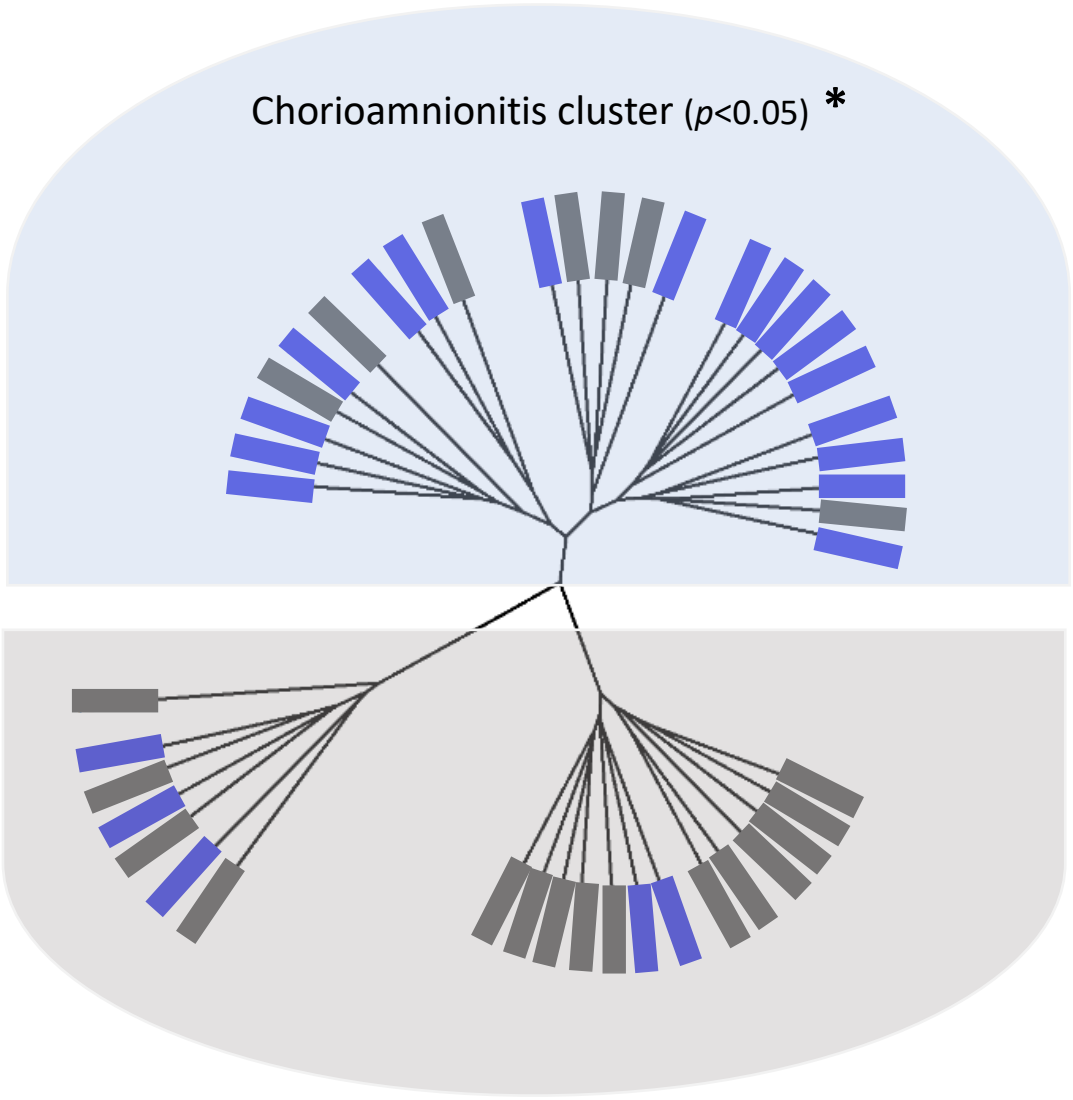

Figure 4.5. Sample clustering based on array-wide neutrophil-specific CpG sites.

Euclidean clustering of our chorionic villi DNA methylation data (n=44 samples) using 2069 neutrophil-specific CpG sites largely separated aCA cases from the non-aCA cases. ***** indicates stable and significantly different clusters as determined by pvclust and sigclust2 packages. Blue labels, aCA. Gray labels, non-aCA.

4.4 Discussion

To our knowledge, this is the first study to investigate genome-wide aCA-associated DNAme alterations in the placenta and fetal membranes. Our EWAS identified 66 DM CpG sites (FDR <0.15 and $\Delta\beta$ >0.05) associated with aCA in chorionic villi. Amongst the 66 were a number of CpGs located in inflammation-related genes including *HLA-E, CXCL14, RAB27A, IRX2, and HSD11B2*. Expression of *HLA-E* molecules in extravillous trophoblast cells of the placenta inhibits the cytotoxic activity of maternal natural killer cells, resulting in immune tolerance to the fetus during pregnancy (349). *CXCL14* is highly expressed in the placental trophoblasts and shown to regulate trophoblast invasion during pregnancy (350). This chemokine acts as a selective chemoattractant for dendritic cells, monocytes, NK cells, and neutrophils, and facilitates leukocyte recruitment under different pathophysiological conditions (351, 352). Furthermore, decreased expression of *CXCL14* was reported in spontaneous PTB placentas (223). *RAB27A* plays a vital role in the regulation of multiple neutrophil functions such as chemotaxis, adhesion to activated surfaces, and exocytosis of granules with anti-microbial properties (353). Transcription factor *IRX2* has been shown to control chemokine expression in breast cancer cells (354). *HSD11B2*, on the other hand, is regulated by pro-inflammatory cytokines and may influence the inflammatory microenvironment (355). Additionally, decreased expression of *HSD11B2* in chorioamnionitis-affected placentas has been reported (356). Overall, our DNAme EWAS study provides an improved understanding of epigenetic changes that occur during placental inflammation, which is an important precursor for developing markers for earlier clinical diagnosis of aCA.

Currently, clinical examination is the routinely used method for diagnosing aCA, but assessment of clinical signs is neither sensitive nor specific. Histologic examination of the placenta is more sensitive and specific for identifying aCA but is only possible after delivery. There has been some promise in utilizing maternal serum biomarkers to predict placental inflammatory responses, including C-reactive protein and cytokines (357-359). However, conflicting reviews on the clinical utility of these maternal serum markers raises concerns on their reliability, sensitivity, and specificity (360-362). Limited studies have identified altered gene expression in candidates such as *TLRs*, and *CXCLs* in chorioamnionitis-affected placentas (225, 226, 236, 363). Some of these inflammation-related mRNA changes were also observed during normal spontaneous labor (228), and therefore may not represent unique mRNA changes in placental inflammation.

DNA methylation is associated with gene expression, but is relatively stable, and more likely to retain a "memory" of earlier *in utero* exposures. In our study, we were successful in confirming some of our array-wide DNAme findings by an alternate technology and validating these DNAme results in an independent set of samples. These DNAme alterations may be useful in the development of biomarkers for rapid prenatal detection of aCA if they are also detectable in maternal blood (70), as has been shown for other conditions including cancer (364-367) and PE (368, 369). However, the aCA-associated DNAme changes reported in this study were small in magnitude and may require highly sensitive detection methods. On the other hand, a subset of aCA-affected placentas may exhibit larger DNAme changes due to increased severity of the inflammatory processes associated with aCA. It is also important to recognize that the distribution of inflammatory lesions associated with aCA is heterogeneous across the placenta,

and depending on the sampling site, changes in DNAme will likely vary from subtle to large effects.

In recent years, there has been increasing interest in DNAme EWAS studies about "cell type correction". Differences in DNAme identified using whole tissue samples, such as chorionic villi may represent a change in DNAme limited to one cell type or suggest a difference in the proportion of cell types between disease groups. These differences in cell type proportions are often thought to be a confounding influence and thus variance due to altered cell type proportions is removed using computational approaches (370). In some conditions, such as in aCA, alterations in cell type proportions may be biologically relevant to the disease pathogenesis, and therefore adjusting for cell composition will significantly reduce the variability due to the pathology, as discussed by Lappalainen and Greally (2017) (183). Numerous studies have documented aCA-associated cellular changes primarily in the context of a microbial invasion that ascends from the lower genital tract. Invasion of the amniotic cavity stimulates a strong inflammatory response in the mother and fetus, and an increase in the concentrations of proinflammatory cytokines can be detected in the amniotic fluid (132, 133, 371). In response to this chemotactic gradient, maternal neutrophils migrate towards the chorionic plate of the placenta. Additionally, placental tissue from cases of aCA exhibit alterations in the number of placental-specific macrophages called Hofbauer cells (23, 24). Placental trophoblasts also mount a specific innate immune response in the presence of a microbial infection (93-95). In our study, we identified DNAme changes associated with aCA which likely reflect an increase in immune cell number such as neutrophils and/or represent changes in placental cell populations as a response to inflammation, such as increased secretion of *IL8* by placental trophoblasts reported during chorioamnionitis (96). It is possible that some of the DNAme changes occurring in the

placental trophoblasts could overlap with the neutrophil-specific changes as these are also a part of the innate immune system. Further, we identified some common aCA-associated DNAme changes between chorionic villi and chorion, and none of the DNAme changes overlapped between chorionic villi and amnion. Because chorionic villi and chorion share a similar trophectoderm-derived cell lineage, the overlapping DNAme changes in these two tissues may reflect similar epigenetic response to aCA-associated inflammation. Further, shared changes between chorionic villi and chorion could also result from a similar alteration in immune cell ratios in chorionic villi and chorion.

We utilized a subset of our matched samples to gain a comprehensive understanding of DNAme landscapes in the placenta and fetal membranes. Our group previously reported on genome-wide tissue-specific DNAme patterns in the placenta, and fetal membranes (207). However, the present study included a larger sample size and matched tissue samples. The DNAme landscape of chorionic villi was more similar to chorion than amnion, possibly because the ectodermal layer of chorion and the outer trophoblast layer of the chorionic villi are both derived from the trophectoderm. In contrast, similarities between chorion and amnion may also occur as the mesenchyme layers of both the chorion and amnion membranes have a common origin from the epiblast.

Our findings should be interpreted within the context of a few inherent limitations. First, our sample size was relatively small which limited power; hence the findings of this study should be replicated in an independent population. It is also important to acknowledge that bisulfite conversion-dependent techniques (850K array and pyrosequencing) cannot distinguish been the canonical 5-methylcytosine mark from its oxidized derivative 5-hmc, though 5-hmC values tend to be low in placenta (190). Although pathological examination confirms that the non-aCA

preterm samples used in this study were not associated with aCA and/or placental inflammation, it is rarely possible to obtain "normal" placentas from 21-37 weeks. Often other placental findings were noted in our non-aCA cases, including placental abruption, spontaneous premature rupture of the membranes, preterm labor, and placenta previa. Multiple etiologies in the non-aCA preterm cases were included to obtain a heterogeneous control population and therefore reduce the likelihood of an association with any given etiology in the non-aCA preterm cases. In addition, though the range of GA overlapped between the aCA and the non-aCA cases, the aCA cases were significantly lower in GA than the non-aCA cases. This is expected, as aCA is associated with preterm birth and therefore the aCA cases were <37 weeks GA. Because GA-dependent DNAme patterns are observed in the placenta (17), GA was included as an additive covariate in our statistical models. Finally, though aCA is mainly characterized by neutrophil infiltration into the chorioamniotic membranes (9), cellular changes in multiple other cell types including but not limited to Hofbauer cells or trophoblasts, are also observed in aCA (10). To fully understand the DNAme variation in aCA-affected placentas, it will be important to study changes in these specific cell populations.

Chapter 5: Altered expression levels of miR-338 and miR-518b is associated with acute chorioamnionitis and *IL6* genotype

5.1 Background

Histologic evidence of inflammation in the placenta, fetal membranes, and umbilical cord is commonly observed in PTB cases (143, 145). This often presents as aCA, defined by an infiltration of maternal neutrophils into the fetal membranes (9, 10), and can also involve the chorionic villous trees (326). Quantification of markers circulating in maternal blood, such as miRNAs, offer great promise as biomarkers for a number of pregnancy outcomes as they are more stable than mRNA and are readily quantifiable in maternal circulation (372).

Small non-coding RNAs such as miRNAs are small ~22 nucleotide, single-stranded RNA molecules which are largely involved in post-transcriptional gene regulation via repressive interactions with their mRNA targets (373, 374). Evidence from various mammalian systems has revealed that the expression patterns of certain miRNA families are highly dependent on tissue type (375, 376). For example, the human placenta has a distinct miRNA profile, largely originating from 2 large miRNA clusters on chromosomes 14 (C14MC), 19 (C19MC), and 2 relatively smaller miRNA clusters on chromosome 13 (miR-17-92) and 19 (miR-371-3) (377, 378). It is now well established that such specific miRNAs produced by the human placenta can be detected in maternal plasma as a result of placental shedding and active secretion (379). Concentrations of placental-specific miRNAs increase in the maternal plasma as pregnancy progresses and return to normal levels after delivery (372).

Aberrant expression of several placental-derived miRNAs in PE-associated placentas has been reported, though there is little reproducibility across these studies (380). The low rate of

reproducibility may be attributed to a number of factors, such as lack of standardized procedures for tissue sampling and case-control ascertainment, differences in study population structure, variable gestational age cut-offs, and other potential confounding factors. While there is an increasing interest in researching placental-specific miRNAs in PE, few investigators have studied placental miRNA changes associated with pregnancies complicated by PTB (94, 233, 234, 236, 381, 382). Importantly, researchers often combine different PTB-linked conditions and do not focus on a specific PTB-related complication such as aCA.

aCA may result from a combination of maternal health exposures, genetic susceptibility, and/or *in utero* exposures to microbes (30, 383). In the context of a microbial infection, alterations in immune cell populations have been reported in aCA (9, 24). Further, trophoblasts in the placenta are capable of eliciting an immune response against a microbial infection (384). Immune cell-type specific changes that occur during aCA may be reflected in altered miRNA profiles, thus quantifying miRNAs in the placentas may be a useful approach to characterize some of these cellular changes associated with inflammation in aCA-affected placentas. To explore this, we sought to investigate the association of aCA with six inflammation-related miRNAs in a population of 57 placentas (33 aCA, 24 non-aCA).

5.2 Methods

5.2.1 Study cohort

To investigate aCA specific miRNA changes in the placenta, a total of 57 placentas were used. Of these, 33 aCA cases were selected based on a diagnosis of aCA determined by histological examination of the placenta and fetal membranes (9) and 24 non-aCA cases were selected to span the same GA and included 17 PTBs of mixed etiologies (incompetent cervix,

premature rupture of membranes, and placental abruption) and 7 term controls. Because this cohort was utilized to investigate miRNA changes in aCA-affected placentas, we excluded placentas with fetal and/or placental chromosomal abnormalities, fetal malformations, congenital abnormalities, and placentas with other PTB-related conditions (PE, IUGR, and hypertension). A subset of this study cohort (n=32) is also described in our recent publication on placental DNAme in aCA (GSE115508) (213).

Demographic and clinical case characteristics of this cohort are presented in Table 5.1. As expected, GA at delivery was significantly different between the groups, as aCA is associated with preterm deliveries.

Table 5.1 Demographic and clinical characteristics of the discovery cohort

Variables	aCA (n=33)	Non-aCA (n=24)	*p* value
Maternal age, years (range)	19.6-43.9	19.6-43.9	ns
GA at delivery, weeks (range)	18-36	22.6-40.7	0.0009
Birth weight (SD) (range)	-0.89-3.49	-1.36-3.1	ns
Fetal sex (M/total)	16/33	13/24	ns

**p*-values are calculated by Wilcoxon-Mann-Whitney rank sum test for continuous variables, Fisher's exact test for fetal sex. ns = non-significant.

Ancestry was described as a continuous measure using the top three coordinates derived from a MDS analysis (See Chapter 2, Section 2.6). Ancestry MDS coordinate 1, which largely separates Europeans and East Asians, was significantly different between aCA and non-aCA groups ($p<0.05$). Distribution of the ancestry MDS coordinates were assesses by a KS test. As the influence of such confounding factors on miRNA expression has been well-demonstrated (385, 386), both GA and ancestry were accounted for in statistical analyses.

5.2.2 miRNA candidate selection

In this study, six inflammation-related candidate miRNA species (miR-223, miR-338-3p, miR-518b, miR-146a, miR-441, and miR-210) were investigated. miR-518b, a member of the C19MC cluster, was chosen as it has been frequently associated with various reproductive pathologies including PE, gestational hypertension, PPROM, and spontaneous PTB (233, 387-389). miR-223 and miR-338 were selected based on published findings of an association with aCA in chorioamniotic membranes (235). Increased expression of miR-223 was demonstrated in aCA-affected fetal organs including lung, liver, and thymus (390). Immune cells, particularly granulocytes exhibit higher expression of miR-223, and altered expression of miR-223 has been reported in inflammatory disorders such as rheumatoid arthritis, obesity, and infection-mediated conditions (391). In the context of inflammation, miR-338 has been shown to enhance immune-specific responses, specifically by promoting the secretion of interleukins such as *IL-1a*, and *IL-6* (392). Similarly, miR-210 regulates the production of proinflammatory cytokines (393), and altered miR-210 expression levels are often associated with pathogen-mediated events (394, 395). Both miR-210 and miR-411 are also linked to PTB-related complications (234, 388), particularly PE (16). In addition, miR-411 expression levels in immune cells such as macrophages are altered upon inflammatory stimuli (396). Finally, the role of mir-146a in inflammation-mediated responses is well-established in tissues other than the placenta (397-399), making mir-146a an important candidate to investigate in our inflammation-associated aCA placentas.

5.2.3 RNA extraction

Total RNA was extracted from 50 mg of *RNAlater* fixed chorionic villi samples followed by an enrichment procedure for small RNAs, using the *mirVana*™ miRNA Isolation Kit (Ambion), as per manufacturer's protocol. Briefly, the cell lysis and tissue disruption protocol for frozen tissue was adopted, followed by the organic extraction step and the enrichment procedure for small RNAs. Chorionic villi samples were eluted in 50ul of water at 95°C. An exogenous plant-based spike-in control, ath-miR-159a, was added to all the samples to monitor inter-sample technical variability. Concentration and quality of the extracted miRNA samples were assessed using a Nanodrop 1000 spectrophotometer (ThermoScientific, USA). For relative miRNA quantification, the extracted miRNA samples from chorionic villi were equalized to 10ng/ul.

5.2.4 Reverse transcription (RT) and quantitative real-time PCR (qPCR)

In the RT step, complementary DNA (cDNA) is reverse transcribed from total miRNA using a stem-loop RT primer which is specific for the mature miRNA target. This is followed by a qPCR step where PCR products are amplified from 15ul of cDNA samples using specific *TaqMan*™ miRNA Assays.

In this study, RT and qPCR were performed simultaneously in two batches of samples. The first batch comprised of the 57 chorionic villus samples (33 aCA, 24 non-aCA) selected to investigate aCA-associated miRNA changes. cDNA was synthesized for the six candidate miRNAs (miR-223, miR-338-3p, miR-518b, miR-146a, miR-441, and miR-210), two endogenous controls (miR-92a, RNU48), and one exogenous control (ath-miR-159a), followed by the qPCR step. While we evaluated multiple endogenous controls for this study, *Normfinder*

(400) identified miR-92a as the optimal endogenous control for chorionic villus samples (Supplementary Figure 5.1). A detailed description on the selection of an endogenous control is provided in Supplementary Methods 5.1. Non-template negative controls were incorporated to detect non-specific amplification. All qPCR reactions were performed in duplicate and run on the ABI ViiA7 system (Applied Biosystems, Foster City, CA).

Data obtained from the ABI ViiA7 system was entered into the Expression Suite Software (Version 1.1) to calculate the expression values for the individual miRNAs. Expression was calculated from a C_q (quantification cycle) value which may be defined as the minimum number of cycles needed to obtain a reliable fluorescent signal distinguishable from the background. Relative expression of the miRNAs was then determined using the $\Delta\Delta C_q$ method (401) and was automatically calculated by the Expression Suite Software.

5.2.5 Target gene prediction and pathway analysis

To investigate the functional effects of the aCA-associated differentially expressed miRNAs, we first sought to identify potential miRNA targets using two publicly available tools (*TargetScan* (402) and *miRDB* (403)) and subsequently performed a gene set enrichment analysis using the *Molecular Signatures Database* (*MSigDB*) (404) to reveal biological pathways and molecular processes involved in aCA.

5.2.6 DNA methylation data and *IL6* genotype data

To investigate whether miRNA-related CpGs were differentially methylated between aCA cases and non-aCA cases, we used our previously obtained DNAme microarray data that was available for a subset of the 57 chorionic villus samples (n=32/57) (GSE115508) (213). CpG sites from the 850K array (204) that mapped to the specific miRNA candidates were identified

using Illumina's annotation, and subsequently tested to identify whether they were differentially methylated between aCA cases (n=19) and non-aCA cases (n=13). Additionally, we used our *IL6* genotype (rs1800796) data available for another subset of the chorionic villus samples (n=48/57) to characterize genetic regulation of miRNA expression (Chapter 3).

5.2.7 Statistical analyses

All statistical analyses were performed using R version 3.4.1. A Shapiro-Wilk normality test showed our miRNA expression data did not follow a normal distribution, and thus miRNA levels were compared using a non-parametric test (Kruskal-Wallis test). Spearman's correlations were calculated to determine whether miRNA expression levels in chorionic villi correlated with expression in matched maternal plasma.

5.3 Results

5.3.1 Expression of mir-518b is associated with fetal sex

We utilized our larger study cohort of 57 placentas to evaluate the effects of clinical and demographic variables on miRNA expression. Expression of miR-518b across GA showed a trend of increased expression in females compared to males (Kruskal-wallis test, p=0.05) (Figure 5.1). Although not significant, miR-518b also showed a trend towards the expected increased expression as gestation progressed, as has been previously reported in maternal plasma (229), while the remaining miRNAs (miR-146a, miR-223, miR-338-3p, and miR-411) except miR-210 , exhibited a teand of decreased expression with increasing GA (Supplementary Figure 5.2).

Neither maternal age nor genetic ancestry were significantly associated with expression in any of the six candidate miRNAs.

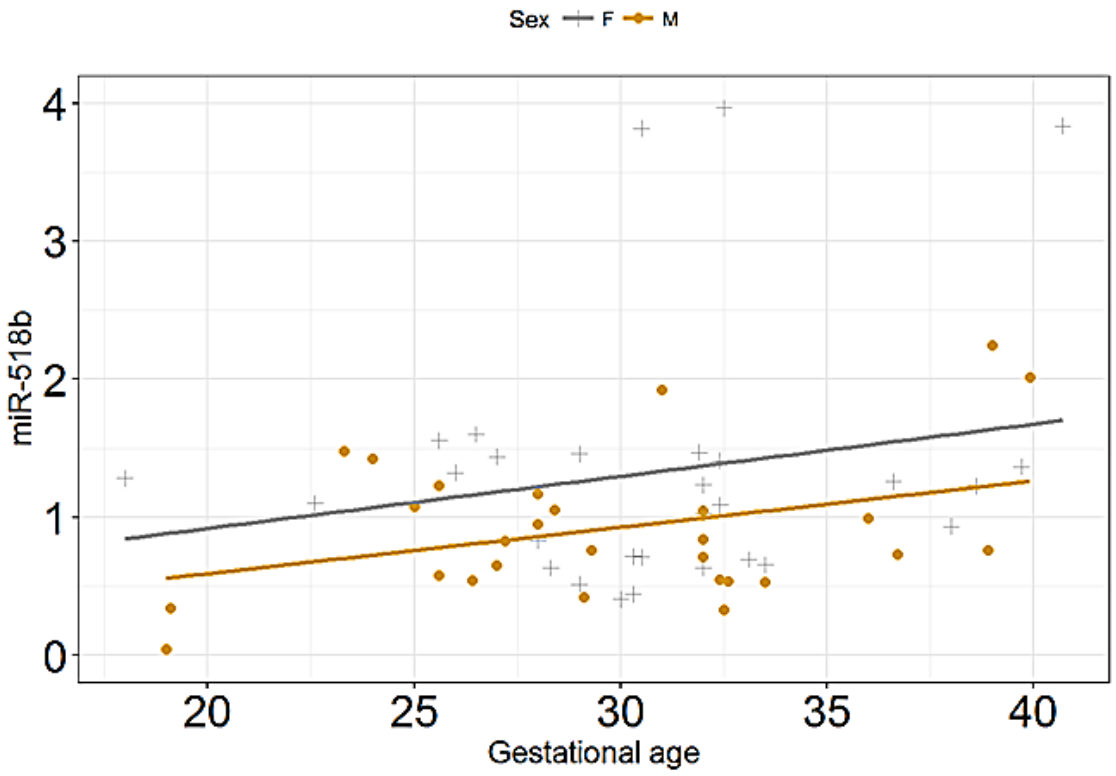

Figure 5.1 Variation in expression of miR-518b between fetal sexes over gestational age.

Although not significant, females showed a trend of increased expression of miR-518b across gestation compared to males (Kruskal-Wallis test, p=0.05). Expression measured by RT-qPCR is on the y-axis and gestational age (weeks) is on the x-axis.

5.3.2 Expression of miR-338-3p and miR-518b is associated with aCA status in the placenta

Although the expression of miR-146a, miR-210, miR-223, and miR-411 were not significantly associated with aCA status, the majority of the miRNAs trended in the expected direction as has been reported in infection-mediated conditions (394, 395) (Supplementary Figure 5.3). Increased expression of miR-338-3p was noted in aCA cases compared to non-aCA cases, while expression of miR-518b was significantly decreased in aCA. Importantly, even after

adjustment of confounding factors including GA at delivery, fetal sex and ancestry, expression of miR-518b was significantly decreased in aCA-affected placentas (p=0.011) and miR-338-3p was significantly increased in placentas with histologic evidence of aCA (p=0.001) (Figure 5.2). Interestingly, both miR-338-3p and miR-518b were also associated with fetal inflammatory responses (Figure 5.2), histologically identified by inflammation of the connective tissue of the umbilical cord (funisitis) and/or umbilical blood vessels (vasculitis).

Male fetuses are at an increased risk of a preterm delivery and are more likely to experience higher rates of postnatal inflammation, infection, and adverse outcomes (345, 348). To determine whether there may be sex-specific miRNA changes linked with aCA, we investigated the expression levels of the aCA-associated miRNAs on male and female placental samples separately. For miR-338-3p, increased expression in aCA cases was observed for both males (p=0.05) and females (p=0.02); however, expression of miR-518b was significantly associated with aCA status in females only (p=0.009) (Supplementary Figure 5.4).

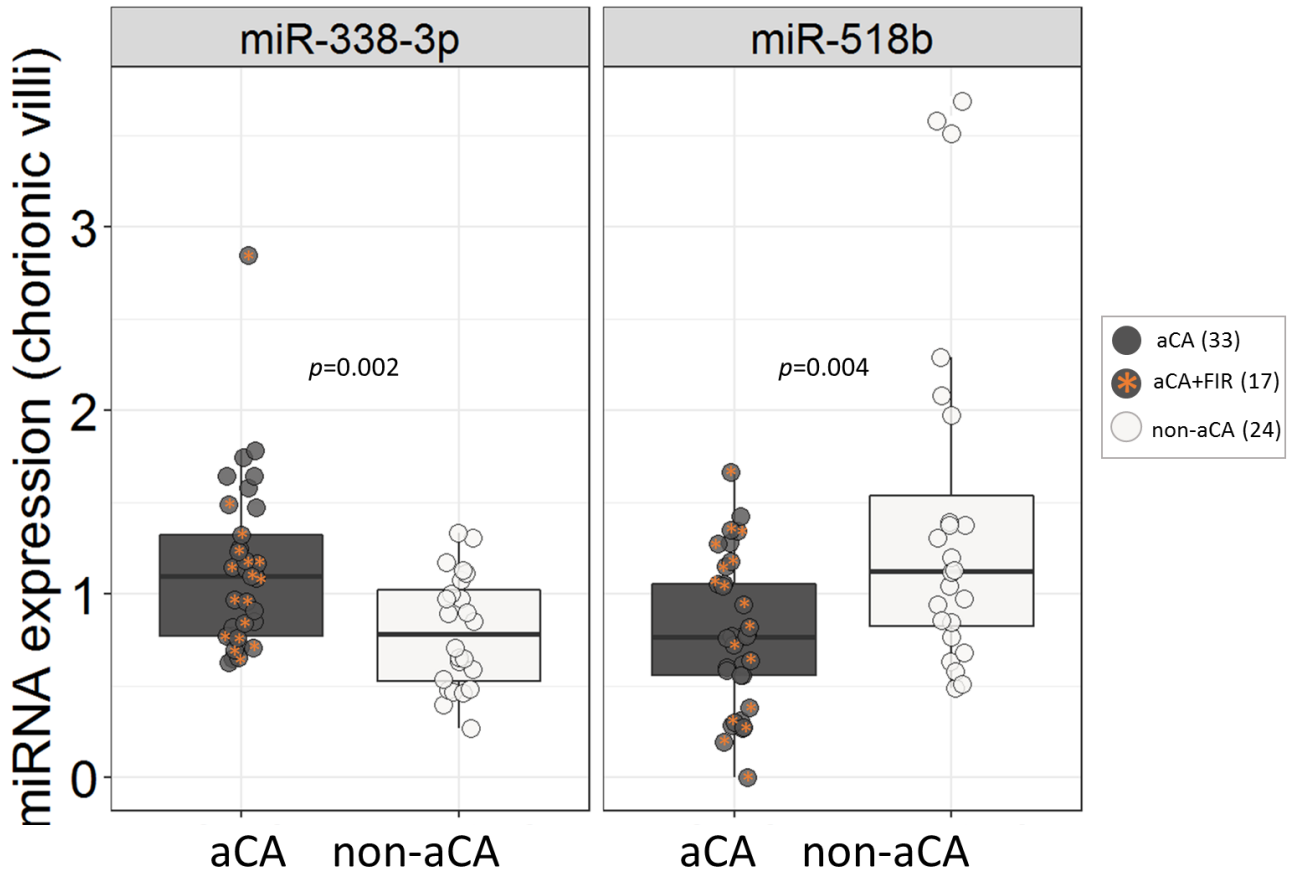

Figure 5.2 Differential expression of miR-338-3p and miR-518b in placentas is associated with aCA status.

Adjusted (for GA, sex and ancestry) expression values are plotted on the y-axis w.r.t study groups on the x-axis. Even after adjustment for GA, fetal sex, and ancestry, altered expression was observed between aCA cases and non-aCA cases. Based on our clinical records, it is unclear why the three females in the non-aCA group showed higher miR-518b expression compared to the remaining individuals within the non-aCA cases; however, we used the non-parametric Kruskal-Wallis test, which is relatively robust to outliers, and thus the magnitude of the difference in expression is less likely to drive the significance between aCA and non-aCA cases.

5.3.3 Predicted gene targets enriched in processes related to general and immune function

Because each miRNA may target multiple mRNA species, identifying the putative target genes of miRNAs is difficult, and many bioinformatic tools have been developed for this purpose (405). As the algorithms and parameters underlying each target prediction tool are

unique, it is prudent to cross-reference the results of multiple target prediction algorithms and use the subset of miRNA targets predicted by two (or more) tools to perform the pathway analysis. Using *TargetScan* and *miRDB*, 27 and 110 gene targets were predicted for miR-518b and miR-338-3p, respectively (Supplementary Figure 5.1). Gene ontology enrichment analysis performed on the target list of mir-338-3p identified gene sets associated with general functions including protein localization, cellular macromolecule localization, and cell projection, and related to specific diseases such as luminal-like breast cancer, Alzheimer's disease, and human alveolar rhabdomyosarcoma (FDR <0.05). Although only 27 gene targets were identified for miR-518b, gene sets were mainly related to immune-system cell types including B cells, thymocytes, macrophages, and T progenitor cells.

5.3.4 Expression of miR-518b and miR-338-3p is not associated with DNA methylation

Because epigenetic modifications such as DNAme may be associated with miRNA expression (406), we investigated whether the CpGs linked to miR-518b and miR-338-3p were differentially methylated between the aCA cases and non-aCA cases. Using Illumina's annotation, we identified 3 CpG sites (*cg06445981*, *cg11251554*, and *cg15993786*) and 11 CpG sites (*cg06807993*, *cg06869212*, *cg11600078*, *cg18637486*, *cg21473782*, *cg23176214*, *cg23295826*, *cg24085713*, *cg26068527*, *cg26766064*, and *cg06332842*) from the 850k array (204) that mapped to miR-518b and miR-338-3p respectively. The 3 CpG sites linked to miR-518b did not overlap with any Illumina-annotated genes; however the 11 CpG sites linked to miR-338-3p were associated with the *AATK* gene and were located 200-1500 base pairs upstream of the transcription start site. The gene list used by Illumina was the RefSeq genes from

UCSC (https://genome.ucsc.edu/). None of the CpGs showed differential methylation associated with aCA in chorionic villi (Supplementary Figure 5.5).

5.3.5 Expression of mir-518b is associated with *IL6* (rs1800796) genotype

We utilized our previously obtained *IL6* genotype (rs1800796) data that was available for a subset (n=48) of the 57 placental samples used to investigate whether expression of the aCA-associated miRNAs (miR-338-3p and miR-518b) was associated with an *IL6* SNP, a genetic polymorphism in placenta that may predisposes some pregnancies to aCA (Chapter 3). We observed that expression of miR-518b was significantly associated with the rs1800796 genotype: homozygous C individuals (n=7) showed significantly decreased miR-518b expression compared to homozygous G individuals (n=35) (Kruskal-Wallis test, p=0.02) (Figure 5.3). As expected the heterozygous CG (n=6) individuals showed intermediate levels of miR-518b expression compared to CC and GG, though not significant at p<0.05 (Figure 5.3). Although, not significant, expression patterns of miR-338-3p also displayed a trend were related to the *IL6* genotype (Supplementary Figure 5.6).

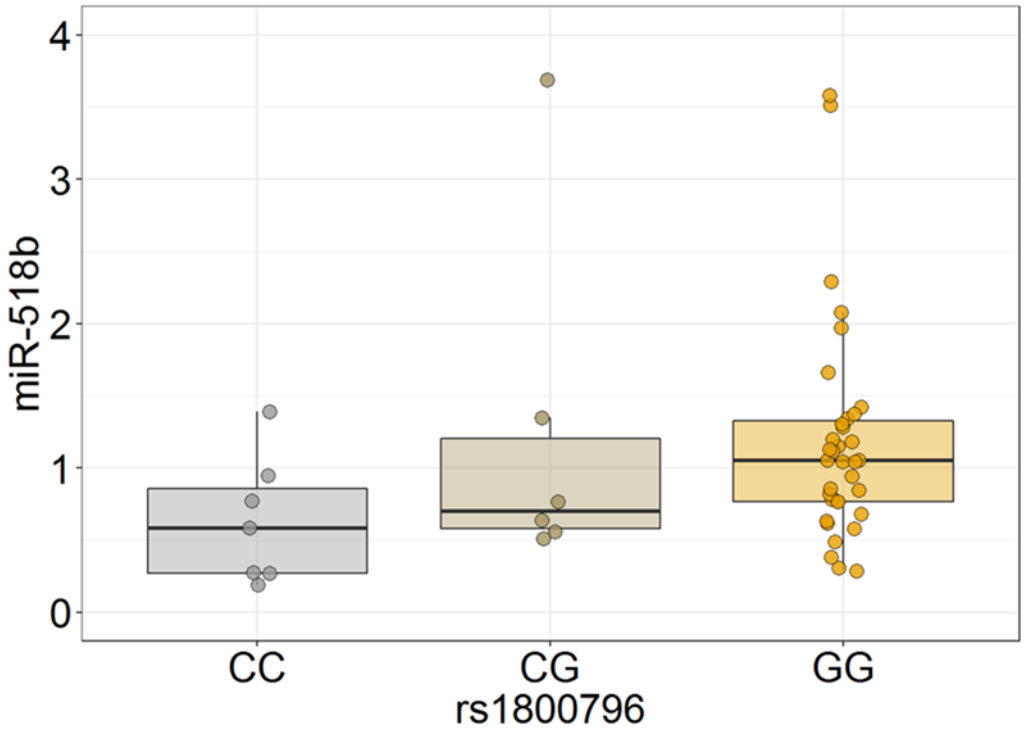

Figure 5.3. Expression of aCA-associated miR-518b in chorionic villi is influenced by *IL6* rs1800786 genotype.

Adjusted (for GA, sex and ancestry) miR-518b expression values are plotted on the y-axis w.r.t *IL6* genotype groups (CC=7, CG=6, GG=35) on the x-axis. Individuals with the CC genotype showed increased expression levels in the placenta compared to individuals of GG genotype (p=0.02). Although not significant, heterozygous CG (n=6) individuals displayed intermediate levels of expression compared to homozygous C (n=7) and G (n=35) individuals.

5.4 Discussion

The present study compared the expression of candidate miRNAs in placentas from pregnancies complicated with aCA to non-aCA placenta by qPCR. Increased expression of miR-338-3p and decreased expression of miR-518b was noted in aCA-affected placentas compared to the non-aCA placentas, suggesting the plausible involvement of these miRNAs in aCA. In alignment with our findings in chorionic villi, an independent study also identified that miR-338-3p showed increased expression in chorioamniotic membranes affected with aCA relative to non-

aCA cases (235). Though the same study also identified miR-223 as differentially expressed between aCA cases and non-aCA, our study did observe this association in the cohort of 57 chorionic villus samples. Differences may be attributed to small sample sizes, accounting for confounding factors and/or reflect tissue-specific expression patterns. While down-regulation of C19MC-specific miRNAs including miR-518b has been observed in PPROM pregnancies (233), expression of miR-518b was significantly increased in spontaneous PTB pregnancies (233). Of note, spontaneous PTB is heterogeneous in etiology (219), and thus it is important to emphasize a specific pathology related to spontaneous PTB, such as aCA.

To characterize miRNA-mediated biological processes involved in aCA, putative gene targets for miR-338-3p and miR-518b were determined using *TargetScan* and *miRDB.* Although gene set enrichment analysis of the predicted targets did not reveal statistically significant pathways related to aCA, our prediction algorithms identified gene targets broadly important for maintenance of a successful pregnancy such as *PLA2G3*, *ADAM17*, and *RAP1B*. Placental expression of the *PLA2* enzymes has been implicated in a number of pregnancy complications including preterm labor (407) and obesity (408). Further, inhibition of miR-338 expression in decidual cells resulted in an increase in mRNA and protein expression of a *PLA2* enzyme (409). Both *PLA2G3* and *ADAM17* are predicted gene targets for miR-338-3p and are involved in eliciting inflammatory responses, specifically *PLA2G3* facilitates mast cell activation (410) and *ADAM17* mediates the production of TNF-α by placental trophoblasts (411).

Decreased placental expression of miR-518b has also been reported in placentas linked to intrauterine growth restriction (412) and in complete hydatidiform moles (413). Although, the exact role of miR-518b in placenta is not established, miR-518b has been shown to repress the

expression of *RAP1B* (414), which was identified as a putative gene target for miR-518b in our target prediction analysis. *RAP1B* regulates key cellular processes such as cell proliferation, angiogenesis, and inflammation; in fact deficiency of *RAP1B* in mice resulted in increased neutrophil recruitment and migration into sites of inflammation (415). Taken together, many of the gene targets for miR-338-3p and miR-518b were involved in inflammation-mediated responses, and therefore may represent potential candidates to understand the downstream effects of the aCA-associated miRNAs orchestrating inflammatory responses in the placenta.

Although the regulatory mechanisms of miRNA expression in placenta have not been extensively investigated, molecular processes such as DNAme and/or genetic alterations such as single nucleotide polymorphisms have been shown to modulate miRNA expression levels in other tissues. For example, Li et al. (2013) identified that CpG sites surrounding the promoter of miR-338-3p, a miRNA also found to be associated with aCA in our study, were significantly more methylated in gastric cancer tumor tissues compared to normal tissues (416). However, in our study, CpG sites that mapped to miR-338-3p and miR-518b were not differentially methylated between aCA cases and non-aCA cases, suggesting DNAme is less likely to participate in regulation of the two aCA-associated miRNAs. Further, the role of genetic variants in modulating miRNA expression levels in infection-mediated diseases have been previously implicated (417); however this relationship is not extensively investigated in placental-mediated complications. Our study demonstrated that placenta expression of miR-518b is associated with *IL6* (rs1800796) genotype, a placental polymorphism that may increase risk of aCA: individuals with the C allele exhibited decreased placental expression of miR-518b compared to carriers of the G allele, and we observed an association between reduced miR-518b expression and aCA status. While *IL6* was not a predicted mRNA target for miR-518b in our analysis with

TargetScan and *miRDB*, it is associated with a broad spectrum of inflammatory and infectious disorders and shown to alter immune responses against microbial infection (418), a well-characterized cause of aCA. However, we cannot rule out the possibility that the *IL6* (rs1800796) genotype may correlate with the genotype of another target gene, which may be a plausible mRNA target for miR-518b.

Overall, we observed placental-specific miRNA changes in aCA-affected placentas and attempted to characterize the processes that regulate expression of aCA-associated miRNAs. As miR-338-3p and miR-518b are detectable in maternal circulation throughout gestation (419, 420), further studies into these miRNAs are warranted.

Chapter 6: Discussion

6.1 Summary of dissertation

The work presented in this dissertation highlights the genetic, epigenetic, and miRNA variation in aCA-affected placentas. First, I adopted a candidate approach and explored the association of 16 innate immune-system SNPs with the presence of aCA in a population of 72 aCA-affected placentas and 197 non-aCA affected placentas. I observed that the C allele in *IL6* promoter SNP (rs1800796) was associated with increased aCA risk. Interestingly, the same allele was also linked with increased DNAme and decreased *IL6* expression, demonstrating the role of *IL6* genetic variants in modulating molecular processes, and may likely influence disease susceptibility. Next, I investigated DNAme patterns in aCA-affected placentas using the 850K array in samples from 44 preterm placentas: 22 aCA cases and non-aCA cases. At less stringent thresholds (FDR <0.15 and $\Delta\beta$ >0.05), this array analysis was capable of capturing some DNAme changes in aCA-affected placentas reflecting an alteration in immune cell number (mainly neutrophils) and/or activation of innate immune responses in placental cells as a response to inflammation. Lastly, miRNA expression changes were investigated in 33 aCA-affected placentas and 24 non-aCA affected placentas, using RT-qPCR. miR-518b, a member of the placental-specific C19MC cluster showed decreased expression in aCA cases, and demonstrated a sex-specific expression profile. Further, miR-518b expression patterns in the placenta were associated with the genotype distribution of the *IL6* SNP (rs1800796), a polymorphism that was previously implicated in aCA risk in the SNP analysis.

While genetic associations may predispose a placenta to aCA, the unique DNAme and miRNA signatures may reflect immune cell infiltration and/or altered gene expression of specific

placental cell types in response to inflammation. Overall, the findings reported in this dissertation lays the groundwork for development of placenta-derived biomarkers for aCA, although it is imperative to validate the results in larger, independent populations.

6.2 Significance of dissertation and future directions

6.2.1 Potential for development of ancestry-specific diagnostic biomarkers

As placental DNA is released into the maternal circulation during pregnancy, this information may be used to identify candidate biomarkers that could be detected in maternal blood for early detection of disease, prior to the onset of clinical symptoms. Nevertheless, signals in maternal fluids that may be predictive of pathology could reflect either placental changes or changes to the maternal immune system directly. In Chapter 4, my EWAS analyses of aCA-affected placentas identified 66 differentially methylated CpGs associated with aCA. Because histologic examination of the placenta after delivery is the current gold standard for a confirmatory diagnosis of aCA, these 66 CpGs may be useful in the development of diagnostic biomarkers for aCA. Similarly, in Chapter 6, I investigated placental-specific miRNAs associated with aCA, and identified miR-338-3p and miR-518b as potential candidates for further exploration as maternal blood biomarkers to facilitate early identification of pregnancies at risk for aCA, though it remains to be seen if these aCA-linked placental miRNAs alterations and DNAme signatures are also detectable in maternal circulation.

Apart from examining aCA-specific placental signatures in maternal blood, it is also important to acknowledge that the pathogenesis of aCA is heterogeneous. Of note, the etiological and genetic heterogeneity in aCA have been rarely considered in studies that have focused on identifying predictive biomarkers for aCA. For example, changes in cytokine concentrations or

genetic variants in cytokines have been frequently associated with aCA; however, individuals are often analyzed together regardless of their genetic background.

In the context of microbial infection, a commonly identified cause of aCA, ethnic variation in chemokine production (*CCL2, CCL11, CXCL8*), cytokine production (*IL1, IL6, IL8*), neutrophil count, antibody levels, and rate of microbe clearance have been well-established (421-423). While our understanding of the factors that may account for this variation is limited, population-specific genetic differences may explain some of the differential host immune responses against pathogens (424). Drawing on the findings in Chapter 4, I found that presence of aCA was associated with the minor C allele of an *IL6* SNP, which was largely confined to individuals of East Asian ancestry. It is likely that there are multiple additional immune-related genetic variants specific to other ancestries which together may explain ancestry-related differences in sPTB conditions such as aCA. For instance, the T allele of a promoter SNP in *SERPINH* enriched in individuals of African ancestry was shown to be associated with an increased risk of a sPTB condition (PPROM) in African Americans (425). Despite this genetic heterogeneity, to date, majority of the disease-focused GWAS have been performed in individuals of European ancestry (>80%), while populations including African American, African, and Hispanic or Latin American merely account for ≤2% of these studies (426), thereby limiting the relevance of the GWAS findings in diverse populations.

Furthermore, genetic polymorphisms that exhibit extreme allelic variation across ancestries have likely undergone positive selection in specific populations (313, 314), demonstrating the role of natural selection in driving population differences in host immune responses. Given that there is significant variation in innate and adaptive immune responses between different ethnic and/or ancestry populations (168, 421, 422, 427, 428), predictive

biomarkers for an inflammatory condition such as aCA are not generalizable across populations, and therefore should be developed and validated in aCA-affected ancestry-specific stratified populations; doing so will also aid in accurately targeting therapeutic treatments.

Additionally, host immune responses may vary depending on the type of microbial trigger. While bacterial species like *Ureaplasma urealyticum, Mycoplasma hominis, Gardnerella vaginalis, Escherichia coli, Fusobacterium nucleatum, and Group B Streptococcus,* are commonly identified causative agents in infection-driven aCA, fungi such as *Candida albicans* and viruses such as adenovirus have also shown to be associated with aCA (429-431); however, aCA-linked inflammatory responses associated with viruses and fungi have not been well-characterized. Furthermore, different species and strains within a microbial genus also exhibit different immune responses suggesting there is no unique immune signature that represents a microbial species/genus (421, 432). As such, future work is needed to understand the impact of species/genus differences at molecular level and subsequently develop pathogen-specific biomarkers.

6.2.2 Potential for identification of functionally-relevant genetic loci of interest

DNAme patterns in tissues including the placenta are under strong genetic control. These genetic influences account for approximately 20-80% of DNAme variance within a tissue and are termed methylation-quantitative trait loci (mQTL) (283, 433-436). To date, the vast majority of mQTL studies have been performed in blood, with only one study focusing exclusively on the human placenta (437). In a comprehensive study of 300 human placentas obtained from low risk pregnant women, the authors identified 4342 placental mQTLs (437). They restricted their analyses to SNP-CpG pairs within 75 kb. Although choosing this window is often arbitrary,

previous mQTL analyses have reported that SNP-CpG associations are more likely to be causal within a 5 kb window (285, 438), and that mQTLs are mostly positioned within 100 kb of SNP loci in multiple tissues including placenta (434, 439).

Previous work in brain and blood have revealed that mQTLs are often enriched in disease-associated GWAS variants facilitating prioritization of genetic candidates involved in disease phenotypes (440, 441), and in turn improve our current understanding of mechanisms underpinning complex diseases. Of note, the GWAS catalogue contains few studies that have investigated the direct role of placental dysfunction in adverse reproductive outcomes, though it is reasonable to assume that placental-specific mQTLs may be utilized to identify loci of interest underlying genetic susceptibility in complex reproductive pathologies. While I did not have genome-wide SNP data available to perform mQTL analyses in my study cohort, genotyping data for *IL6* candidate SNPs and matched DNAme data was available for a subset of my samples. This enabled me to identify a placental mQTL (rs1800796) located in the enhancer region of *IL6*, which was linked to changes in *IL6* expression in the placenta and associated with aCA in individuals of East Asian ancestry (Chapter 3). Because risk variants like the *IL6* SNP (rs1800796) often exhibit population-specific genetic variation (Figure 3.2, Chapter 3), it is important to understand the impact of ancestry on placental DNAme. Ancestry-related DNAme differences in other tissues have been shown to associate with genes involved in immune regulation (442), and thus ancestry-specific mQTLs may be more relevant in identifying predisposing risk factors for diseases with altered immune responses including aCA.

6.2.3 Potential to refine existing classification of pathologies

Molecular profiling has the potential to refine existing clinically-defined groups for heterogeneous pregnancy complications. For example, clustering placentas from diverse outcomes using validated PE-associated DNAme sites, identified unique clusters that were representative of homogeneous clinical groups of PE (293). A similar clustering pattern was also observed using gene expression profiling of healthy and affected placentas of mixed etiologies (297). Similarly, in Chapter 4, hierarchical clustering of placentas with aCA and non-aCA etiologies, using the 2069 neutrophil-specific DNAme signatures, identified two distinct clusters: i) a placental inflammation-mediated cluster predominantly of aCA cases, and ii) a cluster of non-aCA mixed placental-mediated pregnancy pathologies. Additional studies with larger sample sizes are required to validate the clusters, to clarify the key changes that drives the formation of these clusters, and to characterize the predictive value of the possible "inflammation" cluster. While our current understanding of epigenetic changes in the placenta is still in its infancy, these findings provide evidence for the potential role of placental DNAme in classifying and identifying subtypes of heterogeneous pregnancy complications such as aCA and PE, as has been demonstrated for other conditions including cancer (443).

6.3 Considerations & limitations

6.3.1 Case-control ascertainment

Case-control study design is the most commonly used design in association studies, involving comparisons between two well-characterized groups of unrelated individuals: cases that are diagnosed with the disease of interest, and controls who are typically "healthy" and known to be "unaffected" by the disease. Case-control classifications are often poorly defined,

without well-defined inclusion and exclusion criteria, and relevant disease or clinical characteristics are not always consistently recorded. In this dissertation, histological assessment of extraplacental membranes was performed by clinical pathologists to confirm neutrophil infiltration associated with aCA; however, because we obtained samples in a deidentified manner without the full pathology report, information on severity of inflammatory processes related to aCA was not available for all the cases. It is possible that only a subset of the highly severe "Stage 3" aCA-affected placentas may exhibit larger DNAme and/or miRNA expression changes compared to the non-aCA affected placentas, and therefore such effects may be diluted or exaggerated when extreme aCA cases are combined with aCA cases that exhibit a moderate inflammatory phenotype. Moreover, intra- and inter-observer variablity exists in the pathological assessment of aCA severity, which may also add bias the observed relationship betwen aCA and DNAme and/or miRNA expression changes.

Further, aCA may result from multiple factors including maternal health exposures, genetic susceptibility, and/or *in utero* exposures to microbes. While microbial infection was reported in a majority of the aCA cases included in this dissertation, etiology of aCA was not investigated or documented in all the cases. It is important to note that aCA may also occur in a non-infection mediated sterile intraamniotic inflammation setting, which may be caused by tissue injury, hypoxia, or cell death. Additionally, it is challenging to obtain "unaffected/control" placentas from <37 weeks to match the preterm aCA-affected placentas (cases). To address this, I combined multiple placental pathologies to obtain a heterogeneous reference "control/non-aCA" group, which reduces the likelihood of identifying an association with any other pathology in the "control/non-aCA" population. Finally, it is important that the cases and controls have similar demographics including GA, sex, lifestyle, and genetic background, otherwise disease-

associated differences between the groups may actually reflect demographic differences, which may or may not be related to disease. These factors are discussed in detail below.

6.3.2 Potential confounding factors

Confounding influences such as GA, fetal sex, and ancestry can influence DNAme and expression patterns in the placenta (444-447). Some of the GA-dependent DNAme changes in the placenta may be related to changes in cell composition and the differentiation of cells that occurs as gestation progresses (212). Additionally, sex-specific differences in adverse fetal outcomes such as neonatal sepsis, infection, and chronic inflammation have been observed. miR-518b, as shown in Chapter 5, was associated with aCA status in females only, suggesting sex-specific expression of this miRNA species in aCA-affected placentas. In the placenta, sex-dependent expression patterns of many immune-related genes are observed, specifically, male placentas exhibit increased *TLR*, *IL10,* and *TNFα* expression in response to lipopolysaccharide stimulation than the female placentas (448), which may, in part, explain the increased risk of pregnancies carrying a male fetus to deliver prematurely.

Genetic background is another important factor to take into consideration. Association studies are prone to population stratification if cases and controls are not either restricted to a genetically homogeneous population or matched by ancestry. In these unbalanced ancestry case/control situations, it is possible that the variation in allele frequencies, DNAme, and/or expression patterns associated with disease may actually be explained by differences in ancestry between the groups. For example, the *IL6* rs1800796 SNP investigated in Chapter 3, is known to be strongly correlated with ancestry. Based on 1000 Genomes Project data records, the C allele is common in individuals of East Asian (70-80%), and rare in individuals of European ancestry (3-5%).

While I used a panel of 55 AIM SNPs to infer ancestry of my study cohort, unaccounted genetic differences in population structure may still be present as this panel may not be sufficient to capture all ancestry-specific effects, but does provide a cost-effective and less computationally intensive method to assess ancestry. While researchers have attempted to infer population structure from DNAme data by relying on DNAme patterns affected by genetic variants, mQTLs (449, 450), these methods have not been completely validated in different populations and tissues including the placenta. Although such tools are valuable in assessing and correcting for ancestry, they could also be utilized to identify genetically homogeneous sub-populations that may be more ideal to capture disease-associated effects, as ancestry and other related confounding influences may have been filtered out in such populations.

Further, it is important to acknowledge that in a tissue sample of mixed cell population such as chorionic villi, the targeted tissue in this dissertation, DNAme/expression measured is an average across a pool of cells, and thus a change in DNAme could either reflect an average change across all cell types in the sample, or an alteration in the composition of different cell types. Measuring DNAme or gene expression from purified cell types can help to address the challenges in cellular heterogeneity; however isolating pure populations of single placental cell types has practical challenges. As cell deconvolution approaches are eventually developed for the placenta, they can be applied to i) estimate cell ratio variation and its contribution to epigenetic/expression signal or ii) adjust for cell-type differences between samples of whole tissue. Although cell-type variation is often adjusted in EWAS/expression analyses, in certain inflammation-mediated sPTB conditions, such as aCA, changes in placental immune cell ratios are observed, and thus changes in cell type proportions may actually be relevant to the disease pathogenesis. For instance, as DNAme is cell-specific, some of the aCA-associated DNAme

changes in the placenta may be indicative of changes to immune cell composition mainly involving neutrophils, hofbauer cells, and cytokines. In such conditions, cell-specific DNAme profiles could be used to quantify low levels of maternal infiltration, and may be utilized to predict the severity of inflammatory responses in the newborn.

Aside from cell-type heterogeneity, maternal exposures including smoking status, alcohol intake, body mass index, and medication use can influence placental DNAme/expression and may be associated with reproductive pathologies. For example, regions of altered placental DNAme at *AHRR*, *RUNX*, and *CYP1A1* are consistently linked with maternal smoking (453, 454), and have been shown to be associated with preterm birth (<37 weeks GA) (455). I therefore tested for DNAme differences at these CpG sites and did not observe altered DNAme associated with aCA at these sites in my study population. Although I accounted for confounding factors including GA, fetal sex and ancestry in statistical analyses, other potential confounding influences, such as processing time, were not documented for all the cases in our cohorts, and thus could not be accounted for in my analyses.

6.3.3 Methodological constraints

Although the work presented in this dissertation offers new molecular insights into aCA, there are some methodological limitations that should be acknowledged. Given that my sample size was rather small and incomplete pathology information was available for my samples, my statistical power to detect significant associations was low. To work around this limitation, I opted for a candidate gene approach in Chapter 3 and Chapter 5. However, the candidate gene approach is limited to genes with *a priori* evidence suggesting a critical role of the candidates in the disease pathogenesis. A major drawback of such studies is their inability to discover novel

associations beyond those selected as putative candidates. To fully understand the genetic and transcriptomic variation in aCA-affected placentas, it will be important to implement agnostic techniques such as whole-genome SNP arrays and RNA-sequencing; however, larger sample sizes will be required to reduce the burden of multiple test correction. While the 850K array was used to obtain DNAme profiles of aCA-affected placentas (Chapter 4), this array measures less than 4% of the entire human methylome, and therefore it is possible that other aCA-associated CpG sites exist beyond those interrogated by the array. Alternative genome-wide DNAme techniques such as whole genome bisulfite sequencing is an attractive option as it offers a much higher coverage of the methylome, although they are exorbitantly expensive compared to the microarrays, require more amounts of starting material, and would require larger sample sizes which limits their utility in epigenetic analyses.

6.3.4 Association versus causation

The findings described in this dissertation reflect an association of genetic, epigenetic, and miRNA changes with aCA, and do not establish causal mechanisms linked with the pathology, in fact I hypothesize that DNAme and miRNA expression changes may be a consequence of changes in immune cell numbers that occur as a response to inflammation/infection in aCA-affected placentas.

While DNAme has the potential to affect gene transcription, it is unclear if DNAme regulates gene expression or vice-versa, making interpretation of DNAme/gene expression findings extremely difficult. In Chapter 3, I identified a placental *IL6* mQTL (rs1800796), which was also associated with changes in *IL6* expression. Although we did not perform experimental studies to determine the directionality by which *IL6* SNP affects DNAme and gene expression in

placenta, previous work in pancreatic adenocarcinoma cell lines have suggested DNAme dependent *IL6* gene transcription via the MeCP2 protein. MeCP2 has been recognized as a transcriptional repressor by targeting methylated CpGs, and recruiting co-repressors, histone methytransferases, and chromatin remodeling complexes (451-453). Chromatin immunoprecipitation assays confirmed that MeCP2 was only present in non-*IL6* expressing cell lines, and treatment of these cell lines with a DNA methyltransferase inhibitor resulted in the loss of MeCP2, thereby inducing *IL6* expression. Interestingly, the *IL6* SNP rs1800796 was located at position -572, and influenced DNAme patterns at cg01770232 which was located at position -662 relative to the transcription start site, and both (SNP-CpG) were positioned within the MeCP2 binding region. Therefore, it may be reasonable to speculate that the *IL6* SNP may affect the binding of MeCP2 which subsequently alters *IL6* transcription. It is likely that the downstream DNAme changes observed at CpGs further away from MeCP2 binding region may be a product of altered transcription of *IL6*. (Figure 3.3, Chapter 3).

6.4 Placenta, lest we forget

Although discarded at birth, the placenta is an extremely important organ to sustain a healthy pregnancy, as the growth of the fetus is completely dependent on the placenta. This organ is involved in nutrient delivery, immune protection, hormone regulation and secretion, and protection of the baby from harmful exposures. Defects in placental development and function underlie many pregnancy complications such as PE, PTB, miscarriage, and fetal growth restriction (454). Specifically, these defects include shallow trophoblast invasion of the maternal uterus, improper remodeling of maternal spiral arteries due to altered immune signaling at the maternal-placental interface, and placental inflammation related to infectious and non-infectious

triggers during pregnancy. Further, studies in knockout mice have demonstrated placental malformations as one of the major causes of early embryonic lethality (455). For example, placental endothelial defects result in thinning of ventricular walls, edema of the embryonic blood vessels, and reduced vascular branching, that results in mid-gestational lethality (456).

Aside from its crucial role in impacting the outcome of a pregnancy, abnormal placental findings have also been associated with health outcomes in the offspring. For example, autism spectrum disorder is associated with acute and chronic placental inflammatory lesions (457), suggesting that post-delivery assessment of placental health may shed light into the pathophysiology of neurodevelopment disorders. More recently, risk-conferring genetic loci for schizophrenia have been shown to be highly expressed in the placenta, and differentially expressed in PE-affected placentas with/without IUGR compared to unaffected control placentas; the exact mechanism is still unclear but the findings recognize altered placental functioning in association with brain disorders (458). Accumulating evidence also suggests that placental measurements including morphological characteristics and placenta-to-fetal weight ratio are associated with coronary heart diseases and cardiovascular mortality (459-461). These examples suggest that the placental phenotype is reflective of the intrauterine environment, and thus may aid in identifying babies at risk for adverse health consequences, both immediate and long-term.

While articles like “The Placenta, an Afterthought No Longer” (12/3/2018), and “The Mysterious Tree of a Newborn’s Life” (8/14/2014), published by New York Times have appreciated the placenta as a critical organ impacting maternal and fetal health, a significant gap exists in our understanding of the placental processes and the interactions at the maternal-placental interface that lead to adverse pregnancy outcomes. With the advent of 3D culture techniques, recently, genetically stable human trophoblast organoids have been developed from

first trimester placental tissues (462). These complex structures closely recapitulate the organization, physiological and metabolic characteristics of chorionic villi, with the potential to differentiate into syntiotrophoblast and HLA-G^+ extravillous trophoblasts. Models such as trophoblast organoids will become indispensable tools to investigate mechanisms underlying aberrant placental development in various reproductive pathologies, and understand the functional relevance of the placental-specific molecular alterations associated with pregnancy complications.

The work presented in this dissertation is largely aimed at understanding molecular processes involved in the pathophysiology of aCA. While it is important to first validate the molecular signatures reported in this dissertation, and perform genome-wide screens to identify genetic variants and transcriptomic changes linked with aCA, such candidate aCA-associated molecular signatures may be helpful to identify risk profiles for early disease detection. For example, polygenic risk scores defined as the weighted sum of SNPs associated with a disease have been utilized for disease prediction, prevention, and therapeutic intervention (463). Additionally, it is imperative to understand the functional effects of the molecular signatures on placental physiology, if any, using an *in vivo* system such as trophoblast organoids and thereby investigate the downstream effects of the molecular changes orchestrating inflammatory responses in the placenta. Further, future work aimed at integrating diverse molecular data-types will help to gain a comprehensive understanding of altered biological processes in aCA.

With the advent of advanced high-throughput technologies, it is now possible to obtain multi-omics data by interrogating the genome, methylome, transcriptome, proteome and metabolome. By capturing multiple dimensions of biological information, such datasets hold tremendous power to establish interconnections between different molecular layers, and provide

valuable insights into disease etiology. Generally, analysis of only one data type is restricted to associations, whereas integration of diverse omics datatypes may identify causal regulatory patterns relevant to the disease. For instance, module-based analysis that collapses high-dimensional data into fewer modules of highly correlated genes/CpGs/miRNAs may be a useful approach to identify conserved modules between datatypes (464, 465) , thereby identifying common disease-associated dysregulated pathways or hub factors which can then be putative candidates for further experimental validation.

Taken together, the field of placental genetics, epigenetics, and transcriptomics is still young, and only recently the scientific community has started to appreciate the importance of this fascinating organ. Resources like the Placental Atlas Tool (PAT) https:/pat.nichd.nih.gov/, an NICHD (The National Institute of Child Health and Human Development) initiative, are crucial to facilitate data-sharing, replication of associations, and to foster research collaborations and perform integrative multi ‘omic analyses. PAT is a publicly available comprehensive repository that assimilates placental data from various publications and public databases into a single website. Further, large-scale initiatives by NIH such as the Roadmap Epigenomics Consortium (466) have established a comprehensive catalog of reference epigenome profiles for multiple human tissues including placenta, which will enable researchers to gain a deeper understanding of the widespread variation in placental structure and cell composition, and unravel mechanisms that alter placental development and function in numerous reproductive pathologies.

Bibliography

1. Blencowe H, Cousens S, Chou D, Oestergaard M, Say L, Moller A, et al. Born too soon: the global epidemiology of 15 million preterm births. Reprod Health. 2013;10:2.

2. Blencowe H, Cousens S, Oestergaard M, Chou, D, Moller A-B, Narwal R, et al. National, regional, and worldwide estimates of preterm birth rates in the year 2010 with time trends since 1990 for selected countries: a systematic analysis and implications. Lancet. 2012; 379:2162.

3. Moutquin J. Classification and heterogeneity of preterm birth. BJOG. 2003;110:30.

4. Muglia LJ, Katz M. The Enigma of Spontaneous Preterm Birth. N Engl J Med. 2010;362:529.

5. Meis PJ, Goldenberg RL, Mercer B, Moawad A, Das A, McNellis D, et al. The preterm prediction study: significance of vaginal infections. National Institute of Child Health and Human Development Maternal-Fetal Medicine Units Network. Am J Obstet Gynecol. 1995;173:1231.

6. Romero R, Espinoza J, Gonçalves L, Kusanovic J, Friel L, Hassan S. The role of inflammation and infection in preterm birth. Semin Reprod Med. 2007;25:21.

7. Bastek JA, Gómez LM, Elovitz MA. The role of inflammation and infection in preterm birth. Clin Perinatol. 2011;38:385.

8. Romero R, Chaiworapongsa T, Espinosa J. Micronutrients and intrauterine infection, preterm birth and the fetal inflammatory response syndrome. J Nutr. 2003;133:1668.

9. Redline R, Faye-Petersen O, Heller D, Qureshi F, Savell V, Vogler C. Amniotic infection syndrome: nosology and reproducibility of placental reaction patterns. Pediatr Devel Pathol. 2003;6:435.

10. Kim C, Romero R, Chaemsaithong P, Chaiyasit N, Yoon B, Kim Y. Acute chorioamnionitis and funisitis: definition, pathologic features, and clinical significance. Am J Obstet Gynecol. 2015;213:29.

11. Lawn JE, Wilczynska-Ketende K, Cousens SN. Estimating the causes of 4 million neonatal deaths in the year 2000. Int J Epidemiol. 2006;35:706.

12. Liu L, Oza S, Hogan D, Perin J, Rudan I, Lawn JE, et al. Global, regional, and national causes of child mortality in 2000-13, with projections to inform post-2015 priorities: an updated systematic analysis. Lancet. 2015;385:430.

13. Stoll B, Hansen N, Sánchez P, Faix R, Poindexter B, Van Meurs K, et al. Early onset neonatal sepsis: the burden of group B Streptococcal and E. coli disease continues. Pediatrics. 2011;127:817.

14. Saigal S, Doyle L. An overview of mortality and sequelae of preterm birth from infancy to adulthood. Lancet. 2008;371:261.

15. Bernsen RMD, de Jongste JC, Koes BW, Aardoom HA, van der Wouden JC. Perinatal characteristics and obstetric complications as risk factors for asthma, allergy and eczema at the age of 6 years. Clin Exp Allergy. 2005;35:1135.

16. Behrman RE. Preterm birth. Washington, DC: National Academies Press; 2007.

17. Anderson PJ, Doyle LW, Victorian infant collaborative study group. Executive functioning in school-aged children who were born very preterm or with extremely low birth weight in the 1990s. Pediatrics. 2004;114:50.

18. Roberts D, Brown J, Medley N, Dalziel SR. Antenatal corticosteroids for accelerating fetal lung maturation for women at risk of preterm birth. Cochrane Database Syst Rev. 2017;3:44.

19. Benirschke K, Burton G, Baergen R. Early development of the human placenta. In: Pathology of the Human Placenta. 2012;41.

20. Peñaherrera MS, Jiang R, Avila L, Yuen RKC, Brown CJ, Robinson WP. Patterns of placental development evaluated by X chromosome inactivation profiling provide a basis to evaluate the origin of epigenetic variation. Hum Reprod. 2012;27:1745.

21. Robinson WP, McFadden DE, Barrett IJ, Kuchinka B, Peñaherrera MS, Bruyère H, et al. Origin of amnion and implications for evaluation of the fetal genotype in cases of mosaicism. Prenat Diagn. 2002;22:1076.

22. Soares MJ, Varberg KM, Iqbal K. Hemochorial placentation: development, function, and adaptations. Biol Reprod. 2018;99:196.

23. Ben Amara A, Gorvel L, Baulan K, Derain-Court J, Buffat C, Verollet C, et al. Placental macrophages are impaired in chorioamnionitis, an infectious pathology of the placenta. J Immunol. 2013;191:5501.

24. Toti P, Arcuri F, Tang Z, Schatz F, Zambrano E, Mor G, et al. Focal increases of fetal macrophages in placentas from pregnancies with histological chorioamnionitis: potential role of fibroblast monocyte chemotactic protein-1. Am J Reprod Immunol. 2011;65:470.

25. Romero R, Mazor M. Infection and preterm labor. Clin Obstet Gynecol. 1988;31:553.

26. Blanc WA. Pathways of fetal and early neonatal infection. Viral placentitis, bacterial and fungal chorioamnionitis. J Pediatr. 1961;59:473.

27. Fray RE, Davis TP, Brown EA. Clostridium welchii infection after amniocentesis. B Med J. 1984;288:901.

28. Chen G, Nuñez G. Sterile inflammation: sensing and reacting to damage. Nat Rev Immunol. 2010;10:826.

29. Romero R, Chaiworapongsa T, Alpay Savasan Z, Xu Y, Hussein Y, Dong Z, et al. Damage-associated molecular patterns (DAMPs) in preterm labor with intact membranes and preterm PROM: a study of the alarmin HMGB1. J Matern-Fetal Neo M. 2011;24:1444.

30. Romero R, Miranda J, Chaiworapongsa T, Korzeniewski SJ, Chaemsaithong P, Gotsch F, et al. Prevalence and clinical significance of sterile intra-amniotic inflammation in patients with preterm labor and intact membranes. Am J Reprod Immunol. 2014;72:458.

31. Zhou X, Brotman R, Gajer P, Abdo Z, Schüette U, Ma S, et al. Recent advances in understanding the microbiology of the female reproductive tract and the causes of premature birth. Infect Dis Obstet Gynecol. 2010;2010:1.

32. Redline RW. Inflammatory response in acute chorioamnionitis. Semin Fetal Neonat M. 2011;17:20.

33. Bendon RW, Bornstein S, Faye-Petersen OM. Two fetal deaths associated with maternal sepsis and with thrombosis of the intervillous space of the placenta. Placenta. 1998;19:385.

34. Lee J, Kim JS, Park JW, Park CW, Park JS, Jun JK, et al. Chronic chorioamnionitis is the most common placental lesion in late preterm birth. Placenta. 2013;34:681-689.

35. Gersell D, Phillips N, Beckerman K. Chronic chorioamnionitis: a clinicopathologic study of 17 cases. Int J Gynecol Pathol. 1991;10:217.

36. Jacques SM, Qureshi F. Chronic chorioamnionitis: a clinicopathologic and immunohistochemical study. Hum Pathol. 1998;29:1457.

37. Redline RW, Patterson P. Villitis of unknown etiology is associated with major infiltration of fetal tissue by maternal inflammatory cells. Am J Pathol. 1993;143:473.

38. Kim J, Romero R, Kim MR, Kim YM, Friel L, Espinoza J, et al. Involvement of Hofbauer cells and maternal T cells in villitis of unknown aetiology. Histopathology. 2008;52:457.

39. Kim MJ, Romero R, Kim CJ, Tarca AL, Chhauy S, LaJeunesse C, et al. Villitis of unknown etiology is associated with a distinct pattern of chemokine up-regulation in the feto-maternal and

placental compartments: implications for conjoint maternal allograft rejection and maternal anti-fetal graft-versus-host disease. J Immunol. 2009;182:3919.

40. Redline RW. Villitis of unknown etiology: noninfectious chronic villitis in the placenta. Hum Pathol. 2007;38:1439.

41. Kim CJ, Romero R, Kusanovic JP, Yoo W, Dong Z, Topping V, et al. The frequency, clinical significance, and pathological features of chronic chorioamnionitis: a lesion associated with spontaneous preterm birth. Mod Pathol. 2010;23:1000.

42. Labarrere CA, McIntyre JA, Faulk WP. Immunohistologic evidence that villitis in human normal term placentas is an immunologic lesion. Am J Obstet Gynecol. 1990;162:515.

43. Kapur P, Rakheja D, Gomez AM, Sheffield J, Sanchez P, Rogers BB. Characterization of inflammation in syphilitic villitis and in villitis of unknown etiology. Pediatr Dev Pathol. 2004;7:453.

44. Brito H, Juliano P, Altemani C, Altemani A. Is the immunohistochemical study of the inflammatory infiltrate helpful in distinguishing villitis of unknown etiology from non-specific infection villitis? Placenta. 2005;26:839.

45. Salafia C, Vintzileos A, Silberman L, Bantham K, Vogel C. Placental pathology of idiopathic intrauterine growth retardation at term. Amer J Perinatol. 1992;9:179.

46. Labarrere C, Althabe O, Telenta M. Chronic villitis of unknown aetiology in placentae of idiopathic small for gestational age infants. Placenta. 1982;3:309.

47. Russell P, Atkinson K, Krishnan L. Recurrent reproductive failure due to severe placental villitis of unknown etiology. J Reprod Med. 1980;24:93.

48. Redline RW, O'Riordan MA. Placental lesions associated with cerebral palsy and neurologic impairment following term birth. Arch Pathol Lab Med. 2000;124:1785.

49. Tita A, Andrews W. Diagnosis and management of clinical chorioamnionitis. Clin Perinatol. 2010;37:339.

50. Yoon BH, Romero R, Park JS, Kim CJ, Kim M, Oh S, et al. The relationship among inflammatory lesions of the umbilical cord (funisitis), umbilical cord plasma interleukin 6 concentration, amniotic fluid infection, and neonatal sepsis. Am J Obstet Gynecol. 2000;183:1124.

51. Romero R, Emamian M, Quintero R, Wan M, Hobbins JC, Mazor M, et al. The value and limitations of the gramstain examination in the diagnosis of intraamniotic infection. Am J Obstet Gynecol. 1988;159:114.

52. Romero R, Jimenez C, Lohda AK, Nores J, Hanaoka S, Avila C, et al. Amniotic fluid glucose concentration: a rapid and simple method for the detection of intraamniotic infection in preterm labor. Am J Obstet Gynecol. 1990;163:968.

53. Tsuda A, Ikegami T, Hirano H, Sanada H, Ogawa M, Sasaki M, et al. The relationship between amniotic fluid interleukin-6 concentration and histologic evidence of chorioamnionitis. Acta Obstet Gynecol Scand. 1998;77:515.

54. Holst R, Laurini R, Jacobsson B, Samuelsson E, Sävman K, Doverhag C, et al. Expression of cytokines and chemokines in cervical and amniotic fluid: relationship to histological chorioamnionitis. J Matern Fetal Neonatal Med. 2007;20:885.

55. Romero R, Quintero R, Nores J, Avila C, Mazor A, Hanaoka S, et al. Amniotic fluid white blood cell count: a rapid and simple test to diagnose microbial invasion of the amniotic cavity and predict preterm delivery. Am J Obstet Gynecol. 1991;165:821.

56. Park J, Park K, Jung E. Clinical significance of histologic chorioamnionitis with a negative amniotic fluid culture in patients with preterm labor and premature membrane rupture. PLoS One. 2017;12:e0173312.

57. Yoon BH, Romero R, Kim CJ, Jun JK, Gomez R, Choi J, et al. Amniotic fluid interleukin-6: a sensitive test for antenatal diagnosis of acute inflammatory lesions of preterm placenta and prediction of perinatal morbidity. Am J Obstet Gynecol. 1995;172:960.

58. Greig PC, Ernest JM, Teot L, Erikson M, Talley R. Amniotic fluid interleukin-6 levels correlate with histologic chorioamnionitis and amniotic fluid cultures in patients in premature labor with intact membranes. Am J Obstet Gynecol. 1993;169:1035.

59. Kim SM, Romero R, Park JW, Oh KJ, Jun JK, Yoon BH. The relationship between the intensity of intra-amniotic inflammation and the presence and severity of acute histologic chorioamnionitis in preterm gestation. J Matern Fetal Neonatal Med. 2015;28:1500.

60. Caloone J, Rabilloud M, Boutitie F, Traverse-Glehen A, Allias-Montmayeur F, Denis L, et al. Accuracy of several maternal seric markers for predicting histological chorioamnionitis after preterm premature rupture of membranes: a prospective and multicentric study. Eur J Obstet Gynecol Reprod Biol. 2016;205:133.

61. Popowski T, Goffinet F, Maillard F, Schmitz T, Leroy S, Kayem G. Maternal markers for detecting early-onset neonatal infection and chorioamnionitis in cases of premature rupture of membranes at or after 34 weeks of gestation: a two-center prospective study. BMC Pregnancy Childb. 2011;11:26.

62. Martinez-Portilla RJ, Hawkins-Villarreal A, Alvarez-Ponce P, Chinolla-Arellano ZL, Moreno-Espinosa AL, Sandoval-Mejia AL, et al. Maternal serum interleukin-6: a non-invasive

predictor of histological chorioamnionitis in women with preterm-prelabor rupture of membranes. Fetal Diagn Ther. 2018;1.

63. Gulati S, Bhatnagar S, Raghunandan C, Bhattacharjee J. Interleukin-6 as a predictor of subclinical chorioamnionitis in preterm premature rupture of membranes. Am J Reprod Immunol. 2012;67:235.

64. Maeda K, Matsuzaki N, Fuke S, Mitsuda N, Shimoya K, Nakayama M, et al. Value of the Maternal interleukin 6 level for determination of histologic chorioamnionitis in preterm delivery. Gynecol Obstet Invest. 1997;43:225.

65. Kim M, Lee YS, Seo K. Assessment of predictive markers for placental inflammatory response in preterm births. PlOS One. 2014;9:e107880.

66. Trochez-Martinez RD, Smith P. Use of C-reactive protein as a predictor of chorioamnionitis in preterm prelabour rupture of membranes: a systematic review. BJOG. 2007;114:796.

67. van de Laar R, der Ham D, Oei S, Willekes C, Weiner C, Mol B. Accuracy of C-reactive protein determination in predicting chorioamnionitis and neonatal infection in pregnant women with premature rupture of membranes: a systematic review. Eur J Obstet Gynecol Reprod Biol. 2009;147:124.

68. Salazar J, Martínez M, Chávez-Castillo M, Núñez V, Añez R, Torres Y, et al. C-reactive protein: an in-depth look into structure, function, and regulation. Int Sch Res Notices. 2014;2014:1.

69. Manokhina I, Wilson S, Robinson W. Noninvasive nucleic acid–based approaches to monitor placental health and predict pregnancy-related complications. Am J Obstet Gynecol. 2015;213:197.

70. Manokhina I, del Gobbo GF, Konwar C, Wilson SL, Robinson WP. Placental biomarkers for assessing fetal health. Hum Mol Genet. 2017;26:237.

71. Gammill HS, Aydelotte TM, Guthrie KA, Nkwopara EC, Nelson JL. Cellular fetal microchimerism in preeclampsia. Hypertension. 2013;62:1062.

72. Askelund KJ, Chamley LW. Trophoblast deportation part I: review of the evidence demonstrating trophoblast shedding and deportation during human pregnancy. Placenta. 2011;32:716.

73. Rajakumar A, Cerdeira A, Rana S, Zsengeller Z, Edmunds L, Jeyabalan A, et al. Transcriptionally active syncytial aggregates in the maternal circulation may contribute to circulating soluble fms-like tyrosine kinase 1 in preeclampsia. Hypertension. 2012;59:256.

74. Knight M, Redman CW, Linton EA, Sargent IL. Shedding of syncytiotrophoblast microvilli into the maternal circulation in pre-eclamptic pregnancies. BJOG. 1998;105:632.

75. Salomon C, Torres M, Kobayashi M, Scholz-Romero K, Sobrevia L, Dobierzewska A, et al. A gestational profile of placental exosomes in maternal plasma and their effects on endothelial cell migration. PLOS One. 2014;9:e98667.

76. Salomon C, Scholz-Romero K, Sarker S, Sweeney E, Kobayashi M, Correa P, et al. Gestational diabetes mellitus is associated with changes in the concentration and bioactivity of placenta-derived exosomes in maternal circulation across gestation. Diabetes. 2016;65:598.

77. Vargas A, Zhou S, Ethier-Chiasson M, Flipo D, Lafond J, Gilbert C, et al. Syncytin proteins incorporated in placenta exosomes are important for cell uptake and show variation in abundance in serum exosomes from patients with preeclampsia. Faseb J. 2014;28:3703.

78. Alberry M, Maddocks D, Jones M, Abdel Hadi M, Abdel-Fattah S, Avent N, et al. Free fetal DNA in maternal plasma in anembryonic pregnancies: confirmation that the origin is the trophoblast. Prenat Diagn. 2007;27:415.

79. Flori E, Doray B, Gautier E, Kohler M, Ernault P, Flori J, et al. Circulating cell-free fetal DNA in maternal serum appears to originate from cyto- and syncytio-trophoblastic cells. Case report. Hum Reprod. 2004;19:723.

80. Lun FMF, Chiu RWK, Chan KC, Leung T, Lau T, Lo YM. Microfluidics digital PCR reveals a higher than expected fraction of fetal DNA in maternal plasma. Clin Chem. 2008;54:1664.

81. Gil MM, Quezada MS, Revello R, Akolekar R, Nicolaides KH. Analysis of cell-free DNA in maternal blood in screening for fetal aneuploidies: updated meta-analysis. Ultrasound Obstet Gynecol. 2015;45:249.

82. Fan H, Blumenfeld Y, Chitkara U, Hudgins L, Quake S. Noninvasive diagnosis of fetal aneuploidy by shotgun sequencing DNA from maternal blood. Proc Natl Acad Sci USA. 2008;105:16266.

83. Leung TN, Zhang J, Lau TK, Hjelm NM, Lo YMD. Maternal plasma fetal DNA as a marker for preterm labour. Lancet. 1998;352:1904.

84. Farina A, LeShane ES, Romero R, Gomez R, Chaiworapongsa T, Rizzo N, et al. High levels of fetal cell-free DNA in maternal serum: a risk factor for spontaneous preterm delivery. Am J Obstet Gynecol. 2005;193:421.

85. Jakobsen TR, Clausen FB, Rode L, Dziegiel MH, Tabor A. High levels of fetal DNA are associated with increased risk of spontaneous preterm delivery. Prenat Diagn. 2012;32:840.

86. Dugoff L, Barberio A, Whittaker P, Schwartz N, Sehdev H, Bastek J. Cell-free DNA fetal fraction and preterm birth. Am J Obstet Gynecol. 2016;215:231.

87. Poon LCY, Musci T, Song K, Syngelaki A, Nicolaides KH. Maternal plasma cell-free fetal and maternal DNA at 11-13 weeks' gestation: relation to fetal and maternal characteristics and pregnancy outcomes. Fetal Diagn Ther. 2013;33:215.

88. Quezada MS, Francisco C, Dumitrascu-Biris D, Nicolaides KH, Poon LC. Fetal fraction of cell-free DNA in maternal plasma in the prediction of spontaneous preterm delivery. Ultrasound Obstet Gynecol. 2015;45:101.

89. Poon LL, Leung TN, Lau TK, Lo YM. Presence of fetal RNA in maternal plasma. Clin Chem. 2000;46:1832.

90. Ng E, Tsui N, Lau T, Leung T, Chiu R, Panesar N, et al. mRNA of placental origin is readily detectable in maternal plasma. Proc Natl Acad Sci USA. 2003;100:4748.

91. Tsui NBY, Chim SSC, Chiu RWK, Lau TK, Ng EKO, Leung TN, et al. Systematic micro-array based identification of placental mRNA in maternal plasma: towards non-invasive prenatal gene expression profiling. J Med Genet. 2004;41:461.

92. Chim S, Lee W, Ting Y, Chan O, Lee S, Leung T. Systematic identification of spontaneous preterm birth-associated RNA transcripts in maternal plasma. PLoS One. 2012;7:e34328.

93. Stock O, Gordon L, Kapoor J, Walker SP, Whitehead C, Kaitu'u-Lino TJ, et al. Chorioamnionitis occurring in women with preterm rupture of the fetal membranes is associated with a dynamic increase in mRNAs coding cytokines in the maternal circulation. Reprod Sci. 2015;22:852.

94. Mayor-Lynn K, Toloubeydokhti T, Cruz AC, Chegini N. Expression profile of microRNAs and mRNAs in human placentas from pregnancies complicated by preeclampsia and preterm labor. Reprod Sci. 2011;18:46.

95. Chim SSC, Shing TKF, Hung ECW, Leung T, Lau T, Chiu RWK, et al. Detection and characterization of placental microRNAs in maternal plasma. Clin Chem. 2008;54:482.

96. Clausson B, Lichtenstein P, Cnattingius S. Genetic influence on birthweight and gestational length determined by studies in offspring of twins. BJOG. 2000;107:375.

97. Treloar SA, Macones GA, Mitchell LE, Martin NG. Genetic influences on premature parturition in an Australian twin sample. Twin Res Hum Genet. 2000;3:80.

98. Boyd HA, Poulsen G, Wohlfahrt J, Murray JC, Feenstra B, Melbye M. Maternal contributions to preterm delivery. Am J Epidemiol. 2009;170:1358.

99. Svensson AC, Sandin S, Cnattingius S, Reilly M, Pawitan Y, Hultman CM, et al. Maternal effects for preterm birth: a genetic epidemiologic study of 630,000 families. Am J Epidemiol. 2009;170:1365.

100. Porter TF, Fraser AM, Hunter CY, Ward RH, Varner MW. The risk of preterm birth across generations. Obstet Gynecol. 1997;90:63.

101. Kramer MS, Coates AL, Michoud M, Dagenais S, Hamilton EF, Papageorgiou A. Maternal anthropometry and idiopathic preterm labor. Obstet Gynecol. 1995;86:744.

102. Kandel DB, Wu P, Davies M. Maternal smoking during pregnancy and smoking by adolescent daughters. Am J Public Health. 1994;84:1407.

103. Bagaitkar J, Demuth DR, Scott DA. Tobacco use increases susceptibility to bacterial infection. Tob Induc Dis. 2008;4:12.

104. Arcavi L, Benowitz L. Cigarette smoking and infection. Arch Intern Med. 2004;164:2216.

105. Crawford N, Prendergast D, Oehlert JW, Shaw GM, Stevenson DK, Rappaport N, et al. Divergent patterns of mitochondrial and nuclear ancestry are associated with the risk for preterm birth. J Pediatr. 2018;194:46.

106. Little J. Invited Commentary: Maternal Effects in Preterm Birth-Effects of Maternal Genotype, Mitochondrial DNA, Imprinting, or Environment? Am J Epidemiol. 2009;170:1382.

107. Wilcox AJ, Skjærven R, Lie RT. Familial patterns of preterm delivery: maternal and fetal contributions. Am J Epidemiol. 2008;167:474.

108. York TP, Eaves LJ, Lichtenstein P, Neale MC, Svensson A, Latendresse S, et al. Fetal and maternal genes' influence on gestational age in a quantitative genetic analysis of 244,000 Swedish births. Am J Epidemiol. 2013;178:543.

109. Lunde A, Melve KK, Gjessing HK, Skjærven R, Irgens LM. Genetic and environmental influences on birth weight, birth length, head circumference, and gestational age by use of population-based parent-offspring data. Am J Epidemiol. 2007;165:734.

110. Cnattingius S, Reilly M, Pawitan Y, Lichtenstein P. Maternal and fetal genetic factors account for most of familial aggregation of preeclampsia: a population-based Swedish cohort study. Am J Med Genet. 2004;130:365.

111. Kaisho T, Akira S. Toll-like receptor function and signaling. J Allergy Clin Immunol. 2006;117:979.

112. Takeda K, Akira S. Toll-like receptor signalling. Nat Rev Immunol. 2004;4:499.

113. Lorenz E. Association between the Asp299Gly Polymorphisms in the toll-like receptor 4 and premature births in the finnish population. Pediatr Res. 2002;52:373.

114. Rey G, Skowronek F, Alciaturi J, Alonso J, Bertoni B, Sapiro R. Toll receptor 4 Asp299Gly polymorphism and its association with preterm birth and premature rupture of membranes in a south american population. Mol Hum Reprod. 2008;14:555.

115. Simhan HN, Krohn MA, Roberts JM, Zeevi A, Caritis SN. Interleukin-6 promoter −174 polymorphism and spontaneous preterm birth. Am J Obstet Gynecol. 2003;189:915.

116. Karody V, Reese S, Kumar N, Liedel J, Jarzembowski J, Sampath V. A toll-like receptor 9 (rs352140) variant is associated with placental inflammation in newborn infants. J Mat Fetal Neonatal Med. 2016;29:2210.

117. Reiman M, Kujari H, Ekholm E, Lapinleimu H, Lehtonen L, Haataja L. Interleukin-6 polymorphism is associated with chorioamnionitis and neonatal infections in preterm infants. J Pediatr. 2008;153:24.

118. Kazzi SNJ, Jacques SM, Qureshi F, Quasney MW, Kim UO, Buhimschi IA. Tumor necrosis factor-alpha allele lymphotoxin-alpha+250 is associated with the presence and severity of placental inflammation among preterm births. Pediatr Res. 2004;56:94.

119. Simhan HN. Maternal and fetal toll-like receptor 4 genotype and chorionic plate inflammatory lesions. Am J Obstet Gynecol. 2008;199:400.

120. Mingbin Liang, Xun Wang, Jin Li, Fan Yang, Zhian Fang, Lihua Wang, et al. Association of combined maternal-fetal tnf-α gene g308a genotypes with preterm delivery: a gene-gene interaction study. J Biomed Biotechnol. 2010;2010:396184.

121. Pereyra S, Bertoni B, Sapiro R. Interactions between environmental factors and maternal–fetal genetic variations: strategies to elucidate risks of preterm birth. Eur J Obstet Gynecol Reprod Biol. 2016;202:20.

122. Colucci F. The role of KIR and HLA interactions in pregnancy complications. Immunogenet. 2017;69:557.

123. Hiby SE, Walker JJ, O'shaughnessy KM, Redman CW, Carrington M, Trowsdale J, et al. Combinations of maternal KIR and fetal HLA-C genes influence the risk of preeclampsia and reproductive success. J Exp Med. 2004;200:957.

124. Zhang H, Baldwin DA, Bukowski RK, Parry S, Xu Y, Song C, et al. A genome-wide association study of early spontaneous preterm delivery. Genet Epidemiol. 2015;39:217.

125. Wu W, Clark EAS, Manuck TA, Esplin MS, Varner MW, Jorde LB. A genome-wide association study of spontaneous preterm birth in a european population. F1000Research. 2013;2:255.

126. Rappoport N, Toung J, Hadley D, Wong RJ, Fujioka K, Reuter J, et al. A genome-wide association study identifies only two ancestry specific variants associated with spontaneous preterm birth. Sci Rep. 2018;8:1.

127. Zhang G, Feenstra B, Bacelis J, Liu X, Muglia LM, Juodakis J, et al. Genetic associations with gestational duration and spontaneous preterm birth. N Engl J Med. 2017;377:1156.

128. McGinnis R, Steinthorsdottir V, William NO, Thorleifsson G, Shooter S, Hjartardottir S, et al. Variants in the fetal genome near FLT1 are associated with risk of preeclampsia. Nat Genet. 2017;49:1255.

129. Lockwood CJ, Kuczynski E. Risk stratification and pathological mechanisms in preterm delivery. Paediatr Perinat Epidemiol. 2001;15:78.

130. Uzun A, Dewan AT, Istrail S, Padbury JF. Pathway-based genetic analysis of preterm birth. Genomics. 2013;101:163.

131. Capece A, Vasieva O, Meher S, Alfirevic Z, Alfirevic A. Pathway analysis of genetic factors associated with spontaneous preterm birth and pre-labor preterm rupture of membranes. PLOS One. 2014;9:e108578.

132. Hsu C, Meaddough E, Aversa K, Hong S, Lu L, Jones DC, et al. Elevated amniotic fluid levels of leukemia inhibitory factor, interleukin 6, and interleukin 8 in intra-amniotic infection. Am J Obstet Gynecol. 1998;179:1267.

133. Mittal P, Romero R, Kusanovic JP, Edwin SS, Gotsch F, Mazaki-Tovi S, et al. CXCL6 (granulocyte chemotactic protein-2): a novel chemokine involved in the innate immune response of the amniotic cavity. Am J Reprod Immunol. 2008;60:246.

134. Pollard JW, Guleria I. The trophoblast is a component of the innate immune system during pregnancy. Nat Med. 2000;6:589.

135. Moussa M, Roques P, Fievet N, Menu E, Maldonado-Estrada JG, Brunerie J, et al. Placental cytokine and chemokine production in HIV-1-infected women: trophoblast cells show a different pattern compared to cells from HIV-negative women. Clin Exp Immunol. 2001;125:455.

136. Abrahams VM, Schaefer TM, Fahey JV, Visintin I, Wright JA, Aldo PB, et al. Expression and secretion of antiviral factors by trophoblast cells following stimulation by the TLR-3 agonist, Poly(I : C). Hum Reprod. 2006;21:2432.

137. Trautman MS, Dudley DJ, Edwin SS, Collmer D, Mitchell MD. Amnion cell biosynthesis of interleukin-8: regulation by inflammatory cytokines. J Cell Physiol. 1992;153:38.

138. Wadhwa P, Culhane J, Rauh V, Barve S. Stress and preterm birth: neuroendocrine, immune/inflammatory, and vascular mechanisms. Matern Child Health J. 2001;5:119.

139. Liggins G. Premature delivery of foetal lambs infused with glucocorticoids. J Endocrinol. 1969;45:515.

140. Huusko JM, Karjalainen MK, Graham BE, Zhang G, Farrow EG, Miller NA, et al. Whole exome sequencing reveals HSPA1L as a genetic risk factor for spontaneous preterm birth. PLOS Genet. 2018;14:e1007394.

141. Chaiworapongsa T, Erez O, Kusanovic JP, Vaisbuch E, Mazaki-Tovi S, Gotsch F, et al. Amniotic fluid heat shock protein 70 concentration in histologic chorioamnionitis, term and preterm parturition. J Mat Fetal Neonatal Med. 2008;21:449.

142. Fekete A, Vér Á, Bögi K, Treszl A, Rigó J. Is preeclampsia associated with higher frequency of HSP70 gene polymorphisms? Eur J Obstet Gynecol. 2006;126:197.

143. Salafia CM, Vogel CA, Vintzileos AM, Bantham KF, Pezzullo J, Silberman L. Placental pathologic findings in preterm birth. Am J Obstet Gynecol. 1991;165:934.

144. Mueller-Heubach E, Rubinstein D, Schwarz S. Histologic chorioamnionitis and preterm delivery in different patient populations. Obstet Gynecol. 1990;75:622.

145. Andrews WW, Goldenberg RL, Faye-Petersen O, Cliver S, Goepfert AR, Hauth JC. The alabama preterm birth study: polymorphonuclear and mononuclear cell placental infiltrations, other markers of inflammation, and outcomes in 23- to 32-week preterm newborn infants. Am J Obstet Gynecol. 2006;195:803.

146. Perkins R, Zhou S, Butler C, Skipper B. Histologic chorioamnionitis in pregnancies of various gestational ages: implications in preterm rupture of membranes. Obstet Gynecol. 1987;70:856.

147. Lahra MM, Jeffery HE. A fetal response to chorioamnionitis is associated with early survival after preterm birth. Am J Obstet Gynecol. 2004;190:147.

148. Hecht JL, Allred EN, Kliman HJ, Zambrano E, Doss BJ, Husain A, et al. Histological characteristics of singleton placentas delivered before the 28th week of gestation. Pathol. 2008;40:372.

149. Ghidini A, Salafia CM. Histologic placental lesions in women with recurrent preterm delivery. Acta Obstet Gynecol Scand. 2005;84:547.

150. Himes KP, Simhan HN. Risk of recurrent preterm birth and placental pathology. Obstet Gynecol. 2008;112:121.

151. Goldenberg RL, Andrews WW, Faye-Petersen O, Cliver S, Goepfert AR, Hauth JC. The alabama preterm birth project: placental histology in recurrent spontaneous and indicated preterm birth. Am J Obstet Gynecol. 2006;195:792.

152. Nijman T, van Vliet E, Benders M, Mol B, Franx A, Nikkels P, et al. Placental histology in spontaneous and indicated preterm birth: a case control study. Placenta. 2016;48:56.

153. Adams MM, Elam-Evans LD, Wilson HG, Gilbertz DA. Rates of and factors associated with recurrence of preterm delivery. JAMA. 2000;283:1591.

154. Kistka Z, Palomar L, Lee K, Boslaugh S, Wangler M, Cole F, et al. Racial disparity in the frequency of recurrence of preterm birth. Am J Obstet Gynecol. 2007;196:131.

155. Ness RB, Hillier S, Richter HE, Soper DE, Stamm C, Bass DC, et al. Can known risk factors explain racial differences in the occurrence of bacterial vaginosis? J Natl Med Assoc. 2003;95:201.

156. Goldenberg RL, Klebanoff MA, Nugent R, Krohn MA, Hillier S, Andrews WW. Bacterial colonization of the vagina during pregnancy in four ethnic groups. Am J Obstet Gynecol. 1996;174:1618.

157. Hitti J, Nugent R, Boutain D, Gardella C, Hillier SL, Eschenbach DA. Racial disparity in risk of preterm birth associated with lower genital tract infection. Paediatr Perinat Epidemiol. 2007;21:330.

158. Fassett M, Wing D, Getahun D. Temporal trends in chorioamnionitis by maternal race/ethnicity and gestational age (1995–2010). Int J Reprod Med. 2013;2013:1.

159. Shen T, DeFranco E, Stamilio D, Chang J, Muglia L. A population-based study of race-specific risk for preterm premature rupture of membranes. Am J Obstet Gynecol. 2008;199:373.

160. Dammann O, Leviton A, Allred EN. What explains away the increased risk of histological chorioamnionitis in African-American mothers of very-low-birthweight infants? Paediatr Perinat Epidemiol. 2000;14:20.

161. Ogunyemi D, Murillo M, Jackson U, Hunter N, Alperson B. The relationship between placental histopathology findings and perinatal outcome in preterm infants. J Matern Fetal Neonatal Med. 2003;13:102.

162. Blumenshine P, Egerter S, Barclay CJ, Cubbin C, Braveman PA. Socioeconomic disparities in adverse birth outcomes: a systematic review. Am J Prev Med. 2010;39:263.

163. Peacock JL, Bland JM, Anderson HR. Preterm delivery: effects of socioeconomic factors, psychological stress, smoking, alcohol, and caffeine. BMJ. 1995;311:531.

164. McGrady GA, Sung JF, Rowley DL, Hogue CJ. Preterm delivery and low birth weight among first-born infants of black and white college graduates. Am J Epidemiol. 1992;136:266.

165. Gardner MO, Goldenberg RL. The influence of race and previous pregnancy outcome on outcomes in the current pregnancy. Semin Perinatol. 1995;19:191.

166. Culhane J, Goldenberg R. Racial disparities in preterm birth. Semin Perinatol. 2011;35:234.

167. Fettweis JM, Brooks JP, Serrano MG, Sheth NU, Girerd PH, Edwards DJ, et al. Differences in vaginal microbiome in African American women versus women of European ancestry. Microbiol. 2014;160:2272.

168. Menon R, Merialdi M, Lombardi SJ, Fortunato SJ. Differences in the placental membrane cytokine response: a possible explanation for the racial disparity in preterm birth. Am J Reprod Immunol. 2006;56:112.

169. Sadowsky D, Novy M, Witkin S, Gravett M. Dexamethasone or interleukin-10 blocks interleukin-1beta-induced uterine contractions in pregnant rhesus monkeys. Am J Obstet Gynecol. 2003;188:252.

170. Fortunato SJ, Lombardi SJ, Menon R. Racial disparity in membrane response to infectious stimuli: a possible explanation for observed differences in the incidence of prematurity: community award paper. Am J Obstet Gynecol. 2004;190:1557.

171. Vadillo-Ortega F, Estrada-Gutierrez G. Role of matrix metalloproteinases in preterm labour. BJOG. 2005;112:19.

172. Menon R, Thorsen P, Vogel I, Jacobsson B, Morgan N, Jiang L, et al. Racial disparity in amniotic fluid concentrations of tumor necrosis factor (TNF)-α and soluble TNF receptors in spontaneous preterm birth. Am J Obstet Gynecol. 2008;198:533.

173. Menon R, Camargo C, Thorsen P, Lombardi S, Fortunato S. Amniotic fluid interleukin-6 increase is an indicator of spontaneous preterm birth in white but not black americans. Am J Obstet Gynecol. 2008;198:77.

174. Menon R, Williams SM, Fortunato SJ. Amniotic fluid interleukin-1β and interleukin-8 concentrations: racial disparity in preterm birth. Reprod Sci. 2007;14:253.

175. Velez DR, Fortunato SJ, Williams SM, Menon R. Interleukin-6 (IL-6) and receptor (IL6-R) gene haplotypes associate with amniotic fluid protein concentrations in preterm birth. Hum Mol Genet. 2008;17:1619.

176. Reiman M. Interleukin-6 polymorphism is associated with chorioamnionitis and neonatal infections in preterm infants. J Pediatr. 2008;153:24.

177. Holla LI, Fassmann A, Stejskalová A, Znojil V, Vaněk J, Vacha J. Analysis of the interleukin-6 gene promoter polymorphisms in czech patients with chronic periodontitis. J Periodontol. 2004;75:30.

178. Kaemaeraeinen O, Solovieva S, Vehmas T, Luoma K, Riihimaeki H, Ala-Kokko L, et al. Common interleukin-6 promoter variants associate with the more severe forms of distal interphalangeal osteoarthritis. Arthritis Res Ther. 2008;10: 21.

179. Menon R, Pearce B, Velez DR, Merialdi M, Williams SM, Fortunato SJ, et al. Racial disparity in pathophysiologic pathways of preterm birth based on genetic variants. Reprod Biol Endocrinol. 2009;7:62.

180. Deichmann U. Epigenetics: the origins and evolution of a fashionable topic. Dev Biol. 2016;416:249.

181. Haig D. The (dual) origin of epigenetics. Cold Spring Harb Symp Quant Biol. 2004;69:67.

182. Henikoff S, Greally JM. Epigenetics, cellular memory and gene regulation. Curr Biol. 2016;26:648.

183. Lappalainen T, Greally JM. Associating cellular epigenetic models with human phenotypes. Nat Rev Genet. 2017;18:441.

184. Waddington CH. Organisers and genes. Cambridge: Univ Pr. 1940.

185. Waddington CH. The strategy of the genes: a discussion of some aspects of theoretical biology. England: Allen & Unwin. 1957.

186. Greally J. A user's guide to the ambiguous word 'epigenetics'. Nat Rev. 2018;19:207.

187. Bird A. Perceptions of epigenetics. Nature. 2007;447:396.

188. Anonymous, International Human Genome Sequencing Consortium. Initial sequencing and analysis of the human genome. Nature. 2001;409:860.

189. Hashimoto H, Liu Y, Upadhyay AK, Chang Y, Howerton SB, Vertino PM, et al. Recognition and potential mechanisms for replication and erasure of cytosine hydroxymethylation. Nucleic Acids Res. 2012;40:4841.

190. Green BB, Houseman E, Johnson KC, Guerin DJ, Armstrong DA, Christensen BC, et al. Hydroxymethylation is uniquely distributed within term placenta, and is associated with gene expression. Faseb J. 2016;30:2874.

191. Jin S, Wu X, Li AX, Pfeifer GP. Genomic mapping of 5-hydroxymethylcytosine in the human brain. Nucleic Acids Res. 2011;39:5015.

192. Gardiner-Garden M, Frommer M. CpG islands in vertebrate genomes. J Mol Biol. 1987;196:261.

193. Ramsahoye B, Biniszkiewicz D, Lyko F, Clark V, Bird A, Jaenisch R. Non-CpG methylation is prevalent in embryonic stem cells and may be mediated by DNA methyltransferase 3a. Proc Natl Acad Sci USA. 2000;97:5237.

194. Guo J, Su Y, Shin J, Shin J, Li H, Xie B, et al. Distribution, recognition and regulation of non-CpG methylation in the adult mammalian brain. Nat Neurosci. 2014;17:215.

195. Jjingo D, Conley AB, Yi SV, Lunyak VV, Jordan IK. On the presence and role of human gene-body DNA methylation. Oncotarget. 2012;3:462.

196. Cedar H, Bergman Y. Linking DNA methylation and histone modification: patterns and paradigms. Nat Rev Genet. 2009;10:295.

197. Fuks F. DNA methylation and histone modifications: teaming up to silence genes. Curr Opin Genet Dev. 2005;15:490.

198. Hannon E, Lunnon K, Schalkwyk L, Mill J. Interindividual methylomic variation across blood, cortex, and cerebellum: implications for epigenetic studies of neurological and neuropsychiatric phenotypes. Epigenetics. 2015;10:1024.

199. Yuen RK, Neumann SM, Fok AK, Peñaherrera MS, McFadden DE, Robinson WP, et al. Extensive epigenetic reprogramming in human somatic tissues between fetus and adult. Epigenetics Chromatin. 2011;4:7.

200. Farlik M, Halbritter F, Müller F, Choudry FA, Ebert P, Klughammer J, et al. DNA methylation dynamics of human hematopoietic stem cell differentiation. Cell Stem Cell. 2016;19:808.

201. Reinius L, Acevedo N, Joerink M, Pershagen G, Dahlén S, Greco D, et al. Differential DNA methylation in purified human blood cells: implications for cell lineage and studies on disease susceptibility. PLOS One. 2012;7:41361.

202. Bock C, Beerman I, Lien W, Smith Z, Gu H, Boyle P, et al. DNA methylation dynamics during in vivo differentiation of blood and skin stem cells. Mol Cell. 2012;47:633.

203. Pacis A, Tailleux L, Morin AM, Lambourne J, MacIsaac JL, Yotova V, et al. Bacterial infection remodels the DNA methylation landscape of human dendritic cells. Genome Res. 2015;25:1801.

204. Moran S, Arribas C, Esteller M. Validation of a DNA methylation microarray for 850,000 CpG sites of the human genome enriched in enhancer sequences. Epigenomics. 2016;8:389.

205. Robinson MD, Stirzaker C, Statham AL, Coolen MW, Song JZ, Nair SS, et al. Evaluation of affinity-based genome-wide DNA methylation data: effects of cpg density, amplification bias, and copy number variation. Genome Res. 2010;20:1719.

206. Yong W, Hsu F, Chen P. Profiling genome-wide DNA methylation. Epigenet Chromatin. 2016;9:26.

207. Robinson WP, Price EM. The human placental methylome. Cold Spring Harb Perspect Med. 2015;5:023044.

208. Schroeder DI, Blair JD, Lott P, Yu HOK, Hong D, Crary F, et al. The human placenta methylome. Proc Natl Acad Sci USA. 2013;110:6037.

209. Du P, Zhang X, Huang C, Jafari N, Kibbe WA, Hou L, et al. Comparison of beta-value and m-value methods for quantifying methylation levels by microarray analysis. BMC Bioinformatics. 2010;11:587.

210. Novakovic B, Saffery R. Placental pseudo-malignancy from a DNA methylation perspective: unanswered questions and future directions. Front Genet. 2013;4:285.

211. Frendo J, Olivier D, Cheynet V, Blond J, Bouton O, Vidaud M, et al. Direct involvement of HERV-W Env glycoprotein in human trophoblast cell fusion and differentiation. Mol Cell Biol. 2003;23:3566.

212. Novakovic B, Yuen RK, Gordon L, Penaherrera MS, Sharkey A, Moffett A, et al. Evidence for widespread changes in promoter methylation profile in human placenta in response to increasing gestational age and environmental/stochastic factors. BMC Genomics. 2011;12:529.

213. Konwar C, Price M, Wang Li Qing, Wilson S, Terry J, Robinson W. DNA methylation profiling of acute chorioamnionitis-associated placentas and fetal membranes: insights into epigenetic variation in spontaneous preterm births. Epigenet Chromatin. 2018;11:63.

214. Kim J, Pitlick M, Christine P, Schaefer A, Saleme C, Comas B, et al. Genome-wide analysis of DNA methylation in human amnion. Sci World J. 2013;2013:1.

215. Tilley SK, Martin EM, Smeester L, Joseph RM, Kuban KCK, Heeren TC, et al. Placental CpG methylation of infants born extremely preterm predicts cognitive impairment later in life. PlOS One. 2018;13:0193271.

216. Behnia F, Parets S, Kechichian T, Yin H, Dutta E, Saade G, et al. Fetal DNA methylation of autism spectrum disorders candidate genes: association with spontaneous preterm birth. Am J Obstet Gynecol. 2015;212:533.

217. Sundrani DP, Reddy US, Chavan-Gautam PM, Mehendale SS, Chandak GR, Joshi SR. Altered methylation and expression patterns of genes regulating placental angiogenesis in preterm pregnancy. Reprod Sci. 2014;21:1508.

218. Geeleher P, Hartnett L, Egan LJ, Golden A, Raja Ali RA, Seoighe C. Gene-set analysis is severely biased when applied to genome-wide methylation data. Bioinformatics. 2013;29:1851.

219. Esplin MS, Manuck TA, Varner MW, Christensen B, Biggio J, Bukowski R, et al. Cluster analysis of spontaneous preterm birth phenotypes identifies potential associations among preterm birth mechanisms. Am J Obstet Gynecol. 2015;213:429.

220. Nygaard V, Rødland EA, Hovig E. Methods that remove batch effects while retaining group differences may lead to exaggerated confidence in downstream analyses. Biostatistics. 2016;17:29.

221. Toure D, ElRayes W, Barnes-Josiah D, Hartman T, Klinkebiel D, Baccaglini L. Epigenetic modifications of human placenta associated with preterm birth: A systematic review. J Mater Fetal Neonatal Med. 2018;31:530.

222. Eidem HR, Ackerman WE, William E, McGary KL, Abbot P, Rokas A. Gestational tissue transcriptomics in term and preterm human pregnancies: a systematic review and meta-analysis. BMC Med Genomics. 2015;8:27.

223. Chim S, Lee W, Ting Y, Chan O, Lee S, Leung T. Systematic identification of spontaneous preterm birth-associated RNA transcripts in maternal plasma. PLOS One. 2012;7:34328.

224. Lee K, Shim S, Kang K, Kang J, Park D, Kim S, et al. Global gene expression changes induced in the human placenta during labor. Placenta. 2010;31:698.

225. Waring G, Robson S, Bulmer J, Tyson-Capper A. Inflammatory signalling in fetal membranes: increased expression levels of TLR 1 in the presence of preterm histological chorioamnionitis. PLOS One. 2015;10:0124298.

226. Raman K, Wang H, Troncone M, Khan W, Pare G, Terry J. Overlap chronic placental inflammation is associated with a unique gene expression pattern. PLOS One. 2015;10:0133738.

227. Kim YM, Kim GJ, Kim MR, Romero R, Chaiworapongsa T, Kuivaniemi H, et al. Toll-like receptor-2 and -4 in the chorioamniotic membranes in spontaneous labor at term and in preterm parturition that are associated with chorioamnionitis. Am J Obstet Gynecol. 2004;191:1346.

228. Haddad R, Tromp G, Kuivaniemi H, Chaiworapongsa T, Kim YM, Mazor M, et al. Human spontaneous labor without histologic chorioamnionitis is characterized by an acute inflammation gene expression signature. Am J Obstet Gynecol. 2006;195:405.

229. Kotlabova K, Doucha J, Hromadnikova I. Placental-specific microRNA in maternal circulation – identification of appropriate pregnancy-associated microRNAs with diagnostic potential. J Reprod Immunol. 2011;89:185.

230. Mouillet J, Chu T, Sadovsky Y. Expression patterns of placental microRNAs. Birth Defects Res. 2011;91:737.

231. Enquobahrie D, Abetew D, Sorensen T, Willoughby D, Chidambaram K, Williams M. Placental microRNA expression in pregnancies complicated by preeclampsia. Am J Obstet Gynecol. 2011;204:178.

232. Pineles B, Romero R, Montenegro D, Tarca A, Han Y, Kim Y, et al. Distinct subsets of microRNAs are expressed differentially in the human placentas of patients with preeclampsia. Am J Obstet Gynecol. 2007;196:261.

233. Hromadnikova I, Kotlabova K, Ivankova K, Krofta L. Expression profile of C19MC microRNAs in placental tissue of patients with preterm prelabor rupture of membranes and spontaneous preterm birth. Mol Med Rep. 2017;16:3849.

234. Enquobahrie DA, Hensley M, Qiu C, Abetew DF, Hevner K, Tadesse MG, et al. Candidate gene and MicroRNA expression in fetal membranes and preterm delivery risk. Reprod Sci. 2016;23:731.

235. Montenegro D, Romero R, Pineles BL, Tarca AL, Kim YM, Draghici S, et al. Differential expression of microRNAs with progression of gestation and inflammation in the human chorioamniotic membranes. Am J Obstet Gynecol. 2007;197:289.

236. do Imperio G, Bloise E, Javam M, Lye P, Constantinof A, Dunk C, et al. Chorioamnionitis induces a specific signature of placental ABC transporters associated with an increase of miR-331-5p in the human preterm placenta. Cell Physiol Biochem. 2018;45:591.

237. Kramer MS, Platt RW, Wen SW, Joseph KS, Allen A, Abrahamowicz M, et al. A new and improved population-based canadian reference for birth weight for gestational age. Pediatrics. 2001;108:35.

238. Magee LA, Pels A, Helewa M, Rey E, von Dadelszen P. Diagnosis, evaluation, and management of the hypertensive disorders of pregnancy. Pregnancy Hypertens. 2014;4:105.

239. Avila L, Yuen R, Diego-Alvarez D, Peñaherrera M, Jiang R, Robinson WP. Evaluating DNA methylation and gene expression variability in the human term placenta. Placenta. 2010;31:1070.

240. Miller SA, Dykes DD, Polesky HF. A simple salting out procedure for extracting DNA from human nucleated cells. Nucleic Acids Res. 1988;16:1215.

241. Lizio M, Harshbarger J, Shimoji H, Severin J, Kasukawa T, Sahin S, et al. Gateways to the FANTOM5 promoter level mammalian expression atlas. Genome Biol. 2015;16:22.

242. ENCODE Project Consortium. An integrated encyclopedia of DNA elements in the human genome: the ENCODE project consortium. Nature. 2012;489:57.

243. Harper KN, Peters BA, Gamble MV. Batch effects and pathway analysis: two potential perils in cancer studies involving DNA methylation array analysis. Cancer Epidemiol Biomarkers Prev. 2013;22:1052.

244. Buhule OD, Minster RL, Hawley NL, Medvedovic M, Sun G, Viali S, et al. Stratified randomization controls better for batch effects in 450K methylation analysis: a cautionary tale. Front Genet. 2014;5:354.

245. Price EM, Robinson WP. Adjusting for batch effects in DNA methylation microarray data, a lesson learned. Front Genet. 2018;9:83.

246. Leek JT, Johnson WE, Parker HS, Jaffe AE, Storey JD. The sva package for removing batch effects and other unwanted variation in high-throughput experiments. Bioinformatics. 2012;28:882.

247. Dedeurwaerder S, Defrance M, Calonne E, Denis H, Sotiriou C, Fuks F. Evaluation of the infinium methylation 450K technology. Epigenomics. 2011;3:771.

248. Bibikova M, Barnes B, Tsan C, Ho V, Klotzle B, Le JM, et al. High density DNA methylation array with single CpG site resolution. Genomics. 2011;98:288.

249. Fortin J, Labbe A, Lemire M, Zanke BW, Hudson TJ, Fertig EJ, et al. Functional normalization of 450k methylation array data improves replication in large cancer studies. Genome Biol. 2014;15:503.

250. Maksimovic J, Gordon L, Oshlack A. SWAN: Subset-quantile within array normalization for illumina infinium HumanMethylation450 BeadChips. Genome Biol. 2012;13:44.

251. Triche J, Timothy J, Weisenberger DJ, Van Den Berg D, Laird PW, Siegmund KD. Low-level processing of Illumina Infinium DNA Methylation BeadArrays. Nucleic Acids Res. 2013;41:90.

252. Teschendorff AE, Marabita F, Lechner M, Bartlett T, Tegner J, Gomez-Cabrero D, et al. A beta-mixture quantile normalization method for correcting probe design bias in Illumina Infinium 450 k DNA methylation data. Bioinformatics. 2013;29:189.

253. Gabriel S, Ziaugra L, Tabbaa D. SNP genotyping using the sequenom MassARRAY iPLEX platform. Curr Protoc Hum Genet. 2009;2:2.

254. Förster T. Zwischenmolekulare Energiewanderung und Fluoreszenz. Annalen der Physik. 1948;437:55.

255. Phillips C, Salas A, Sánchez JJ, Fondevila M, Gómez-Tato A, Álvarez-Dios J, et al. Inferring ancestral origin using a single multiplex assay of ancestry-informative marker SNPs. Forensic Sci Int Genet. 2007;1:273.

256. Fondevila M, Phillips C, Santos C, Freire Aradas A, Vallone PM, Butler JM, et al. Revision of the SNPforID 34-plex forensic ancestry test: Assay enhancements, standard reference sample genotypes and extended population studies. Forensic Sci Int Genet. 2013;7:63.

257. Phillips C, Freire Aradas A, Kriegel AK, Fondevila M, Bulbul O, Santos C, et al. Eurasiaplex: a forensic SNP assay for differentiating european and south asian ancestries. Forensic Sci Int Genet. 2013;7:359.

258. Del Gobbo GF, Price EM, Hanna CW, Robinson WP. No evidence for association of MTHFR 677C>T and 1298A>C variants with placental DNA methylation. Clin Epigenetics. 2018;10:34.

259. Beck S, Wojdyla D, Say L, Betran AP, Merialdi M, Requejo JH, et al. The worldwide incidence of preterm birth: a systematic review of maternal mortality and morbidity. Bull World Health Organ. 2010;88:31.

260. Behrman RE. Preterm birth. Washington, DC: National Academies Press; 2007.

261. Wilcox AJ, Skjærven R, Lie RT. Familial patterns of preterm delivery: maternal and fetal contributions. Am J Epidemiol. 2008;167:474.

262. Goldenberg RL, Andrews WW, Faye-Petersen O, Cliver S, Goepfert AR, Hauth JC. The alabama preterm birth project: placental histology in recurrent spontaneous and indicated preterm birth. Am J Obstet Gynecol. 2006;195:792.

263. Shiono PH, Klebanoff MA. Ethnic differences in preterm and very preterm delivery. Am J Public Health. 1986;76:1317.

264. Kistka ZA, Palomar L, Lee KA, Boslaugh SE, Wangler MF, Cole FS, et al. Racial disparity in the frequency of recurrence of preterm birth. Am J Obstet Gynecol. 2007;196:131.

265. Menon R, Dunlop AL, Kramer MR, Fortunato SJ, Hogue CJ. An overview of racial disparities in preterm birth rates: caused by infection or inflammatory response? Acta Obstet Gynecol Scand. 2011;90:1325.

266. Genc M, Onderdonk A. Endogenous bacterial flora in pregnant women and the influence of maternal genetic variation. BJOG. 2011;118:154.

267. Chapman SJ, Hill AVS. Human genetic susceptibility to infectious disease. Nat Rev Genet. 2012;13:175.

268. Segal S, Hill A. Genetic susceptibility to infectious disease. Trends Microbiol. 2003;11:445.

269. Petersen L, Nielsen GG, Andersen PK, Sørensen TIA. Case-control study of genetic and environmental influences on premature death of adult adoptees. Genet Epidemiol. 2002;23:123.

270. Rovers MM, Haggard MP, Gannon M, Koeppen-Schomerus G, Plomin R. Heritability of symptom domains in otitis media: a longitudinal study of 1,373 twin pairs. Am J Epidemiol. 2002;155:958.

271. Stene LC, Honeyman MC, Hoffenberg EJ, Haas JE, Sokol RJ, Emery L, et al. Rotavirus infection frequency and risk of celiac disease autoimmunity in early childhood: a longitudinal study. Am J Gastroenterol. 2006;101:2333.

272. Koch A, Melbye M, Sørensen P, Homøe P, Madsen HO, Mølbak K, et al. Acute respiratory tract infections and mannose-binding lectin insufficiency during early childhood. JAMA. 2001;285:1316.

273. Krediet TG, Wiertsema SP, Vossers MJ, Hoeks SB, Fleer A, Ruven HJ, et al. Toll-like receptor 2 polymorphism is associated with preterm birth. Pediatr Res. 2007;62:474.

274. Thaxton J, Nevers T, Sharma S. TLR-mediated preterm birth in response to pathogenic agents. Infect Dis Obstet Gynecol. 2010;2010:1.

275. Speer EM, Gentile DA, Zeevi A, Pillage G, Huo D, Skoner DP. Role of single nucleotide polymorphisms of cytokine genes in spontaneous preterm delivery. Hum Immunol. 2006;67:915.

276. El-Bastawissi AY, Williams MA, Riley DE, Hitti J, Krieger JN. Amniotic fluid interleukin-6 and preterm delivery: a review. Obstet Gynecol. 2000;95:1056.

277. Wenstrom KD, Andrews WW, Hauth JC, Goldenberg RL, DuBard MB, Cliver SP. Elevated second-trimester amniotic fluid interleukin-6 levels predict preterm delivery. Am J Obstet Gynecol. 1998;178:546.

278. Sorokin Y, Romero R, Mele L, Wapner R, Iams J, Dudley D, et al. Maternal serum interleukin-6, c-reactive protein, and matrix metalloproteinase-9 concentrations as risk factors for preterm birth <32 weeks and adverse neonatal outcomes. Am J Perinatol. 2010;27:631.

279. Goepfert AR, Goldenberg RL, Andrews WW, Hauth JC, Mercer B, Iams J, et al. The preterm prediction study: association between cervical interleukin 6 concentration and spontaneous preterm birth. Am J Obstet Gynecol. 2001;184:483.

280. Ma Y, Smith CE, Lai C, Irvin MR, Parnell LD, Lee Y, et al. The effects of omega-3 polyunsaturated fatty acids and genetic variants on methylation levels of the interleukin-6 gene promoter. Mol Nutr Food Res. 2016;60:410.

281. Soto-Ramírez N, Arshad SH, Holloway JW, Zhang H, Schauberger E, Ewart S, et al. The interaction of genetic variants and DNA methylation of the interleukin-4 receptor gene increase the risk of asthma at age 18 years. Clin Epigenetics. 2013;5:1.

282. Zhang H, Tong X, Holloway JW, Rezwan FI, Lockett GA, Patil V, et al. The interplay of DNA methylation over time with Th2 pathway genetic variants on asthma risk and temporal asthma transition. Clin Epigenetics. 2014;6:8.

283. Bell JT, Pai AA, Pickrell JK, Gaffney DJ, Pique-Regi R, Degner JF, et al. Correction: DNA methylation patterns associate with genetic and gene expression variation in HapMap cell lines. Genome Biol. 2011;12:405.

284. Han H, Cortez CC, Yang X, Nichols PW, Jones PA, Liang G. DNA methylation directly silences genes with non-CpG island promoters and establishes a nucleosome occupied promoter. Hum Mol Genet. 2011;20:4299.

285. Gutierrez-Arcelus M, Lappalainen T, Montgomery SB, Buil A, Ongen H, Yurovsky A, et al. Passive and active DNA methylation and the interplay with genetic variation in gene regulation. Elife. 2013;2:00523.

286. Nile CJ, Read RC, Akil M, Duff GW, Wilson AG. Methylation status of a single CpG site in the IL6 promoter is related to IL6 messenger RNA levels and rheumatoid arthritis. Arthritis Rheum. 2008;58:2686.

287. van Eijk K, de Jong S, Boks M, Langeveld T, Colas F, Veldink J, et al. Genetic analysis of DNA methylation and gene expression levels in whole blood of healthy human subjects. BMC Genomics. 2012;13:636.

288. Annells MF, Hart PH, Mullighan CG, Heatley SL, Robinson JS, McDonald HM. Polymorphisms in immunoregulatory genes and the risk of histologic chorioamnionitis in Caucasoid women: a case control study. BMC Pregnancy Childb. 2005;5:4.

289. Simhan HN, Krohn MA, Zeevi A, Daftary A, Harger G, Caritis SN. Tumor necrosis factor–α promoter gene polymorphism -308 and chorioamnionitis. Obstet Gynecol. 2003;102:162.

290. Kerk J, Dördelmann M, Bartels DB, Brinkhaus MJ, Dammann C, Dörk T, et al. Multiplex measurement of cytokine/receptor gene polymorphisms and interaction between interleukin-10 (-1082) genotype and chorioamnionitis in extreme preterm delivery. J Soc Gynecol Investig. 2006;13:350.

291. Abu-Maziad A, Schaa K, Bell EF, Dagle JM, Cooper M, Marazita ML, et al. Role of polymorphic variants as genetic modulators of infection in neonatal sepsis. Pediatr Res. 2010;68:323.

292. Esposito S, Zampiero A, Pugni L, Tabano S, Pelucchi C, Ghirardi B, et al. Genetic polymorphisms and sepsis in premature neonates. PLOS One. 2014;9:101248.

293. Wilson SL, Leavey K, Cox BJ, Robinson WP. Mining DNA methylation alterations towards a classification of placental pathologies. Hum Mol Genet. 2018;27:135.

294. Auton A, Abecasis GR, Altshuler DM, Durbin RM, Abecasis GR, Bentley DR, et al. A global reference for human genetic variation. Nature. 2015;526:68.

295. Sandoval J, Heyn H, Moran S, Serra-Musach J, Pujana MA, Bibikova M, et al. Validation of a DNA methylation microarray for 450,000 CpG sites in the human genome. Epigenetics. 2011;6:692.

296. Blair JD, Yuen RKC, Lim BK, McFadden DE, von Dadelszen P, Robinson WP. Widespread DNA hypomethylation at gene enhancer regions in placentas associated with early-onset pre-eclampsia. Mol Hum Reprod. 2013;19:697.

297. Leavey K, Wilson SL, Bainbridge SA, Robinson WP, Cox BJ. Epigenetic regulation of placental gene expression in transcriptional subtypes of preeclampsia. Clin Epigenetics. 2018;10:28.

298. Solé X, Guinó E, Valls J, Iniesta R, Moreno V. SNPStats: a web tool for the analysis of association studies. Bioinformatics. 2006;22:1928.

299. Indumathi, B., Katkam, S. K., Krishna, L. S. R., & Kutala, V. K. Dual Effect of IL-6 -174 G/C polymorphism and promoter methylation in the risk of coronary artery disease among South Indians. Indian J Clin Biochem. 2018:1.

300. Ryan J, Pilkington L, Neuhaus K, Ritchie K, Ancelin M, Saffery R. Investigating the epigenetic profile of the inflammatory gene IL-6 in late-life depression. BMC Psychiatry. 2017;17:354.

301. Stefani FA, Viana MB, Dupim AC, Brito JAR, Gomez RS, da Costa JE, et al. Expression, polymorphism and methylation pattern of interleukin-6 in periodontal tissues. Immunobiology. 2012;218:1012.

302. Gaunt TR, Shihab HA, Hemani G, Min JL, Woodward G, Lyttleton O, et al. Systematic identification of genetic influences on methylation across the human life course. Genome Biol. 2016;17:61.

303. Abrahams VM, Schaefer TM, Fahey JV, Visintin I, Wright JA, Aldo PB, et al. Expression and secretion of antiviral factors by trophoblast cells following stimulation by the TLR-3 agonist, Poly(I:C). Hum Reprod. 2006;21:2432.

304. Hunter C, Jones S. IL-6 as a keystone cytokine in health and disease. Nat Immunol. 2015;16:448.

305. Fielding CA, McLoughlin RM, McLeod L, Colmont CS, Najdovska M, Grail D, et al. IL-6 regulates neutrophil trafficking during acute inflammation via STAT3. J Immunol. 2008;181:2189.

306. Hoge J, Yan I, Jaenner N, Schumacher V, Chalaris A, Steinmetz OM, et al. IL-6 controls the innate immune response against listeria monocytogenes via classical IL-6 signaling. J Immunol. 2013;190:703.

307. Foster CB, Lehrnbecher T, Samuels S, Stein S, Mol F, Metcalf JA, et al. An IL6 promoter polymorphism is associated with a lifetime risk of development of Kaposi sarcoma in men infected with human immunodeficiency virus. Blood. 2000;96:2562.

308. Ad'hiah AH, Mahmood AS, Al-kazaz AA, Mayouf KK. Gene expression and six single nucleotide polymorphisms of interleukin-6 in rheumatoid arthritis: A case-control study in Iraqi patients. Alexandria J Med. 2018;54:639.

309. Kaemaeraeinen O, Solovieva S, Vehmas T, Luoma K, Riihimaeki H, Ala-Kokko L, et al. Common interleukin-6 promoter variants associate with the more severe forms of distal interphalangeal osteoarthritis. Arthritis Res Ther. 2008;10:21.

310. Fishman D, Faulds G, Jeffery R, Mohamed-Ali V, Yudkin JS, Humphries S, et al. The effect of novel polymorphisms in the interleukin-6 (IL-6) gene on IL-6 transcription and plasma IL-6 levels, and an association with systemic-onset juvenile chronic arthritis. J Clin Invest. 1998;102:1369.

311. Gao S, Liang S, Pan M, Sun R, Chen C, Luan H, et al. Interleukin-6 genotypes and serum levels in Chinese Hui population. Int J Clin Exp Med. 2014;7:2851.

312. Pan M, Gao S, Jiang M, Guo J, Zheng J, Zhu J. Interleukin 6 promoter polymorphisms in normal Han Chinese population: frequencies and effects on inflammatory markers. J Invest Med. 2011;59:272.

313. Li J, Hong X, Mesiano S, Muglia LJ, Wang X, Snyder M, et al. Natural selection has differentiated the progesterone receptor among human populations. Am J Hum Genet. 2018;103:45.

314. Barreiro LB, Quach H, Laval G, Patin E, Quintana-Murci L. Natural selection has driven population differentiation in modern humans. Nat Genet. 2008;40:340.

315. Kameda T, Matsuzaki N, Sawai K, Okada T, Saji F, Matsuda T, et al. Production of interleukin-6 by normal human trophoblast. Placenta. 1990;11:205.

316. Champion H, Innes BA, Robson SC, Lash GE, Bulmer JN. Effects of interleukin-6 on extravillous trophoblast invasion in early human pregnancy. Mol Hum Reprod. 2012;18:391.

317. Benyo DF, Smarason A, Redman CW, Sims C, Conrad KP. Expression of inflammatory cytokines in placentas from women with preeclampsia. J Clin Endocrinol Metab. 2001;86:2505.

318. Dalrymple S, Slattery R, Aud D, Krishna M, Lucian L, Murray R. Interleukin-6 is required for a protective immune response to systemic Escherichia coli infection. Infect Immun. 1996;64:3231.

319. Romani L, Mencacci A, Cenci E, Spaccapelo R, Toniatti C, Puccetti P, et al. Impaired neutrophil response and CD4+ T helper cell 1 development in interleukin 6-deficient mice infected with Candida albicans. J Exp Med. 1996;183:1345.

320. Liu Z, Simpson R, Cheers C. Recombinant interleukin-6 protects mice against experimental bacterial infection. Infect Immun. 1992;60:4402.

321. Hume EBH, Cole N, Garthwaite LL, Khan S, Willcox MDP. A protective role for IL-6 in staphylococcal microbial keratitis. Invest Ophthalmol Vis Sci. 2006;47:4926.

322. Dandrea M, Donadelli M, Costanzo C, Scarpa A, Palmieri M. MeCP2/H3meK9 are involved in IL-6 gene silencing in pancreatic adenocarcinoma cell lines. Nucleic Acids Res. 2009;37:6681.

323. Klose RJ, Sarraf SA, Schmiedeberg L, McDermott SM, Stancheva I, Bird AP. DNA binding selectivity of MeCP2 due to a requirement for A/T sequences adjacent to methyl-CpG. Mol Cell. 2005;19:667.

324. Kim CJ, Romero R, Chaemsaithong P, Kim J. Chronic inflammation of the placenta: definition, classification, pathogenesis, and clinical significance. Am J Obstet Gynecol. 2015;213:69.

325. Lee J, Romero R, Dong Z, Xu Y, Qureshi F, Jacques S, et al. Unexplained fetal death has a biological signature of maternal anti-fetal rejection: chronic chorioamnionitis and alloimmune anti-human leucocyte antigen antibodies. Histopath. 2011;59:928.

326. Redline RW. Classification of placental lesions. Am J Obstet Gynecol. 2015;213:28.

327. Jones PA. Functions of DNA methylation: islands, start sites, gene bodies and beyond. Nat Rev Genet. 2012;13:484.

328. Liu Y, Hoyo C, Murphy S, Huang Z, Overcash F, Thompson J, et al. DNA methylation at imprint regulatory regions in preterm birth and infection. Am J Obstet Gynecol. 2013;208:395.

329. Du P, Kibbe WA, Lin SM. lumi: a pipeline for processing Illumina microarray. Bioinformatics. 2008;24:1547.

330. Price EM, Peñaherrera MS, Portales-Casamar E, Pavlidis P, Van Allen MI, McFadden DE, et al. Profiling placental and fetal DNA methylation in human neural tube defects. Epigenet Chromatin. 2016;9:6.

331. Pidsley R, Zotenko E, Peters TJ, Lawrence MG, Risbridger GP, Molloy P, et al. Critical evaluation of the Illumina MethylationEPIC BeadChip microarray for whole-genome DNA methylation profiling. Genome Biol. 2016;17:208.

332. Price ME, Cotton AM, Lam LL, Farré P, Emberly E, Brown CJ, et al. Additional annotation enhances potential for biologically-relevant analysis of the Illumina Infinium HumanMethylation450 BeadChip array. Epigenet Chromatin. 2013;6:4.

333. Edgar RD, Jones MJ, Robinson WP, Kobor MS. An empirically driven data reduction method on the human 450K methylation array to remove tissue specific non-variable CpGs. Clin Epigenetics. 2017;9:11.

334. Pidsley R, Wong C, Volta M, Lunnon K, Mill J, Schalkwyk L. A data-driven approach to preprocessing Illumina 450K methylation array data. BMC Genomics. 2013;14:293.

335. Benjamini Y, Hochberg Y. Controlling the false discovery rate: a practical and powerful approach to multiple testing. J R Stat Soc Ser B. 1995;57:289.

336. Martin A, Murakami P, Irizarry R. Using the charm package to estimate DNA methylation levels and find differentially methylated regions. Bioconductor Package. 2011.

337. Smyth GK. Limma: linear models for microarray data. Bioinformatics and Computational Biology Solutions Using R and Bioconductor. New York:Springer. 2005.

338. Reinius LE, Acevedo N, Joerink M, Pershagen G, Dahlén SE, Greco D, et al. Differential DNA methylation in purified human blood cells: implications for cell lineage and studies on disease susceptibility. PLOS One. 2012;7:41361.

339. Hanna CW, Peñaherrera MS, Saadeh H, Andrews S, McFadden DE, Kelsey G, et al. Pervasive polymorphic imprinted methylation in the human placenta. Genome Res. 2016;26:756.

340. Suzuki R, Shimodaira H. Pvclust: an R package for assessing the uncertainty in hierarchical clustering. Bioinformatics. 2006;22:1540.

341. Liu Y, Hayes DN, Nobel A, Marron JS. Statistical significance of clustering for high-dimension, low-sample size data. J Am Stat Assoc. 2008;103:1281.

342. Gillis J, Mistry M, Pavlidis P. Gene function analysis in complex data sets using ErmineJ. Nat Protoc. 2010;5:1148.

343. Cooperstock M, Campbell J. Excess males in preterm birth: interactions with gestational age, race, and multiple birth. Obstet Gynecol. 1996;88:189.

344. McGregor J, Leff M, Orleans M, Baron A. Fetal gender differences in preterm birth: findings in a north american cohort. Amer J Perinatol. 1992;9:43.

345. Mondal D, Galloway T, Bailey T, Mathews F. Elevated risk of stillbirth in males: systematic review and meta-analysis of more than 30 million births. BMC Med. 2014;12:220.

346. Ghidini A, Salafia CM. Gender differences of placental dysfunction in severe prematurity. BJOG. 2005;112:140.

347. Khoury MJ, Marks JS, McCarthy BJ, Zaro SM. Factors affecting the sex differential in neonatal mortality: the role of respiratory distress syndrome. Am J Obstet Gynecol. 1985;151:777.

348. Zeitlin J, Saurel-Cubizolles M, De Mouzon J, Rivera L, Ancel P, Blondel B, et al. Fetal sex and preterm birth: are males at greater risk? Hum Reprod. 2002;17:2762.

349. Veenstra van Nieuwenhoven AL, Heineman MJ, Faas MM. The immunology of successful pregnancy. Hum Reprod Update. 2003;9:347.

350. Kuang H, Chen Q, Zhang Y, Zhang L, Peng H, Ning L, et al. The cytokine gene CXCL14 restricts human trophoblast cell invasion by suppressing gelatinase activity. Endocrinology. 2009;150:5596.

351. Lu J, Chatterjee M, Schmid H, Beck S, Gawaz M. CXCL14 as an emerging immune and inflammatory modulator. J Inflamm. 2016;13:1.

352. Hara T, Tanegashima K. Pleiotropic functions of the CXC-type chemokine CXCL14 in mammals. J Biochem. 2012;151:469.

353. Catz SD. The role of Rab27a in the regulation of neutrophil function. Cell Microbiol. 2014;16:1301.

354. Werner S, Stamm H, Pandjaitan M, Kemming D, Brors B, Pantel K, et al. Iroquois homeobox 2 suppresses cellular motility and chemokine expression in breast cancer cells. BMC Cancer. 2015;15:896.

355. Chapman K, Holmes M, Seckl J. 11β-Hydroxysteroid Dehydrogenases: Intracellular Gate-Keepers of Tissue Glucocorticoid Action. Physiol Rev. 2013;93:1139.

356. Johnstone JF, Bocking AD, Unlugedik E, Challis JRG. The effects of chorioamnionitis and betamethasone on 11beta hydroxysteroid dehydrogenase types 1 and 2 and the glucocorticoid receptor in preterm human placenta. J Soc Gynecol Investig. 2005;12:238.

357. Shimoya K, Matsuzaki N, Taniguchi T, Okada T, Saji F, Murata Y. Interleukin-8 level in maternal serum as a marker for screening of histological chorioamnionitis at term. Int J Gynecol Obstet. 1997;57:153.

358. Ibarra Chavarría V, Sanhueza Smith P, Mota González M, del Rey Pineda G, Karchmer S. C-reactive protein as early marker of chorioamnionitis in premature rupture of membranes. Ginecol Obstet Mex. 1989;57:203.

359. Kim M, Lee Y, Seo K. Assessment of predictive markers for placental inflammatory response in preterm births. PLoS One. 2014;9:107880.

360. Trochez-Martinez R, Smith P, Lamont R. Use of C-reactive protein as a predictor of chorioamnionitis in preterm prelabour rupture of membranes: a systematic review. BJOG. 2007;114:796.

361. Sereepapong W, Limpongsanurak S, Triratanachat S, Wannakrairot P, Charuruks N, Krailadsiri P. The role of maternal serum C-reactive protein and white blood cell count in the prediction of chorioamnionitis in women with premature rupture of membranes. J Med Assoc Thai. 2001;84:360.

362. Smith EJ, Muller CL, Sartorius JA, White DR, Maslow AS. C-reactive protein as a predictor of chorioamnionitis. J Am Osteopath Assoc. 2012;112:660.

363. Kim Y, Romero R, Chaiworapongsa T, Kim G, Kim M, Kuivaniemi H, et al. Toll-like receptor-2 and -4 in the chorioamniotic membranes in spontaneous labor at term and in preterm parturition that are associated with chorioamnionitis. Am J Obstet Gynecol. 2004;191:1346.

364. deVos T, Tetzner R, Model F, Weiss G, Schuster M, Distler J, et al. Circulating methylated SEPT9 DNA in plasma is a biomarker for colorectal cancer. Clin Chem. 2009;55:1337.

365. Grützmann R, Molnar B, Pilarsky C, Habermann J, Schlag P, Saeger H, et al. Sensitive detection of colorectal cancer in peripheral blood by septin 9 DNA methylation assay. PLOS One. 2008;3:3759.

366. Belinsky SA. Gene-promoter hypermethylation as a biomarker in lung cancer. Nat Rev Cancer. 2004;4:707.

367. Fujiwara K, Fujimoto N, Tabata M, Nishii K, Matsuo K, Hotta K, et al. Identification of epigenetic aberrant promoter methylation in serum DNA is useful for early detection of lung cancer. Clin Cancer Res. 2005;11:1219.

368. Tsui DWY, Chan KCA, Chim SSC, Chan L, Leung T, Lau T, et al. Quantitative aberrations of hypermethylated RASSF1A gene sequences in maternal plasma in pre-eclampsia. Prenat Diagn. 2007;27:1212.

369. Papantoniou N, Bagiokos V, Agiannitopoulos K, Kolialexi A, Destouni A, Tounta G, et al. RASSF1A in maternal plasma as a molecular marker of preeclampsia. Prenat Diagn. 2013;33:682.

370. Rahmani E, Zaitlen N, Baran Y, Eng C, Hu D, Galanter J, et al. Sparse PCA corrects for cell type heterogeneity in epigenome-wide association studies. Nat Methods. 2016;13:443.

371. Romero R, Sepulveda W, Kenney JS, Archer LE, Allison AC, Sehgal PB. Interleukin 6 determination in the detection of microbial invasion of the amniotic cavity. Ciba F Symp. 1992;167:205.

372. Chim SSC, Shing TKF, Hung ECW, Leung T, Lau T, Chiu RWK, et al. Detection and characterization of placental microRNAs in maternal plasma. Clin Chem. 2008;54:482.

373. Lee RC, Ambros V. An extensive class of small RNAs in caenorhabditis elegans. Sci. 2001;294:862.

374. Lagos-Quintana M, Rauhut R, Lendeckel W, Tuschl T. Identification of novel genes coding for small expressed RNAs. Sci. 2001;294:853.

375. Minami K, Uehara T, Morikawa Y, Omura K, Kanki M, Horinouchi A, et al. miRNA expression atlas in male rat. Sci Data. 2014;1:140005.

376. Ludwig N, Leidinger P, Becker K, Backes C, Fehlmann T, Pallasch C, et al. Distribution of miRNA expression across human tissues. Nucleic Acids Res. 2016;44:3865.

377. Morales-Prieto D, Ospina-Prieto S, Chaiwangyen W, Schoenleben M, Markert U. Pregnancy-associated miRNA-clusters. J Reprod Immunol. 2012;97:51.

378. Luo S, Ishibashi O, Ishikawa G, Ishikawa T, Katayama A, Mishima T, et al. Human villous trophoblasts express and secrete placenta-specific microRNAs into maternal circulation via exosomes. Biol Reprod. 2009;81:717.

379. Ouyang Y, Mouillet J, Coyne C, Sadovsky Y. Review: placenta-specific microRNAs in exosomes – good things come in nano-packages. Placenta. 2013;35:73.

380. Chen D, Wang W. Human placental microRNAs and preeclampsia. Biol Reprod. 2013;88:130.

381. Montenegro D, Romero R, Pineles B, Tarca A, Kim Y, Draghici S, et al. Differential expression of microRNAs with progression of gestation and inflammation in the human chorioamniotic membranes. Am J Obstet Gynecol. 2007;197:289.

382. Ackerman W, Buhimschi I, Eidem H, Rinker D, Rokas A, Rood K, et al. Comprehensive RNA profiling of villous trophoblast and decidua basalis in pregnancies complicated by preterm birth following intra-amniotic infection. Placenta. 2016;44:23.

383. Pankuch G, Appelbaum P, Lorenz R, Botti J, Schachter J, Naeye R. Placental microbiology and histology and the pathogenesis of chorioamnionitis. Obstet Gynecol. 1984;64:802.

384. Shimoya K, Matsuzaki N, Taniguchi T, Kameda T, Koyama M, Neki R, et al. Human placenta constitutively produces interleukin-8 during pregnancy and enhances its production in intrauterine infection. Biol Reprod. 1992;47:220.

385. Gu Y, Sun J, Groome L, Wang Y. Differential miRNA expression profiles between the first and third trimester human placentas. Am J Physiol Endocrinol Metab. 2013;304:836.

386. Huang RS, Gamazon ER, Ziliak D, Wen Y, Im HK, Zhang W, et al. Population differences in microRNA expression and biological implications. RNA Biol. 2011;8:692.

387. Hromadnikova I, Kotlabova K, Ivankova K, Krofta L. First trimester screening of circulating C19MC microRNAs and the evaluation of their potential to predict the onset of preeclampsia and IUGR. PLOS One. 2017;12:0171756.

388. Zhu X, Han T, Sargent I, Yin G, Yao Y. Differential expression profile of microRNAs in human placentas from preeclamptic pregnancies vs normal pregnancies. Am J Obstet Gynecol. 2009;200:661.

389. Hromadnikova I, Kotlabova K, Ondrackova M, Pirkova P, Kestlerova A, Novotna V, et al. Expression profile of C19MC microRNAs in placental tissue in pregnancy-related complications. DNA Cell Biol. 2015;34:437.

390. Lee J, Kim CJ, Kim J, Lee D, Ahn S, Yoon BH. Increased miR-223 expression in foetal organs is a signature of acute chorioamnionitis with systemic consequences. J Cell Mol Med. 2018;22:1179.

391. Haneklaus M, Gerlic M, O'Neill LAJ, Masters SL. miR-223: infection, inflammation and cancer. J Intern Med. 2013;274:215.

392. Yang Y, Wang Y, Liang Q, Yao L, Gu S, Bai X. MiR-338-5p Promotes Inflammatory Response of Fibroblast-Like Synoviocytes in Rheumatoid Arthritis via Targeting SPRY1. J Cell Biochem. 2017;118:2295.

393. Qi J, Qiao Y, Wang P, Li S, Zhao W, Gao C. MicroRNA-210 negatively regulates LPS-induced production of proinflammatory cytokines by targeting NF-κB1 in murine macrophages. FEBS Lett. 2012;586:1201.

394. Lemaire J, Mkannez G, Guerfali FZ, Gustin C, Attia H, Sghaier RM, et al. MicroRNA Expression Profile in Human Macrophages in Response to Leishmania major Infection. PLOS Negl Trop Dis. 2013;7:2478.

395. Kiga K, Mimuro H, Suzuki M, Shinozaki-ushiku A, Kobayashi T, Sanada T, et al. Epigenetic silencing of miR-210 increases the proliferation of gastric epithelium during chronic Helicobacter pylori infection. Nat Commun. 2014;5:4497.

396. Ortega FJ, Moreno M, Mercader JM, Moreno-Navarrete JM, Fuentes-Batllevell N, Sabater M, et al. Inflammation triggers specific microRNA profiles in human adipocytes and macrophages and in their supernatants. Clin Epigenetics. 2015;7:49.

397. Taganov K, Boldin M, Chang K, Baltimore D. NF-κB-dependent induction of microRNA miR-146, an inhibitor targeted to signaling proteins of innate immune responses. Proc Natl Acad Sci USA. 2006;103:12481.

398. Xie Y, Shu R, Jiang S, Liu D, Ni J, Zhang X. MicroRNA-146 inhibits pro-inflammatory cytokine secretion through IL-1 receptor-associated kinase 1 in human gingival fibroblasts. J Inflamm. 2013;10:20.

399. Sharma N, Verma R, Kumawat KL, Basu A, Singh SK. miR-146a suppresses cellular immune response during Japanese encephalitis virus JaOArS982 strain infection in human microglial cells. J Neuroinflammation. 2015;12:30.

400. Perkins J, Dawes J, McMahon S, Bennett D, Orengo C, Kohl M. ReadqPCR and NormqPCR: R packages for the reading, quality checking and normalisation of RT-qPCR quantification cycle (Cq) data. BMC Genomics. 2012;13:296.

401. Livak KJ, Schmittgen TD. Analysis of relative gene expression data using real-time quantitative PCR and 2− ΔΔCT method. Methods. 2001;25:402.

402. Lewis BP, Shih I, Jones-Rhoades MW, Bartel DP, Burge CB. Prediction of mammalian microRNA targets. Cell. 2003;115:787.

403. Wang X. miRDB: a microRNA target prediction and functional annotation database with a wiki interface. RNA. 2008;14:1012.

404. Liberzon A, Subramanian A, Pinchback R, Thorvaldsdóttir H, Tamayo P, Mesirov JP. Molecular signatures database (MSigDB) 3.0. Bioinformatics. 2011;27:1739.

405. Riffo-Campos ÁL, Riquelme I, Brebi-Mieville P. Tools for Sequence-Based miRNA Target Prediction: What to Choose? Int J Mol Sci. 2016;17:1987.

406. Han L, Witmer PD, Casey E, Valle D, Sukumar S. DNA methylation regulates microRNA expression. Cancer Biol Ther. 2007;6:1284.

407. Bernal AL, Newman GE, Phizackerley PJR, Bryant-Greenwood G, Keeling JW. Human placental phospholipase A2 activity in term and preterm labour. Eur J Obstet Gyn R B. 1992;43:185.

408. Varastehpour A, Radaelli T, Minium J, Ortega H, Herrera E, Catalano P, et al. Activation of phospholipase A2 is associated with generation of placental lipid signals and fetal obesity. J Clin Endocr Metab. 2006;91:248.

409. Montenegro D, Romero R, Kim SS, Tarca AL, Draghici S, Kusanovic JP, et al. Expression patterns of microRNAs in the chorioamniotic membranes: a role for microRNAs in human pregnancy and parturition. J Pathol. 2009;217:113.

410. Starkl P, Marichal T, Galli SJ. PLA2G3 promotes mast cell maturation and function. Nat Immunol. 2013;14:527.

411. Ma R, Gu Y, Groome LJ, Wang, Y. ADAM17 regulates TNFα production by placental trophoblasts. Placenta. 2011;32:975.

412. Wang D, Na Q, Song W, Song G. Altered Expression of miR-518b and miR-519a in the placenta is associated with low fetal birth weight. Amer J Perinatol. 2014;31:729.

413. Na Q, Wang D, Song W. Underexpression of 4 placenta-associated microRNAs in complete hydatidiform moles. Int J Gynecol Cancer. 2012;22:1075.

414. Liu M, Wang Y, Lu H, Wang H, Shi X, Shao X, et al. miR-518b enhances human trophoblast cell proliferation through targeting Rap1b and activating Ras-MAPK signal. Front Endocrinol. 2018;9:100.

415. Kumar S, Xu J, Kumar RS, Lakshmikanthan S, Kapur R, Kofron M, et al. The small GTPase Rap1b negatively regulates neutrophil chemotaxis and transcellular diapedesis by inhibiting Akt activation. J Exp Med. 2014;211:1741.

416. Li P, Chen X, Su L, Li C, Zhi Q, Yu B, et al. Epigenetic silencing of miR-338-3p contributes to tumorigenicity in gastric cancer by targeting SSX2IP. PLOS One. 2013;8:e66782.

417. Siddle KJ, Deschamps M, Tailleux L, Nédélec Y, Pothlichet J, Lugo-Villarino G, et al. A genomic portrait of the genetic architecture and regulatory impact of microRNA expression in response to infection. Genome Res. 2014;24:850.

418. Hoge J, Yan I, Jaenner N, Schumacher V, Chalaris A, Steinmetz OM, et al. IL-6 Controls the innate immune response against listeria monocytogenes via classical IL-6 signaling. J Immunol. 2013;190:703.

419. Kotlabova K, Doucha J, Hromadnikova I. Placental-specific microRNA in maternal circulation - identification of appropriate pregnancy-associated microRNAs with diagnostic potential. J Reprod Immunol. 2011;89:185.

420. Miura K, Miura S, Yamasaki K, Higashijima A, Kinoshita A, Yoshiura KI, et al. Identification of pregnancy-associated microRNAs in maternal plasma. Clin Chem. 2010;56:1767.

421. Nahid P, Jarlsberg LG, Kato-Maeda M, Segal MR, Osmond DH, Gagneux S, et al. Interplay of strain and race/ethnicity in the innate immune response to M. tuberculosis. PLOS One. 2018;13:e0195392.

422. Coussens AK, Wilkinson RJ, Nikolayevskyy V, Elkington PT, Hanifa Y, Islam K, et al. Ethnic variation in inflammatory profile in tuberculosis. PLOS Pathog. 2013;9:e1003468.

423. D. Modiano, V. Petrarca, B. S. Sirima, I. Nebie, D. Diallo, F. Esposito, et al. Different response to plasmodium falciparum malaria in West African sympatric gthnic Groups. P Natl Acad Sci USA. 1996;93:13206.

424. Nédélec Y, Sanz J, Baharian G, Szpiech ZA, Pacis A, Dumaine A, et al. Genetic ancestry and natural selection drive population differences in immune responses to pathogens. Cell. 2016;167:669.

425. Wang H, Parry S, Macones G, Sammel MD, Kuivaniemi H, Tromp G, et al. A functional SNP in the promoter of the SERPINH1 gene increases risk of preterm premature rupture of membranes in African Americans. P Natl Acad Sci USA. 2006;103:13463.

426. Mills MC, Rahal C. A scientometric review of genome-wide association studies. Comm Biol. 2019;2:9.

427. Pennington R, Gatenbee C, Kennedy B, Harpending H, Cochran G. Group differences in proneness to inflammation. Infect Genet Evol. 2009;9:1371.

428. Haralambieva IH, Salk HM, Lambert ND, Ovsyannikova IG, Kennedy RB, Warner ND. Associations between race, sex and immune response variations to rubella vaccination in two independent cohorts. Vaccine. 2014;32:1946.

429. Tsekoura EA, Konstantinidou A, Papadopoulou S, Athanasiou S, Spanakis N, Kafetzis D, et al. Adenovirus genome in the placenta: association with histological chorioamnionitis and preterm birth. J Med Virol. 2010;82:1379.

430. Bruner J, Elliott J, Kilbride H, Garite T, Knox G. Candida chorioamnionitis diagnosed by amniocentesis with subsequent fetal infection. Amer J Perinatol. 1986;3:213.

431. Whyte RK, Hussain Z, deSa D. Antenatal infections with Candida species. Arch Dis Child. 1982;57:528.

432. Sela U, Euler CW, da Rosa JC, Fischetti VA. Strains of bacterial species induce a greatly varied acute adaptive immune response: the contribution of the accessory genome. PLOS Pathog. 2018;14:e1006726.

433. Cheung WA, Shao X, Morin A, Siroux V, Kwan T, Ge B, et al. Functional variation in allelic methylomes underscores a strong genetic contribution and reveals novel epigenetic alterations in the human epigenome. Genome Biol. 2017;18:1.

434. Do C, Lang C, Lin J, Darbary H, Krupska I, Gaba A, et al. Mechanisms and disease associations of haplotype-dependent allele-mpecific DNA Methylation. Am J Hum Genet. 2016;98:934.

435. Gertz J, Varley K, Reddy T, Bowling K, Pauli F, Parker S, et al. Analysis of DNA Methylation in a three-generation family reveals widespread genetic influence on epigenetic regulation. PLOS Genet. 2011;7: e1002228.

436. Chen S, Chen L, Ge B, Casale FP, Vasquez L, Kwan T, et al. Genetic drivers of epigenetic and transcriptional variation in human immune cells. Cell. 2016;167:1398.

437. Delahaye F, Do C, Kong Y, Ashkar R, Salas M, Tycko B, et al. Genetic variants influence on the placenta regulatory landscape. PLOS Genet. 2018;14:e1007785.

438. Teh AL, Pan H, Chen L, Ong M, Dogra S, Wong J, et al. The effect of genotype and in utero environment on interindividual variation in neonate DNA methylomes. Genome Res. 2014;24:1064.

439. Shi J, Marconett CN, Duan J, Hyland PL, Li P, Wang Z, et al. Characterizing the genetic basis of methylome diversity in histologically normal human lung tissue. Nat Commun. 2014;5:3365.

440. Starr J, Visscher P, Wray N, Deary I, Martin N, Murphy L, et al. Identification of 55,000 replicated DNA methylation QTL. Sci Rep. 2017;8:17605.

441. Hannon E, Spiers H, Viana J, Pidsley R, Burrage J, Murphy TM, et al. Methylation QTLs in the developing brain and their enrichment in schizophrenia risk loci. Nat Neurosci. 2016;19:48.

442. Husquin LT, Rotival M, Fagny M, Quach H, Zidane N, McEwen LM, et al. Exploring the genetic basis of human population differences in DNA methylation and their causal impact on immune gene regulation. Genome Biol. 2018;19:222.

443. Stefansson OA, Moran S, Gomez A, Sayols S, Arribas-Jorba C, Sandoval J, et al. A DNA methylation-based definition of biologically distinct breast cancer subtypes. Mol Oncol. 2015;9:555.

444. Martin E, Smeester L, Bommarito PA, Grace MR, Boggess K, Kuban K, et al. Sexual epigenetic dimorphism in the human placenta: implications for susceptibility during the prenatal period. Epigenomics. 2017;9:267.

445. Mayne BT, Leemaqz SY, Smith AK, Breen J, Roberts CT, Bianco-Miotto T. Accelerated placental aging in early onset preeclampsia pregnancies identified by DNA methylation. Epigenomics. 2017;9:279.

446. Sood R, Zehnder JL, Druzin ML, Brown PO. Gene expression patterns in human placenta. P Natl Acad Sci Biol. 2006;103:5478.

447. Buckberry S, Bianco-Miotto T, Bent SJ, Dekker GA, Roberts CT. Integrative transcriptome meta-analysis reveals widespread sex-biased gene expression at the human fetal-maternal interface. Mol Hum Reprod. 2014;20:810.

448. Yeganegi M, Watson CS, Martins A, Kim SO, Reid G, Challis JR, et al. Effect of Lactobacillus rhamnosus GR-1 supernatant and fetal sex on lipopolysaccharide-induced cytokine and prostaglandin-regulating enzymes in human placental trophoblast cells: implications for treatment of bacterial vaginosis and prevention of preterm labor. Am J Obstet Gynecol. 2009;200:532.

449. Rahmani E, Shenhav L, Schweiger R, Yousefi P, Huen K, Eskenazi B, et al. Genome-wide methylation data mirror ancestry information. Epigenet Chromatin. 2017;10:1.

450. Barfield RT, Almli LM, Kilaru V, Smith AK, Mercer KB, Duncan R, et al. Accounting for population stratification in DNA methylation studies. Genet Epidemiol. 2014;38:231.

451. Hendrich B, Bird A. Identification and characterization of a family of mammalian methyl CpG-binding proteins. Genet Res. 1998;72:59.

452. Wade PA, Strouboulis J, Jones PL, Vermaak D, Wolffe AP, Jan Veenstra GC, et al. Methylated DNA and MeCP2 recruit histone deacetylase to repress transcription. Nat Genet. 1998;19:187.

453. Laherty CD, Eisenman RN, Ng H, Bird A, Johnson CA, Nan X, et al. Transcriptional repression by the methyl-CpG-binding protein MeCP2 involves a histone deacetylase complex. Nature. 1998;393:386.

454. Morgan T. Role of the placenta in preterm birth: a review. Amer J Perinatol. 2016;33:258.

455. Perez-Garcia V, Fineberg E, Wilson R, Murray A, Mazzeo CI, Tudor C, et al. Placentation defects are highly prevalent in embryonic lethal mouse mutants. Nature. 2018;555:468.

456. Shaut CAE, Keene DR, Sorensen LK, Li DY, Stadler HS. HOXA13 is essential for placental vascular patterning and labyrinth endothelial specification. PLOS Genet. 2008;4:e1000073.

457. Straughen JK, Misra DP, Divine G, Shah R, Perez G, VanHorn S, et al. The association between placental histopathology and autism spectrum disorder. Placenta. 2017;57:183.

458. Ursini G, Punzi G, Chen Q, Marenco S, Robinson JF, Porcelli A, et al. Convergence of placenta biology and genetic risk for schizophrenia. Nat Med. 2018;24:792.

459. Risnes KR, Romundstad PR, Nilsen TIL, Eskild A, Vatten LJ. Placental weight relative to birth weight and long-term cardiovascular mortality: findings from a cohort of 31,307 men and women. Am J Epidemiol. 2009;170:622.

460. Godfrey KM. The role of the placenta in fetal programming. Placenta. 2002;23:27.

461. Martyn C, Barker D, Osmond C. Mothers' pelvic size, fetal growth, and death from stroke and coronary heart disease in men in the UK. Lancet. 1996;348:1264.

462. Turco MY, Gardner L, Kay RG, Hamilton RS, Prater M, Hollinshead MS, et al. Trophoblast organoids as a model for maternal-fetal interactions during human placentation. Nature. 2018;564:263.

463. Torkamani A, Wineinger NE, Topol EJ. The personal and clinical utility of polygenic risk scores. Nature Rev Genet. 2018;19:581.

464. Langfelder P, Horvath S. WGCNA: an R package for weighted correlation network analysis. BMC Bioinformatics. 2008;9:559.

465. Mitra K, Carvunis A, Ramesh SK, Ideker T. Integrative approaches for finding modular structure in biological networks. Nature Rev Genet. 2013;14:719.

466. Lander ES, Stamatoyannopoulos JA, Farnham PJ, Ecker JR, Ren B, Hirst M, et al. The NIH roadmap epigenomics mapping consortium. Nat Biotechnol. 2010;28:1045.

Appendix A Supplementary Material for Chapter 1

A.1 Supplementary tables

Supplementary Table 1.1 Studies assessing amniotic fluid markers and maternal serum markers for predicting aCA

Tissue	Biomarker performance assessment	Citation
Maternal blood	ROC curve reported low diagnostic accuracy (area under the curve (AUC) - 0.56).	Le, Ray., et al. (2015)
Maternal blood	ROC curve with the largest AUC was for CRP (0.70).	Caloone, J., et al. (2016)
Maternal blood	ROC curve with the largest AUC was for NLR (0.80), and optimal NLR cut-off was 6.48mg/l for predicting HCA (sensitivity 71.4%, specificity 77.9%).	Kim, M. A., et al. (2014)
Maternal blood	Optimal IL-8 cut-off was 90pg/ml for predicting aCA (sensitivity 64%, specificity 81%) (AUC not reported).	Shimoya, K., et al. (1997)
Maternal blood	ROC curve with largest AUC was for CRP (0.56) and optimal CRP cut-off was >5 mg/dl for predicting aCA(sensitivity 77%, specificity 32%).	Smith, E. J., et al. (2012)
Maternal blood	Sensitivities of 50–80% .	Trochez-Martinez, R. D., et al. (2007)
Maternal blood	ROC curve couldn't be estimated due to unreliable information.	van de Laar, R., et al. (2009)
Maternal blood	ROC curve for CRP shows AUC of 0.62 and optimal CRP cut-off was 5mg/dl for predicting aCA (sensitivity 59%, specificity 47%).	Popowski, T., et al. (2011)
Maternal blood	ROC curve with largest AUC was using maternal characteristics and IL-6 (0.85). The optimal IL-6 cut-off was 19.5 pg/dL for predicting aCA (sensitivity 68%, specificity 88%).	Martinez-Portilla, R. J., et al. (2018)
Maternal blood	Not evaluated.	Sayed Ahmed, W. A., et al. (2016)
Maternal blood	IL-6 showed higher odds ratio (9.78, 95% confidence interval 1.50-63.82).	Maeda, K., et al. (1997)

Tissue	Biomarker performance assessment	Citation
Maternal blood	ROC curve with largest AUC was for ICAM-1 (0.995). The optimal ICAM-1 cut-off was 106ng/ml for predicting aCA (sensitivity 98%, specificity 93.8%).	Steinborn, A.,et al. (2000)
Maternal blood	Optimal IL-6 cut-off was > 8 pg/mL for predicting infection (sensitivity 82.6% , specificity of 86.3%).	Gulati, S., et al. (2012)
Amniotic fluid	Sensitivity (100%) and specificity (50%) for predicting aCA before 34 weeks.	Romero, R., et al. (1991)
Amniotic fluid	The optimal AF glucose cut-off was <20mg/dl for predicting aCA(specificity >90%, sensitivity <20%). AUC not reported.	Odibo, A. O., et al. (1999)
Amniotic fluid	Not evaluated.	Hillier, S. L., et al. (1993)
Amniotic fluid	Optimal IL-8 cut-off was 1561 ng/mL for predicting aCA(sensitivity 67%, specificity 74%), AUC not reported.	Kacerovsky, M., et al. (2009)
Amniotic fluid	Optimal IL-6 cut-off was > 17 ng/ml for predicting aCA (sensitivity 79% , specificity 100%). AUC - 0.89.	Yoon, B. H., et al. (1995)
Amniotic fluid	Optimal cut-off IL-6 was >1000 pg/mL for predicting aCA (sensitivity 60%, specificity 94%). AUC - 0.78.	Kacerovsky, M., et al. (2014)
Amniotic fluid	Not evaluated.	Kim, S. M., et al. (2015)
Amniotic fluid	Optimal IL-6 cut-off was >3500 pg/ml for predicting stage II/III aCA (sensitivity 87.5%, specificity 89.5%). AUC not reported.	Tsuda, A., et al. (1998)
Amniotic fluid and maternal blood	ROC curve with the largest AUC was for AF IL-6 (0.74) and optimal AF IL-6 cut-off was 2.4ng/ml for predicting aCA (sensitivity 62%, specificity 78%).	Kim, S. A.,et al. (2016)
Amniotic fluid and maternal blood	ROC curve with largest AUC was for AF MMP-9 (0.78) and optimal AF MMP-9 cut-off was 15.0ng/ml for predicting aCA.	Oh, K. J., et al. (2011)
Amniotic fluid and maternal blood	ROC curve with largest AUC was for AF IL-8 (0.76) and optimal AF IL-8 cut-off was for ≥9.9 ng/mL , ≥17.3 ng/mL, ≥55.9 ng/mL) for predicting stage I,II,and III aCA respectively.	Yoneda, S., et al. (2015)

Note: aCA was diagnosed based on histological assessement of the placenta. The studies mentioned in this table often used the terminology histologic chorioamnionitis/acute histologic chorioamnionitis

Appendix B Supplementary Material for Chapter 3

B.1 Supplementary figures

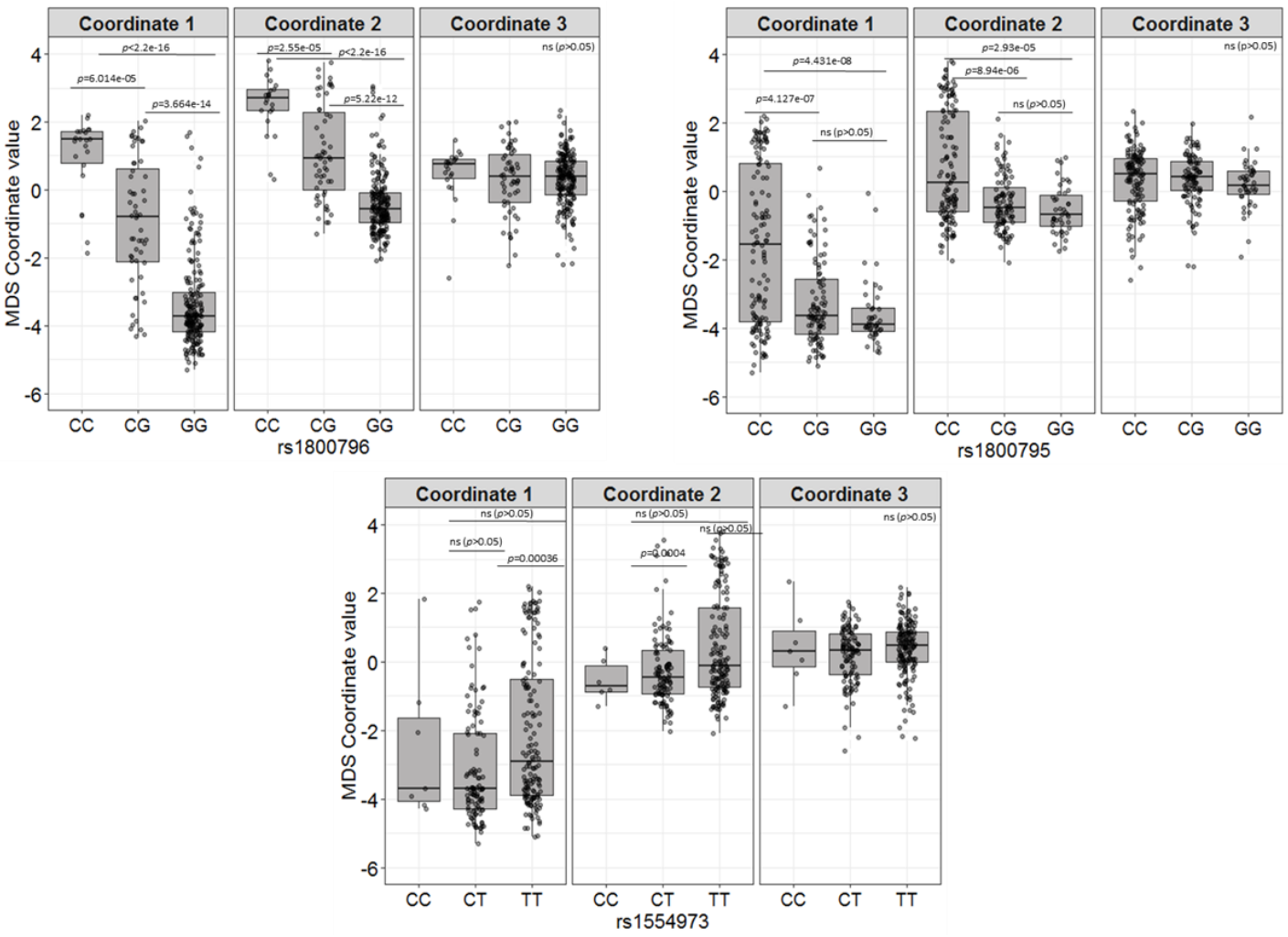

Supplementary Figure 3.1. Association of SNP genotypes (rs1800795, rs1800796, and rs1554973) with ancestry in study cohort. Ancestry is described as a continuous measure using the top three ancestry MDS coordinates. There were significant differences in the distribution of the top two ancestry MDS coordinates between the genotypes; however, ancestry MDS coordinate 3 was not significantly different between the genotypes for the three SNPs.

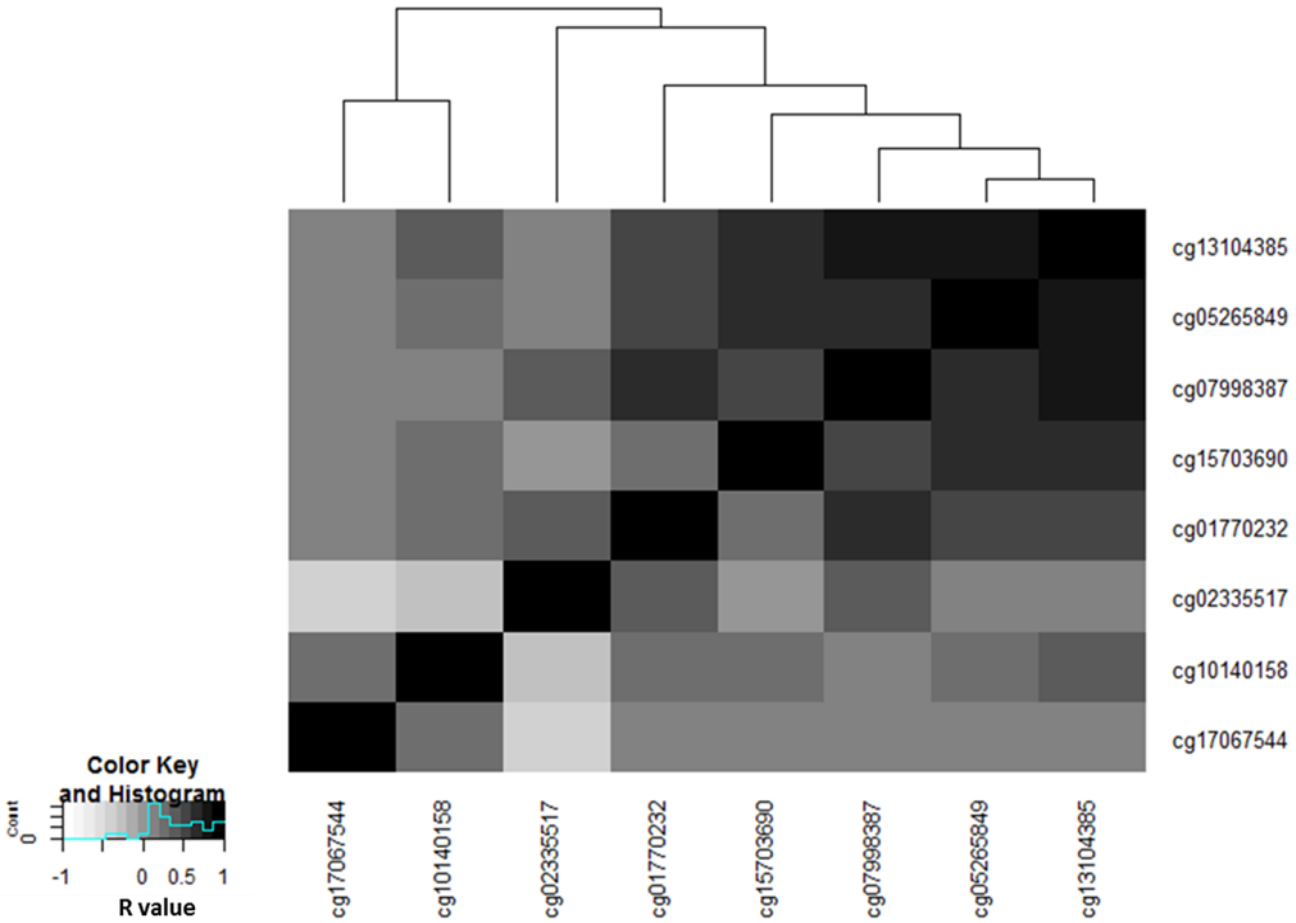

Supplementary Figure 3.2. Correlation of β values across eight *IL6*-related CpGs. Using Spearman's correlation, modest (r>0.5) to strong (r>0.7) correlations were observed across most of the *IL6*-related CpGs. Stronger correlations were observed among CpGs that were physically closer to one another (bps).

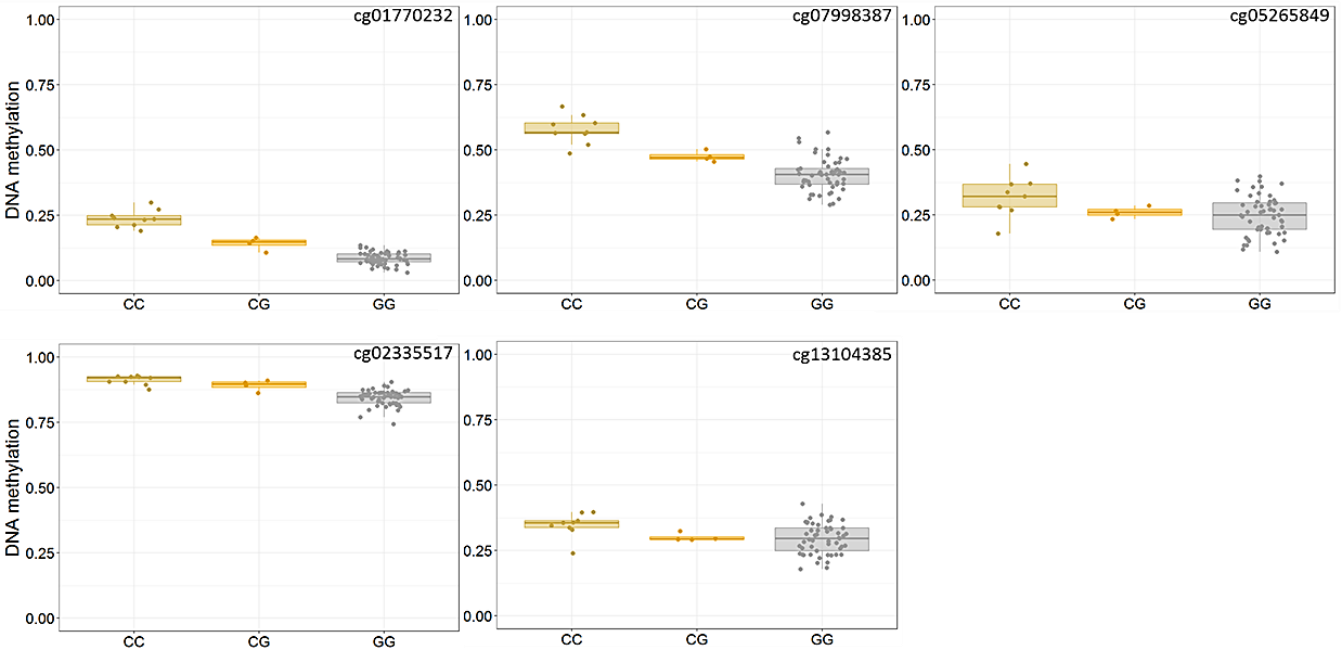

Supplementary Figure 3.3. Differential methylation of *IL6*-related CpGs based on *IL6* genotype status at rs1800796. In a subset of the study population (n=67), individuals with CC genotype (n=9) showed increased DNAm levels compared to carriers of GG genotype (n=54) at five of the tested CpGs (Bonferroni-corrected $p<0.05$). As expected, the four heterozygotes (CG) showed intermediate DNAme levels.

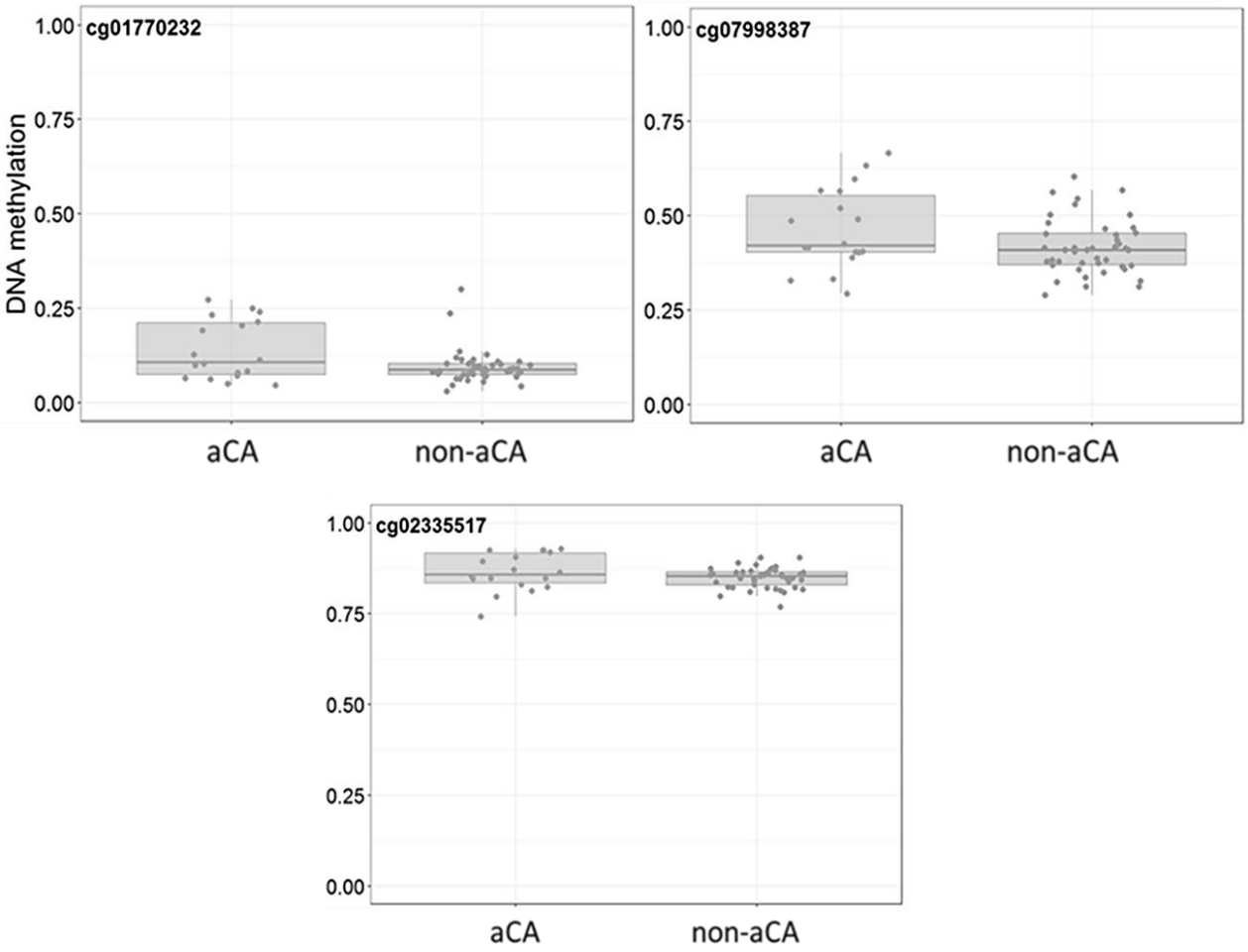

Supplementary Figure 3.4. Altered DNAm at *IL6*-related CpGs is associated with aCA status. In a subset of the study population for which genotype and DNAme data was available (n=67), aCA-a placentas showed increased DNAme compared to non-aCA associated placentas ($p<0.05$, Kruskal-Wallis test).

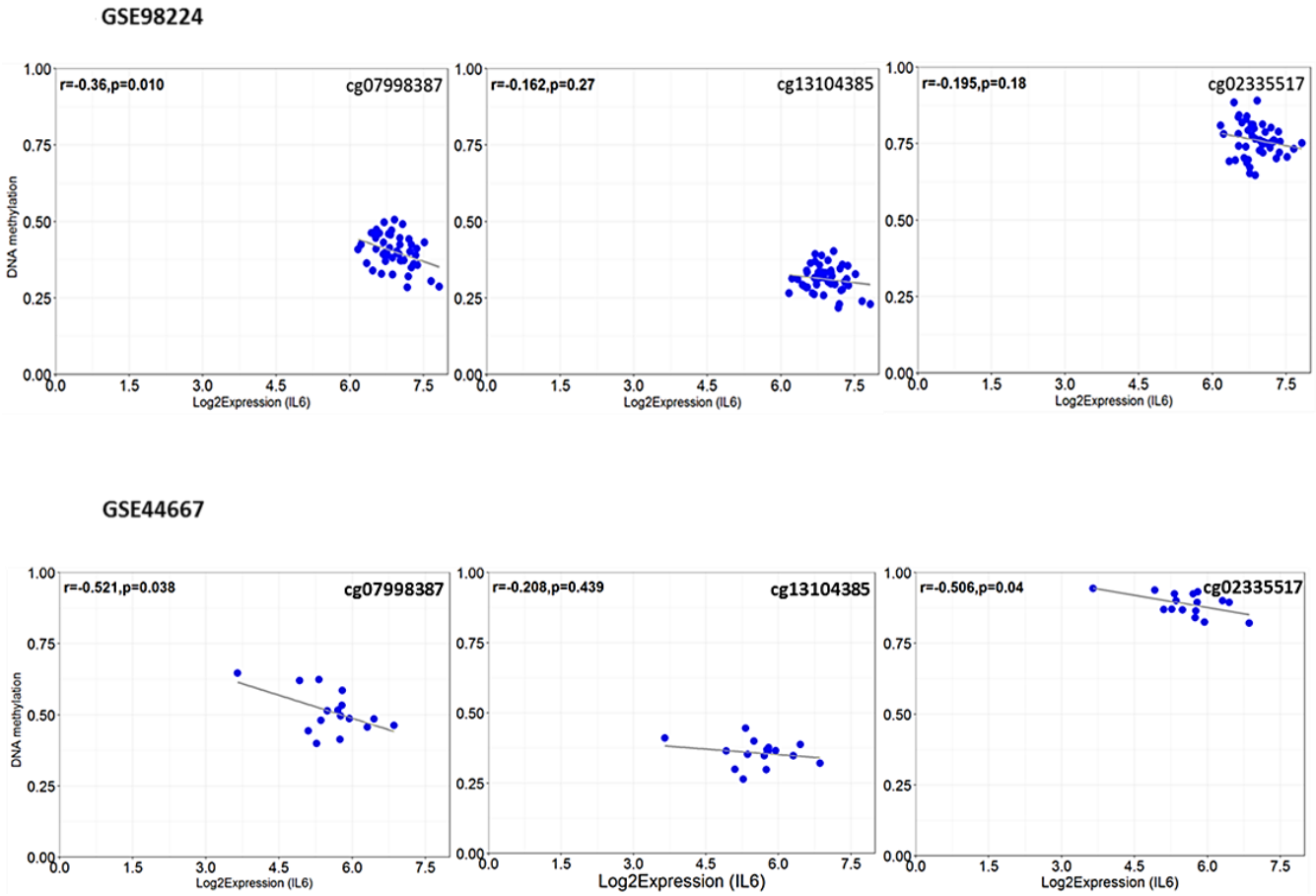

Supplementary Figure 3.5. Correlation between placental DNAme and gene expression at *IL6* locus. A non-significant negative trend between DNAme and gene expression was observed in both the publicly available datasets: GSE98224 (n=48 placentas); GSE44667 (n=16 placentas).

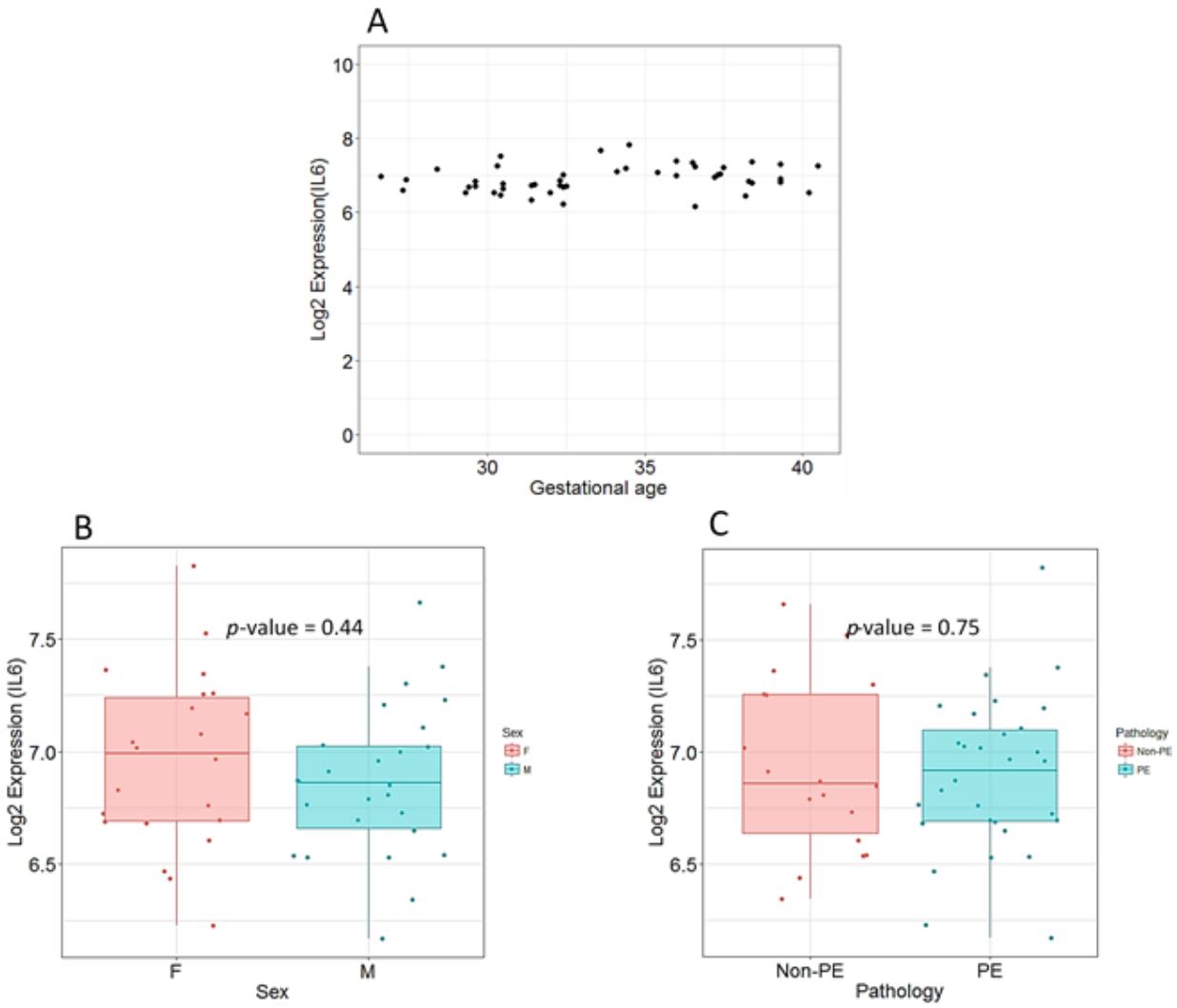

Supplementary Figure 3.6. No association of *IL6* expression with gestational age, fetal sex and preeclampsia status. In each graph, *IL6* gene expression, measured as log2 transformed, is depicted on the y-axis in comparison to A) gestational age, B) fetal sex C) preeclampsia status

B.2 Supplementary tables

Supplementary Table 3.1. Allele counts and frequencies for the SNPs used in the study

Marker	Alleles	Count		Frequency		*p-value*	OR
		aCA	non-aCA	aCA	non-aCA		
rs1800450	C	115	342	0.81	0.87	0.10	0.65
	T	27	52	0.19	0.13		
rs3804099	A	84	227	0.59	0.58	0.77	1.06
	G	58	167	0.41	0.42		
rs1554973	C	37	84	0.26	0.59	0.24	1.30
	T	105	310	0.74	0.79		
rs2149356	A	48	129	0.34	0.33	0.84	1.05
	C	94	265	0.66	0.67		
rs5744105	C	69	160	0.49	0.42	0.14	1.36
	G	71	224	0.51	0.00		
rs2228144	C	126	337	0.89	0.87	0.77	1.14
	T	16	49	0.11	0.13		
rs1800796	C	35	65	0.25	0.16	0.04*	1.65
	G	107	329	0.75	0.84		
rs1800795	C	91	262	0.64	0.66	0.61	0.90
	G	51	132	0.36	0.34		
rs1143643	A	46	132	0.32	0.34	0.84	0.95
	G	96	262	0.68	0.66		
rs1800896	C	54	145	0.38	0.37	0.92	1.04
	T	88	245	0.62	0.63		
rs2222202	A	50	139	0.37	0.37	1.00	1.01
	G	86	241	0.63	0.63		
rs4073	A	63	176	0.44	0.45	1.00	0.99
	T	79	218	0.56	0.55		
rs2664349	C	51	124	0.36	0.31	0.35	1.22
	T	91	270	0.64	0.69		
rs2569190	C	70	205	0.50	0.52	0.69	0.92
	T	70	189	0.50	0.48		
rs352140	C	78	212	0.55	0.54	0.84	1.05
	T	64	182	0.45	0.46		

Supplementary Table 3.2. Counts per genotype

	rs1800796						rs1800795					
	Cluster 1		Cluster 2		Cluster 3		Cluster 1		Cluster 2		Cluster 3	
Genotypes	aCA	non-aCA	aCA	non-aCA	aCA	non-aCA	aCA	non-aCA	aCA	non-aCA	aCA	non-aCA
CC	0	0	3	1	8	10	14	46	8	21	11	28
CG	4	13	5	16	4	14	19	61	5	10	1	1
GG	42	122	5	16	0	5	13	28	0	2	0	0

Appendix C Supplementary Material for Chapter 4

C.1 Supplementary figures

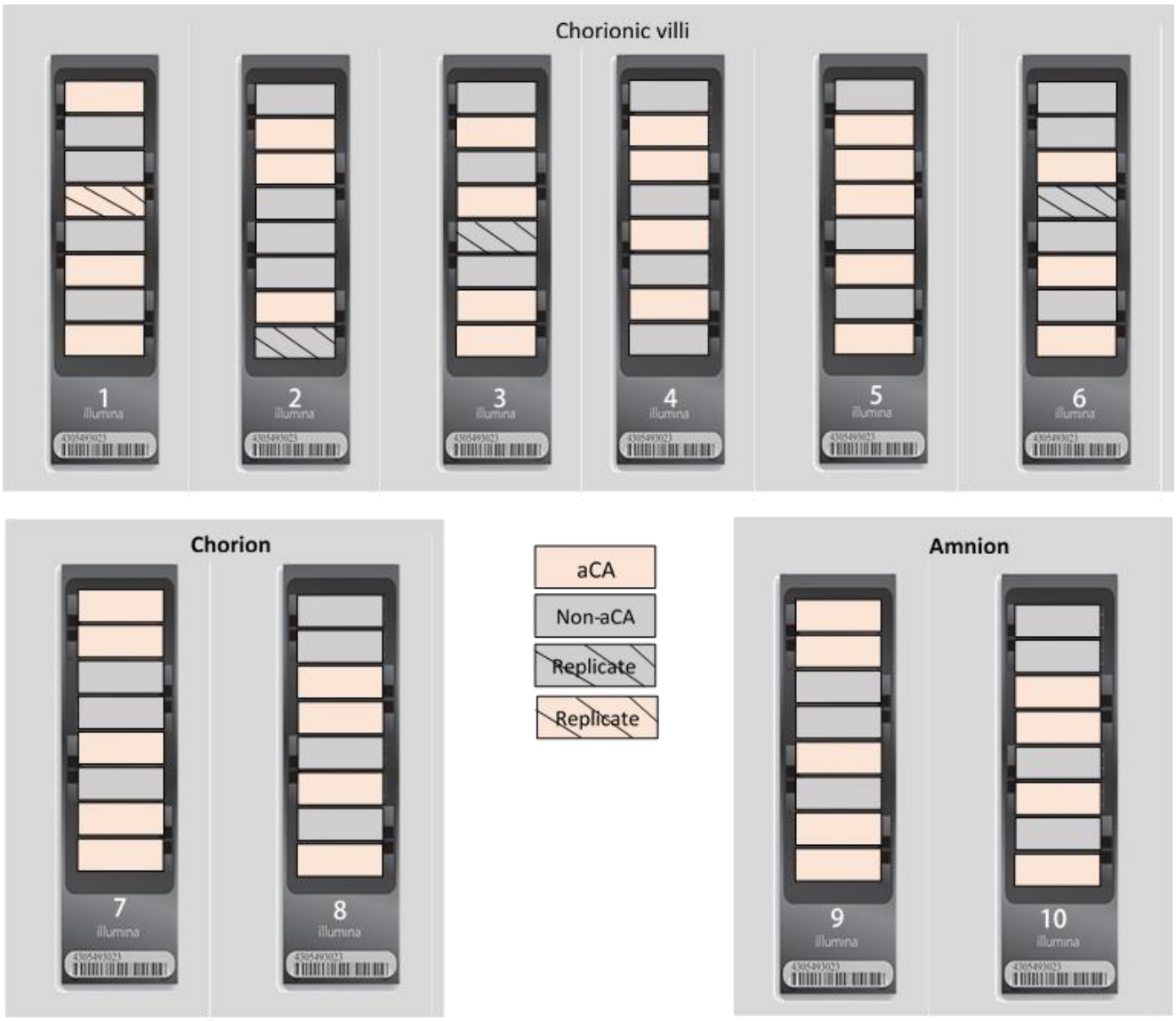

Supplementary Figure 4.1. Distribution of samples across the ten chips for the discovery cohort. The study included 44 chorionic villous samples (4 run in duplicate for technical controls: replicates), 16 matched amnion samples, and 16 matched chorion samples.

4.2a

4.2b

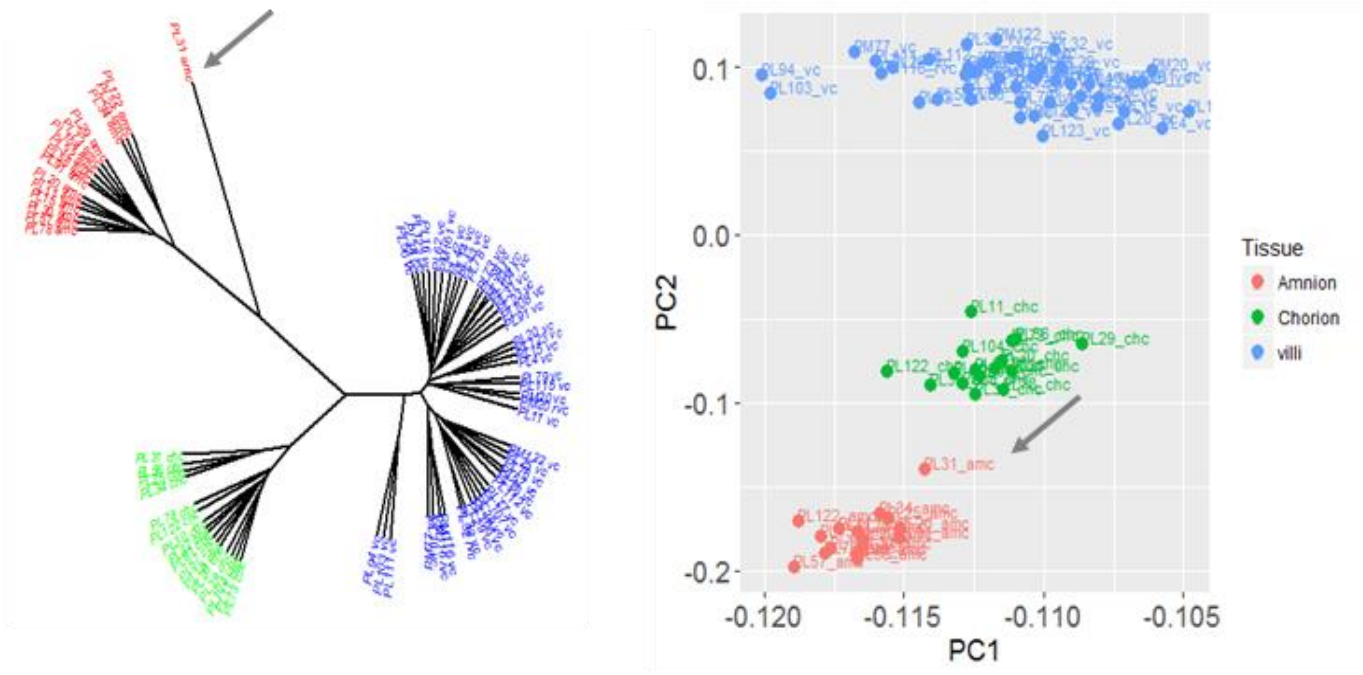

Supplementary Figure 4.2a and 4.2b. Unsupervised hierarchical clustering and PCA on all probes in the 850k array (866,895 CpGs). Samples clustered primarily by tissue type (chorionic villi – blue, chorion – green, amnion – red). However, one amnion sample clustered further away from the amnion group (as indicated by the arrow) suggesting it is not representative of its tissue type and was therefore, removed from further analysis.

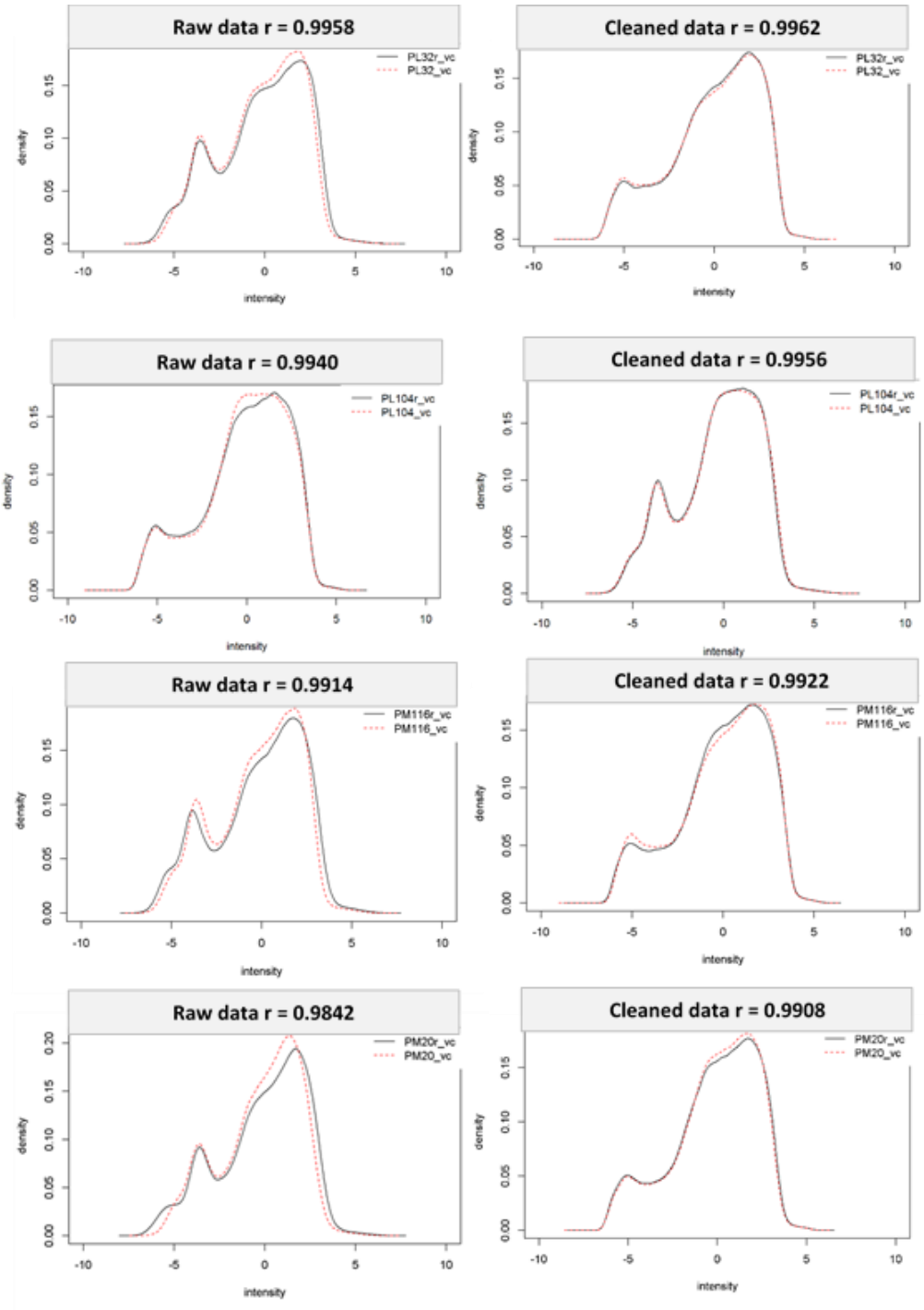
Raw data r = 0.9958
PL32r_vc
PL32_vc
density
intensity
Cleaned data r = 0.9962
PL32r_vc
PL32_vc
density
intensity
Raw data r = 0.9940
PL104r_vc
PL104_vc
density
intensity
Cleaned data r = 0.9956
PL104r_vc
PL104_vc
density
intensity
Raw data r = 0.9914
PM116r_vc
PM116_vc
density
intensity
Cleaned data r = 0.9922
PM116r_vc
PM116_vc
density
intensity
Raw data r = 0.9842
PM20r_vc
PM20_vc
density
intensity
Cleaned data r = 0.9908
PM20r_vc
PM20_vc
density
intensity

Supplementary Figure 4.3. Distribution of M values was plotted for each pair of technical replicate samples. The pairwise correlation of probes improved from raw data to batch corrected cleaned data for the four replicates.

	cg11340524 (*RAB27A*)	cg21962324 (*IRX2*)	cg01276475 (*RIMS1*)
Primer sequences			
Forward	5'-GTGATTTTTTTAAAAGGTAAATGAGAG-3'	5'-GTTTTGGCGTTTTTTTTATAATGATAAATG-3'	5'-ATTGAGTGGTTGGTAGTTATGTT-3'
Reverse	5'-Biosg/ACCCCAATTTAAAAACCACTTAACT-3'	5'-Biosg/AACTCTAATTACCAAACAAATATTCT-3'	5'-Biosg/ACTCTACTACCTCCAATTTAAAACT-3'
Sequencing	5'-ATAAGTTGTTAGAGTTTAGTTAT-3'	5'-GTAAATGAACGTGAAGTGTTTTAGT-3'	5'-GGTTGGTAGTTATGTTTG-3'
PCR cycling conditions			
Step 1	95°C/15 min	95°C/15 min	95°C/15 min
Step 2	95°C/40 sec	95°C/40 sec	95°C/40 sec
Step 3	53°C/40 sec	56°C/40 sec	60°C/40 sec
Step 4	72°C/40 sec	72°C/40 sec	72°C/40 sec
Step 5	Go to 2, 39 times	Go to 2, 39 times	Go to 2, 39 times
Step 6	72°C/7 min	72°C/7 min	72°C/7 min

Supplementary Figure 4.4. Primer sequences and reaction conditions used for pyrosequencing assays.

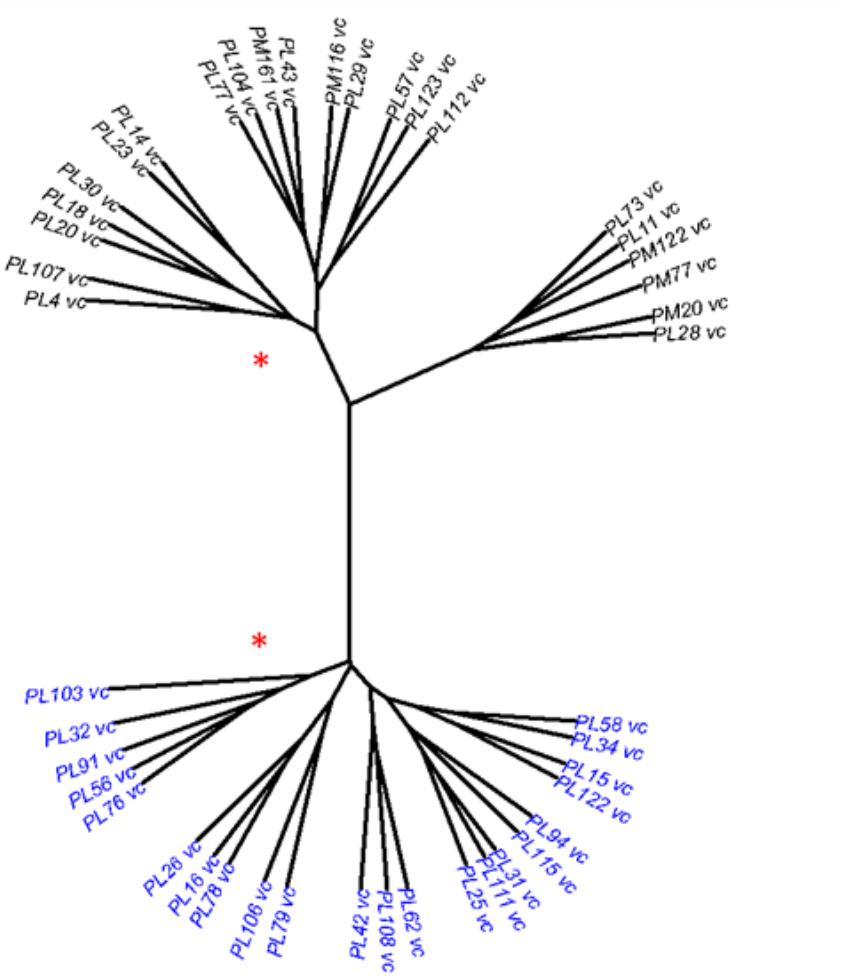

Supplementary Figure 4.5. Hierarchical clustering on the 66 differentially methylated CpG sites in chorionic villi. Samples clustered by acute chorioamnionitis status. Black labels, non-aCA; blue labels, aCA. * indicates stable and significantly different clusters as determined by pvclust and sigclust2 packages

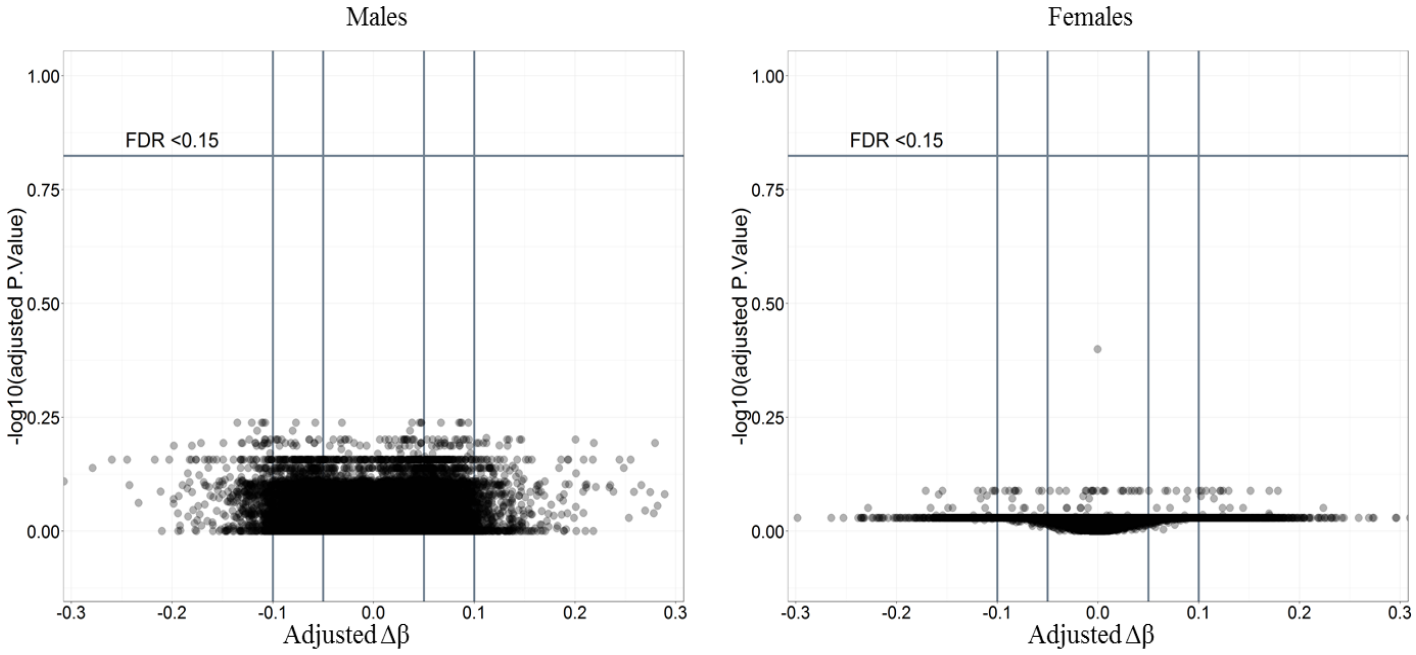

Supplementary Figure 4.6. Sex-specific array-wide volcano plots in chorionic villi. For each probe, FDR corrected p-values from fitted linear models were plotted against group differences in DNAm, for males and females separately. The flat volcano plots demonstrate a lack of differential methylation associated with aCA in either of the sexes, after correction for multiple comparisons.

Supplementary Figure 4.7. Differential methylation at the three candidate CpG sites in males and females. In males, we confirmed significant differential DNAme in the discovery cohort and validated in the independent set of samples for cg21962324 and cg11340524. In females, none of the three CpG sites were differentially methylated in the validation cohort; however similar DNAme trends were observed. % DNA methylation plotted on y-axis was measured by pyrosequencing.

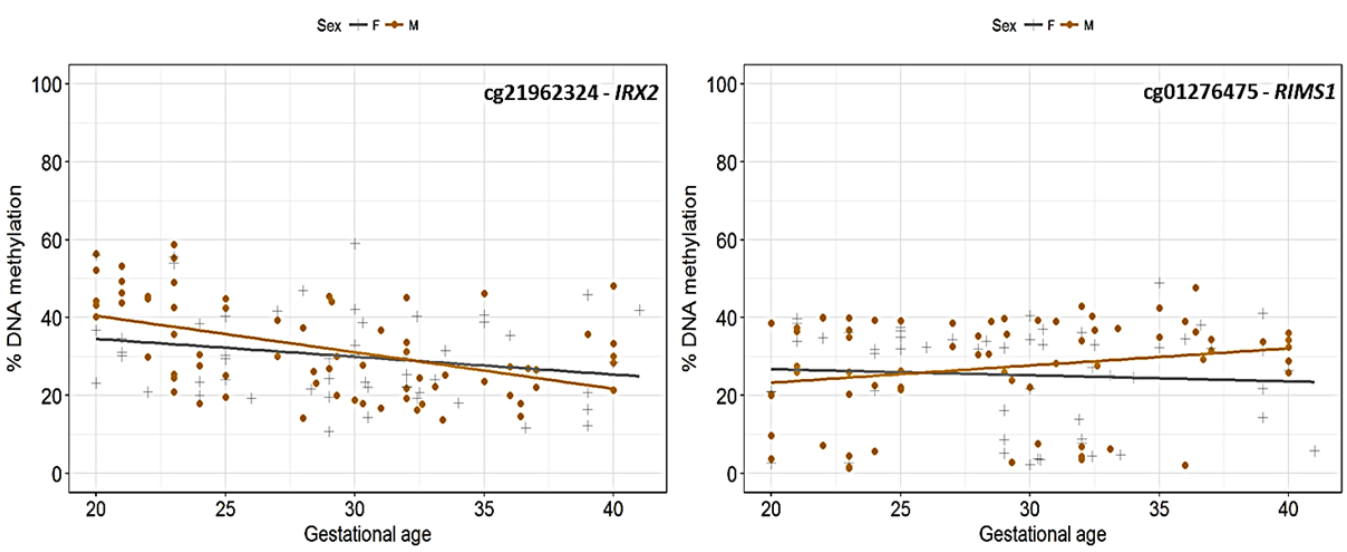

Supplementary Figure 4.8. Variation in DNAme between fetal sexes over gestational age. Though not significant, sex-specific trends in DNAme across gestation was observed for cg21962324 (*IRX2)* and cg01276475 (*RIMS1*). % DNAme measured by pyrosequencing is on the y-axis and gestational age (weeks) is on the x-axis.

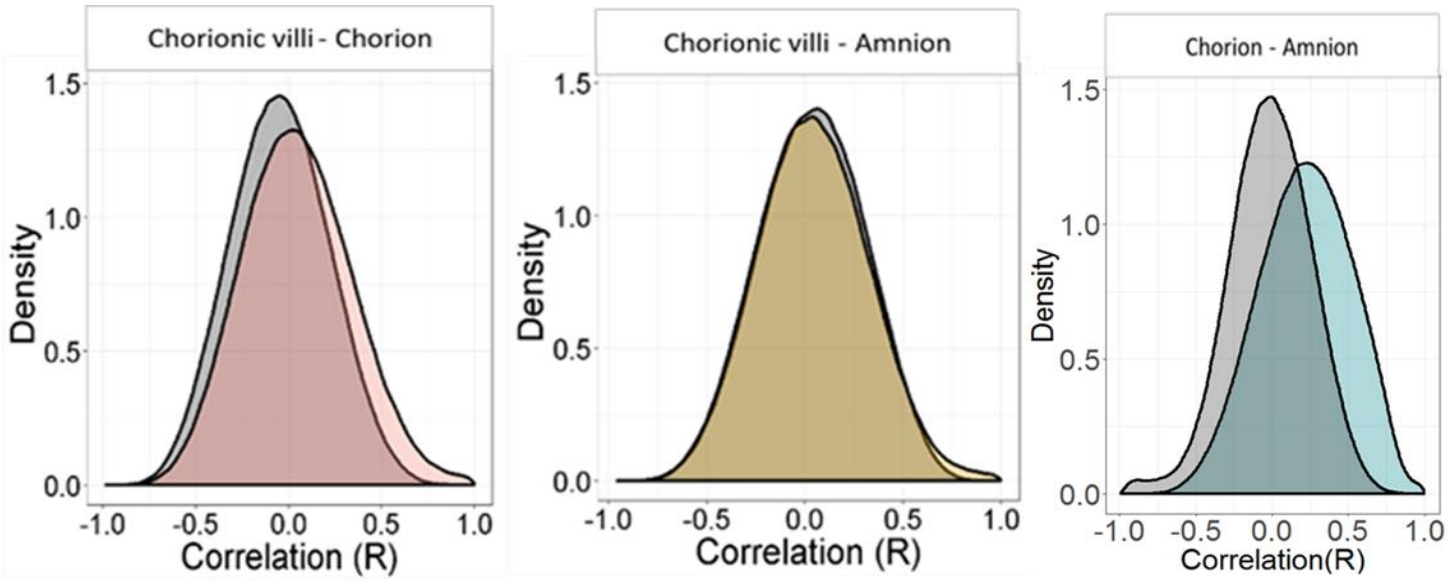

Supplementary Figure 4.9. Distributions of correlation coefficients (R) between DNAme in chorionic villi and fetal membranes were compared against the null distribution (grey). Chorionic villi is more similar to chorion than amnion as evident by skewing of the distribution of correlation coefficient (R) towards stronger positive correlations. As expected, positive skewing was most pronounced when correlations were run between the fetal membranes as both chorion and amnion have a common inner cell mass origin.

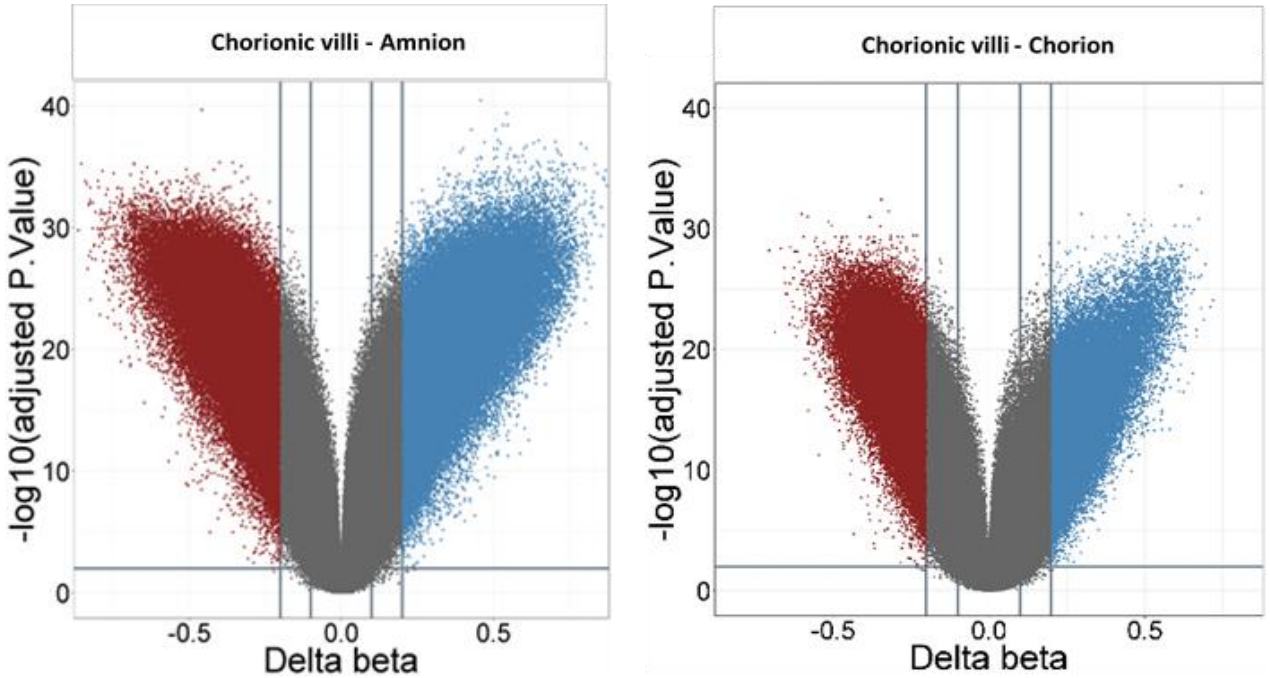

Supplementary Figure 4.10. Array-wide volcano plots of the differential methylation analysis between the tissue pairs (chorionic villi and amnion; and chorionic villi and chorion). The x-axis indicates a DNAme difference (Δβ) between the compared tissues. The y-axis represents FDR corrected p-value. Points are colored to highlight CpGs sites that met biological ($\Delta\beta > 0.20$) and statistical thresholds (FDR < 0.01). Sites highlighted in red are those that are hypermethylated in chorionic villi compared to amnion/chorion. Sites highlighted in blue are those that are hypomethylated in chorionic villi compared to amnion/chorion.

C.2 Supplementary tables

Supplementary Table 4.1. Probe filtering characteristics for chorionic villi, amnion and chorion

Criteria	Chorionic villi	Chorion	Amnion
SNP probes	59	59	59
Probes targeting sex chromosomes	19,681	19,681	19,681
Probes with evidence of cross hybridization	53,241	53,241	53,241
Probes with a SNP at the site of bp extension or at the site of the CpG being measured	10,262	10,262	10,262
Poor quality probes (detection p value >0.01 in >20 % of samples or <3 bead replicates in >20 % of samples)	4386	2020	1573
Non variable probes	67,429	75,991	79,969

Supplementary Table 4.2. Probes investigated for biologically relevant candidate CpG site analysis

Probe	Chromosome	UCSC_Refgene_Name	UCSC_Refgene_Group
cg02544380	1	IL10	TSS1500
cg02901679	1	IL10	TSS200
cg03239976	1	IL10	Body
cg04321197	1	IL10	1stExon
cg10978799	1	IL10	TSS200
cg15096505	1	IL10	Body
cg16247264	1	IL10	Body
cg16284789	1	IL10	Body
cg17067005	1	IL10	Body
cg17744604	1	IL10	TSS1500
cg18442793	1	IL10	TSS1500
cg24274865	1	IL10	TSS1500
cg01290568	2	IL1B	5'UTR
cg02596281	2	IL1B	TSS1500
cg07250315	2	IL1B	Body
cg07935264	2	IL1B	TSS200
cg10486274	2	IL1B	Body
cg14117934	2	IL1B	3'UTR
cg15218327	2	IL1B	Body
cg15836722	2	IL1B	Body
cg18773937	2	IL1B	TSS1500
cg19890119	2	IL1B	Body
cg20983042	2	IL1B	TSS1500
cg23149881	2	IL1B	TSS1500
cg01770232	7	IL6	TSS1500
cg02335517	7	IL6	Body
cg05265849	7	IL6	Body
cg07998387	7	IL6	Body
cg10140158	7	IL6	TSS1500
cg13104385	7	IL6	Body
cg15703690	7	IL6	Body
cg17067544	7	IL6	TSS1500
cg04392234	4	IL8	3'UTR
cg16468729	4	IL8	Body
cg01592588	3	IRAK2	Body
cg01793179	3	IRAK2	Body
cg01962199	3	IRAK2	Body

Probe	Chromosome	UCSC_Refgene_Name	UCSC_Refgene_Group
cg03215701	3	IRAK2	TSS200
cg03886837	3	IRAK2	Body
cg04455646	3	IRAK2	TSS1500
cg04733838	3	IRAK2	TSS1500
cg06391377	3	IRAK2	Body
cg07463991	3	IRAK2	Body
cg07631359	3	IRAK2	Body
cg08110661	3	IRAK2	Body
cg08424512	3	IRAK2	Body
cg08819120	3	IRAK2	Body
cg09386682	3	IRAK2	Body
cg10106965	3	IRAK2	TSS1500
cg10317164	3	IRAK2	Body
cg11753709	3	IRAK2	Body
cg11851603	3	IRAK2	Body
cg12204957	3	IRAK2	Body
cg12484135	3	IRAK2	Body
cg13302664	3	IRAK2	Body
cg13419330	3	IRAK2	Body
cg13933891	3	IRAK2	Body
cg14433987	3	IRAK2	Body
cg14527942	3	IRAK2	Body
cg14784004	3	IRAK2	Body
cg15292072	3	IRAK2	Body
cg16286142	3	IRAK2	Body
cg18007850	3	IRAK2	TSS200
cg18091848	3	IRAK2	Body
cg18527651	3	IRAK2	3'UTR
cg18716706	3	IRAK2	Body
cg19275895	3	IRAK2	Body
cg19518265	3	IRAK2	Body
cg19553158	3	IRAK2	Body
cg20854791	3	IRAK2	Body
cg21387009	3	IRAK2	Body
cg21393095	3	IRAK2	Body
cg25458727	3	IRAK2	Body
cg25503542	3	IRAK2	Body
cg26060132	3	IRAK2	Body
cg26592283	3	IRAK2	Body
cg27032569	3	IRAK2	TSS1500
cg00524814	10	MBL2	TSS200

Probe	Chromosome	UCSC_Refgene_Name	UCSC_Refgene_Group
cg05759948	10	MBL2	TSS1500
cg08253748	10	MBL2	TSS1500
cg08780887	10	MBL2	TSS1500
cg09545806	10	MBL2	1stExon
cg13882988	10	MBL2	1stExon
cg14802408	10	MBL2	Body
cg18972123	10	MBL2	TSS1500
cg27418851	10	MBL2	TSS200
cg02526439	8	MMP16	3'UTR
cg05139829	8	MMP16	Body
cg05991513	8	MMP16	Body
cg06908058	8	MMP16	Body
cg10474091	8	MMP16	Body
cg10525327	8	MMP16	Body
cg10945860	8	MMP16	Body
cg11452992	8	MMP16	Body
cg13521251	8	MMP16	Body
cg14989234	8	MMP16	Body
cg15728672	8	MMP16	Body
cg16433873	8	MMP16	Body
cg16699632	8	MMP16	Body
cg18182787	8	MMP16	Body
cg23051059	8	MMP16	Body
cg26680202	8	MMP16	Body
cg00646813	4	TLR1	5'UTR
cg02016764	4	TLR1	5'UTR
cg03430998	4	TLR1	TSS1500
cg08757862	4	TLR1	TSS1500
cg08888038	4	TLR1	5'UTR
cg09316306	4	TLR1	TSS1500
cg11918910	4	TLR1	5'UTR
cg14003984	4	TLR1	TSS1500
cg20054786	4	TLR1	Body
cg22809983	4	TLR1	5'UTR
cg22839308	4	TLR1	TSS1500
cg00000884	4	TLR2	5'UTR
cg01249659	4	TLR2	TSS1500
cg01554777	4	TLR2	5'UTR
cg03523945	4	TLR2	5'UTR
cg03610073	4	TLR2	TSS1500
cg06405222	4	TLR2	TSS200

Probe	Chromosome	UCSC_Refgene_Name	UCSC_Refgene_Group
cg06618866	4	TLR2	TSS1500
cg12940473	4	TLR2	5'UTR
cg14581949	4	TLR2	TSS1500
cg15801357	4	TLR2	TSS200
cg15852258	4	TLR2	TSS200
cg16547110	4	TLR2	TSS200
cg18652319	4	TLR2	Body
cg19037167	4	TLR2	5'UTR
cg24295442	4	TLR2	TSS1500
cg00073181	1	TLR5	5'UTR
cg00244959	1	TLR5	5'UTR
cg01181681	1	TLR5	TSS1500
cg02619544	1	TLR5	TSS1500
cg04219417	1	TLR5	TSS1500
cg05696109	1	TLR5	TSS200
cg05858079	1	TLR5	5'UTR
cg06155710	1	TLR5	3'UTR
cg07015886	1	TLR5	TSS1500
cg11209549	1	TLR5	5'UTR
cg12095594	1	TLR5	5'UTR
cg14849237	1	TLR5	5'UTR
cg15448366	1	TLR5	5'UTR
cg15630422	1	TLR5	5'UTR
cg16409474	1	TLR5	5'UTR
cg16585333	1	TLR5	5'UTR
cg17599809	1	TLR5	5'UTR
cg18201671	1	TLR5	TSS1500
cg20357670	1	TLR5	5'UTR
cg20542622	1	TLR5	5'UTR
cg23039250	1	TLR5	5'UTR
cg23291900	1	TLR5	TSS1500
cg23343408	1	TLR5	5'UTR
cg24861436	1	TLR5	Body
cg00755496	3	TLR9	Body
cg01045723	3	TLR9	Body
cg01395047	3	TLR9	TSS200
cg05778154	3	TLR9	TSS1500
cg08721301	3	TLR9	TSS200
cg09595853	3	TLR9	Body
cg11855705	3	TLR9	TSS200
cg13380109	3	TLR9	Body

Probe	Chromosome	UCSC_Refgene_Name	UCSC_Refgene_Group
cg14528193	3	TLR9	Body
cg16302310	3	TLR9	TSS1500
cg17716965	3	TLR9	TSS200
cg17722393	3	TLR9	Body
cg18452449	3	TLR9	TSS1500
cg22484793	3	TLR9	TSS1500
cg23021329	3	TLR9	Body
cg23949087	3	TLR9	Body
cg26207095	3	TLR9	TSS1500
cg01360627	6	TNF	Body
cg01569083	6	TNF	TSS200
cg02137984	6	TNF	3'UTR
cg03037030	6	TNF	TSS200
cg04425624	6	TNF	1stExon
cg04472685	6	TNF	3'UTR
cg06825478	6	TNF	3'UTR
cg08553327	6	TNF	1stExon
cg08639424	6	TNF	TSS1500
cg10650821	6	TNF	1stExon
cg10717214	6	TNF	1stExon
cg11484872	6	TNF	TSS200
cg12681001	6	TNF	1stExon
cg15989608	6	TNF	3'UTR
cg17741993	6	TNF	Body
cg19124225	6	TNF	3'UTR
cg19648923	6	TNF	TSS200
cg19978379	6	TNF	TSS1500
cg20477259	6	TNF	Body
cg21222743	6	TNF	1stExon
cg21370522	6	TNF	TSS200
cg21467614	6	TNF	1stExon
cg23384708	6	TNF	Body
cg24452282	6	TNF	TSS1500
cg26729380	6	TNF	1stExon
cg26736341	6	TNF	3'UTR

Supplementary Table 4.3. Probe filtering characteristics for tissue-tissue comparison analysis.

Criteria	Number of probes eliminated
SNP probes	59
Probes targeting sex chromosomes	19,681
Probes with evidence of cross hybridization	53,241
Probes with a SNP at the site of bp extension or at the site of the CpG being measured	10,262
Poor quality probes (detection p value >0.01 in >20 % of samples or <3 bead replicates in >20 % of samples)	4386

Supplementary Table 4.4. Probes identified as differentially methylated in the discovery cohort (chorionic villi).

Probe	Chromosome	UCSC_Refgene_ Name	UCSC_Refgene_ Group	Adjusted P-value	Δβ (Deltaβ)
cg01276475	6	RIMS1	TSS1500	0.08241	0.23988
cg19696329	6	LTV1	Body	0.08861	0.18219
cg16545496	16	HSD11B2	TSS1500	0.05184	0.16503
cg17444090	1	SIPA 1L2		0.12202	0.15335
cg24895142	7	ST7	Body	0.12306	0.11496
cg18143564	11	RIC3	Body	0.09908	0.1108
cg08627825	22	LINC00229		0.12202	0.11042
cg18624016	2	SNED1	Body	0.09864	0.09479
cg19179332	17			0.1229	0.09118
cg11340524	15	RAB27A	TSS1500	0.12492	0.08996
cg26224223	19	TSHZ3	TSS1500	0.09864	0.08963
cg00715092	5			0.09433	0.0864
cg09140778	2	GBX2		0.09908	0.0828
cg04402021	19	POLR2E	Body	0.12306	0.08102
cg15013171	22			0.08861	0.08056
cg14803324	12			0.12306	0.08008
cg20710266	15	NR2F2	Body	0.02891	0.07896
cg03928041	8	ANGPT2	Body	0.13149	0.07653
cg11862635	4			0.0465	0.07569
cg00539858	2			0.04786	0.07513
cg05293930	22	SUN2	5'UTR	0.0465	0.07261
cg18694418	7	AMZ1	Body	0.09908	0.07175
cg01597130	11			0.09908	0.07158
cg09275023	6	HLA-E	TSS1500	0.09954	0.06711
cg14853341	1	KCNK1	Body	0.12202	0.06649
cg21606707	19	RAB11B	Body	0.08241	0.06542
cg01860944	13	AK097816		0.09908	0.06375
cg04498921	22			0.08861	0.06362
cg25313383	4			0.14752	0.06356
cg02782634	17	TMEM49	Body	0.12202	0.06294
cg20437986	7			0.08861	0.05831
cg25139649	1	SKI	Body	0.14024	0.05666
cg16241107	22			0.1229	0.05583
cg26525592	5	CXCL14	TSS1500	0.1229	0.05519
cg24244235	20			0.08861	0.05324
cg19788186	21	KCNJ15	5'UTR	0.09908	0.05049
cg18326021	10	SORCS3	1stExon	0.04786	-0.0509

Probe	Chromosome	UCSC_Refgene_Name	UCSC_Refgene_Group	Adjusted P-value	Δβ (Deltaβ)
cg01408508	20			0.08861	-0.0526
cg03321020	1	KIAA2013		0.12202	-0.0536
cg26852723	10	FAM171A1	Body	0.1229	-0.0573
cg15971243	1			0.12202	-0.061
cg17351418	2			0.09908	-0.0648
cg17052497	18			0.14129	-0.0661
cg09905635	7	TNS3	5'UTR	0.1229	-0.0685
cg16008054	8	DLGAP2		0.1229	-0.0686
cg21368375	7			0.14941	-0.072
cg02552292	2	GPR39	Body	0.1229	-0.0786
cg02540975	6			0.14752	-0.0794
cg03073060	7	TNS3	5'UTR	0.09908	-0.083
cg26679964	7			0.1229	-0.087
cg12567780	4	ANK2	Body	0.12202	-0.0876
cg03547623	2	LRP1B	Body	0.1229	-0.0883
cg26922019	3	ZBTB20	TSS1500;5'UTR	0.09908	-0.0888
cg11993043	13			0.14656	-0.0905
cg23706187	4	MIR2054		0.09908	-0.0915
cg22952895	2	TMEM18		0.1229	-0.0936
cg03089016	9			0.07541	-0.0954
cg24244500	13	AK05545		0.1229	-0.1019
cg02332293	5	IRX1		0.1229	-0.1027
cg19571721	8	DLGAP2	5'UTR	0.08277	-0.1142
cg17611614	1			0.12202	-0.1198
cg24975986	7	ZNF727	TSS200	0.09908	-0.1206
cg21962324	5	IRX2		0.12202	-0.1236
cg21665850	2	TMEM18		0.14024	-0.1518
cg12771935	2			0.1103	-0.1569
cg24760768	6	DNAH8	Body	0.13933	-0.1719

C.3 Supplementary methods

Supplementary Method 4.1. Data preprocessing of matched tissue cohort

15 samples with matched chorionic villi, amnion and chorion were identified for the matched tissue comparison analysis. Functional normalization was used to account for type I- type II probe bias on the 850K array. Because the primary objective of this study was to characterize DNAme signatures between aCA cases and controls within a tissue, samples were not randomized by tissue type. It is also important to acknowledge that some of the tissue-specific DM sites may be associated with batch as each tissue type was run on separate 850k chips, but we don't expect this to affect the result for one comparison more than the other. Additionally, we anticipate tissue-associated DNAm effects to be of larger magnitude than any other technical batch effects.

Supplementary Method 4.2. Differential methylation analysis on matched tissue comparison dataset

To quantify the similarity between fetal membranes and placental chorionic villi, differential DNAm analysis on a per CpG level was performed between the tissue pairs (chorionic villi-chorion and chorionic villi-amnion) by applying a linear model to M values using *limma*. In modeling DNAme, tissue type was considered as the main effect and GA, fetal sex, and ancestry were included as covariates. Because each tissue type was collected from the same individuals it is likely that DNAme may be influenced by inter-individual differences. To account for this, the model included a within-individual consensus correlation value estimated by the duplicateCorrelation( ) function in *limma*. Multiple test correction was done on the nominal p values of each tissue pair comparison, using Benjamini and Hochberg false detection rate (FDR) method. M values corrected for the additive covariates were logit-transformed to β values and

average DNAme for every CpG site was calculated by obtaining the mean β value for each of the tissue type. Magnitude of DNAme differences (Δβ) between tissues was then calculated. Differentially methylated sites were identified based on i) statistical significance (FDR <0.01); and ii) biological significance (Δβ >0.2).

Appendix D Supplementary Material for Chapter 5

D.1 Supplementary figures

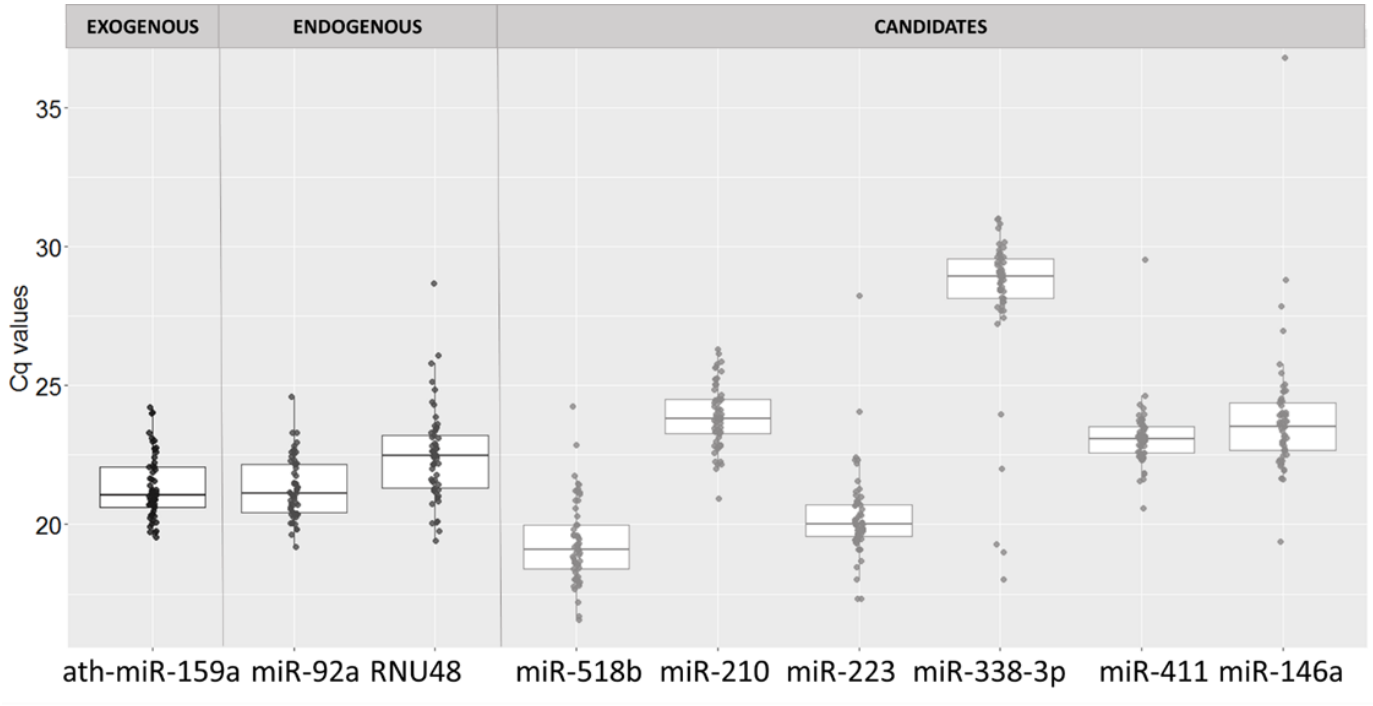

Supplementary Figure 5.1. Expression measured as raw C_q values are plotted for the exogenous control (ath-miR-159a), the two endogenous controls (miR-92a, RNU48) and the six candidate miRNAs (miR-518b, miR-210, miR-338-3p, miR-411, and miR-146a). As expected the expression of the exogenous control and the endogenous controls, particularly, miR-92a were most stable across the 57 placental samples.

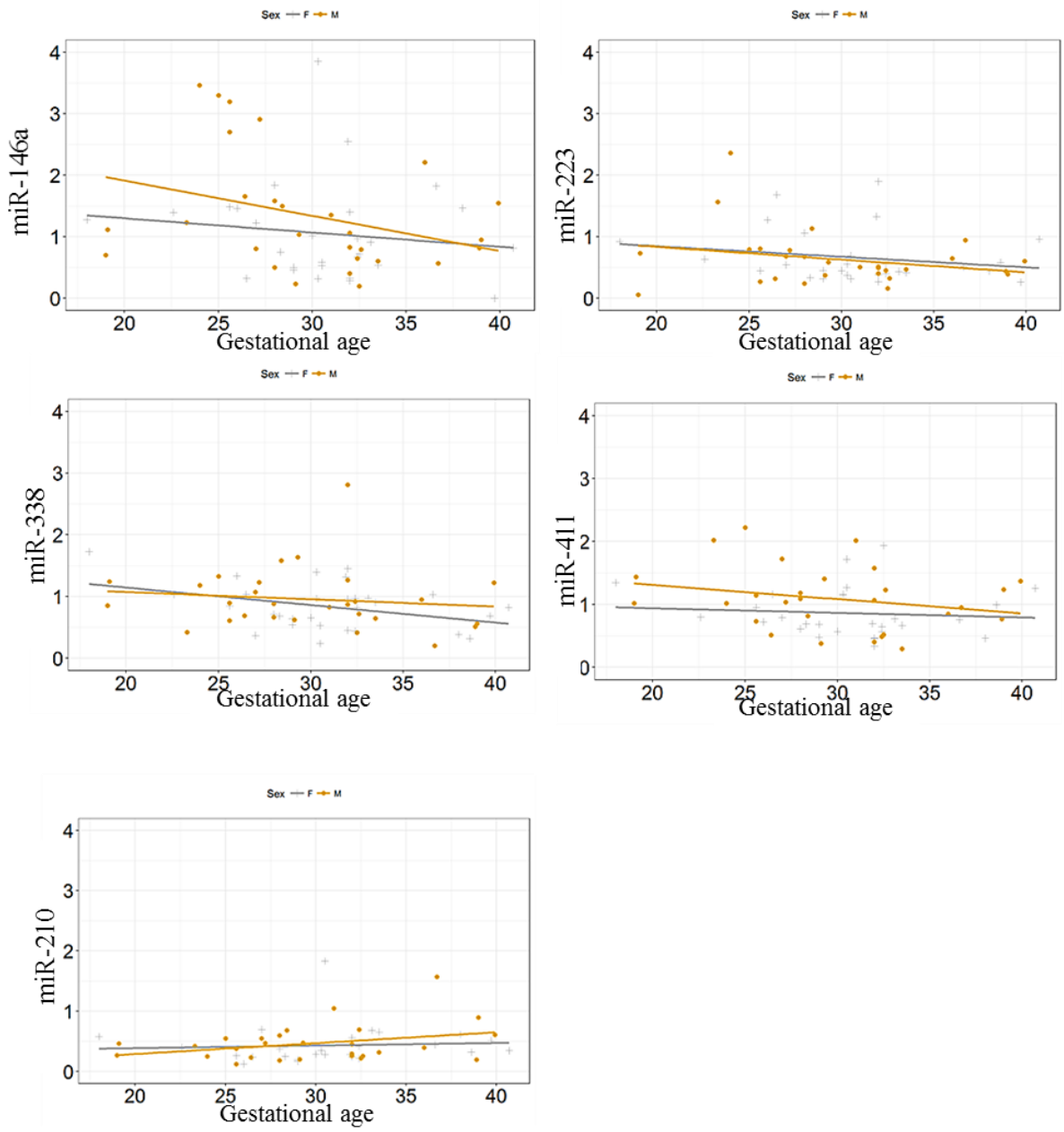

Supplementary Figure 5.2. Placental expression of the six candidate miRNAs across gestational age with respect to fetal sex is shown. Although not significant, miR-146a, miR-223, miR-338, and miR-411 displayed a trend towards decreased expression with gestational age at delivery.

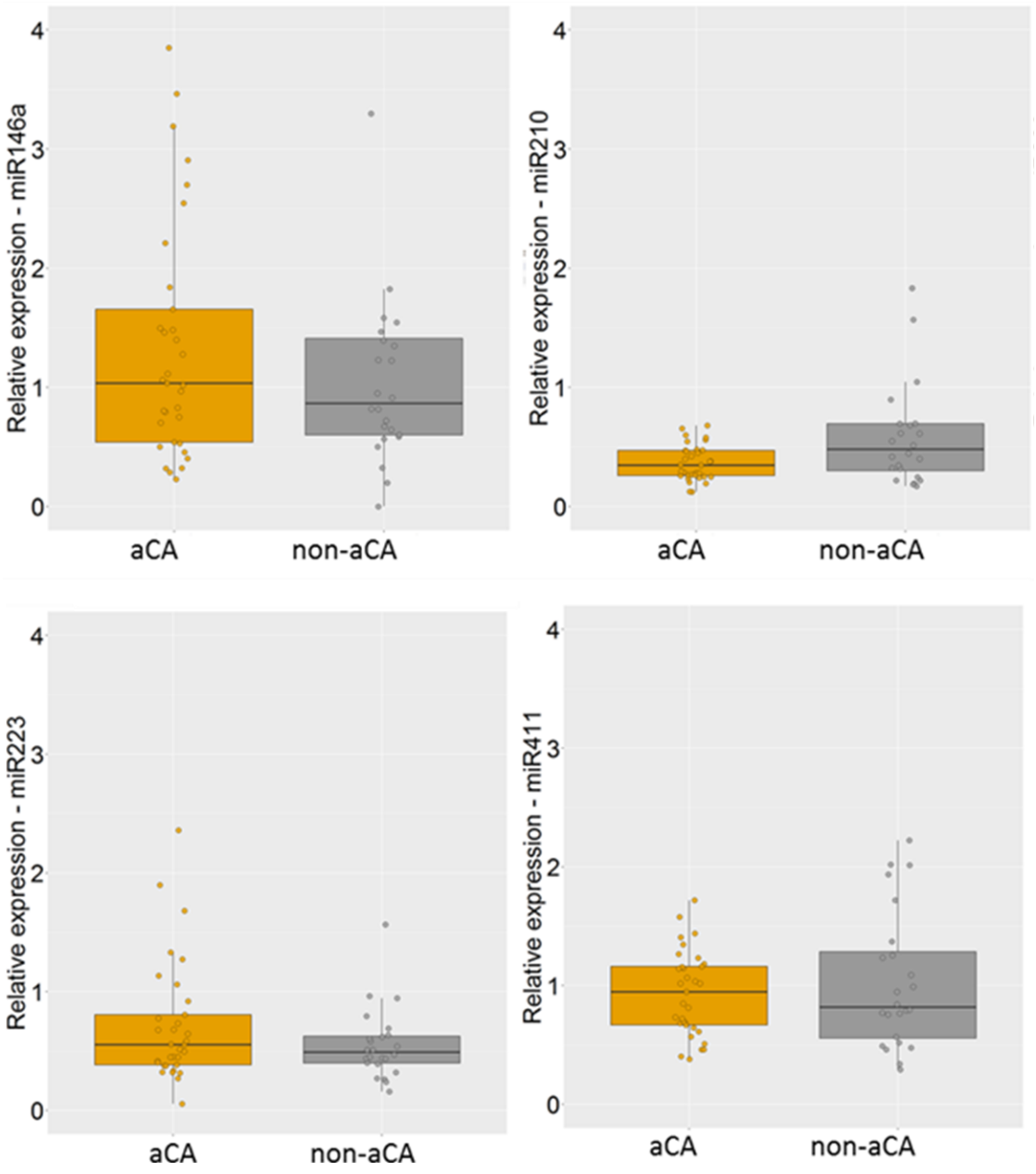

Supplementary Figure 5.3. Expression of mir-146a, miR-210, miR-223, and miR-411 did not exhibit a significant association with aCA status (Kruskal-Wallis test, $p>0.05$); however they trended in the expected direction as observed in response to an infection.

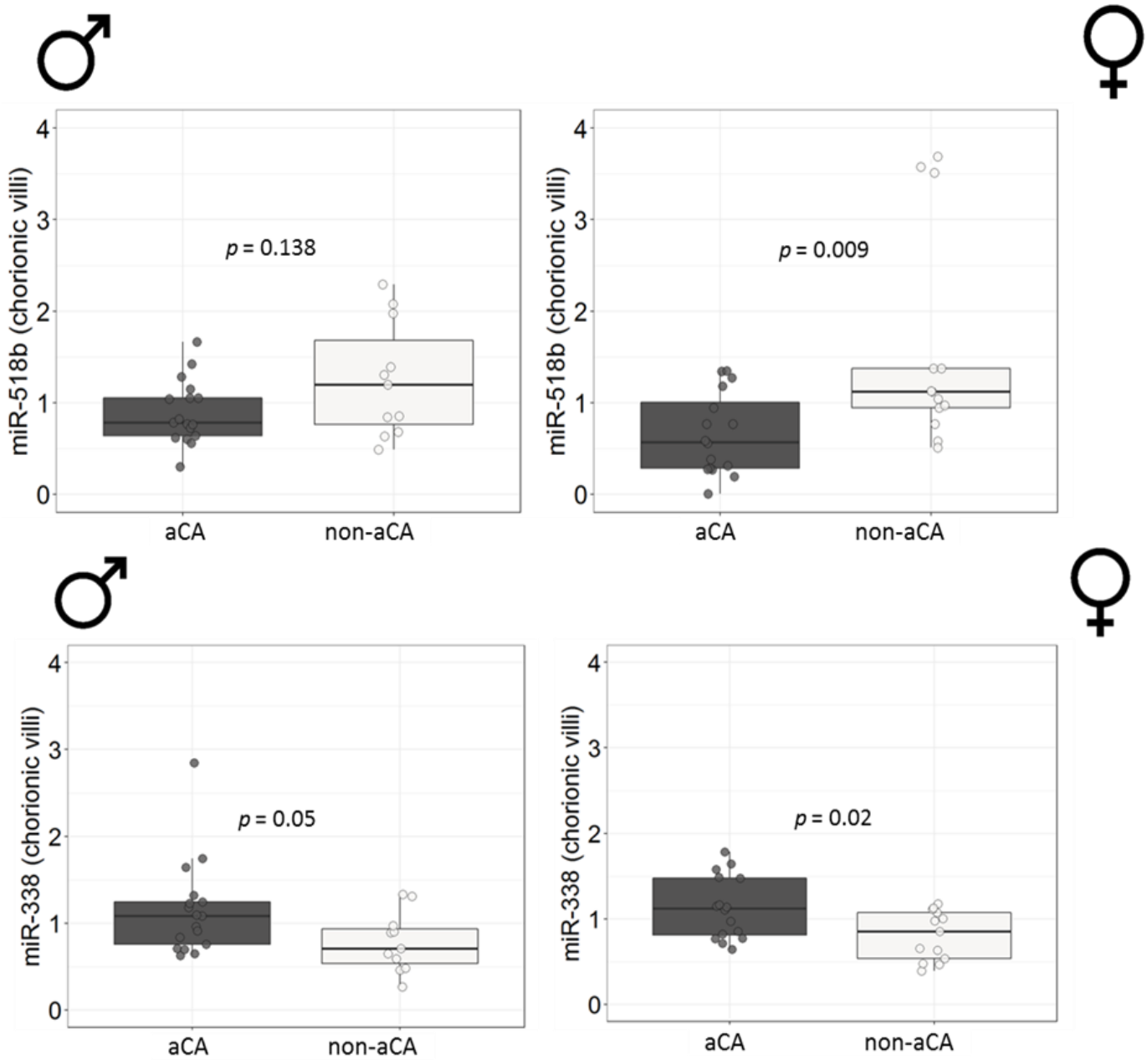

Supplementary Figure 5.4. For miR-338, significant association with aCA status was noted for both males and females (Kruskal-Wallis test, $p<0.05$); however, for miR-518b expression was significantly associated with aCA in female placentas only (Kruskal-Wallis test, $p<0.05$).

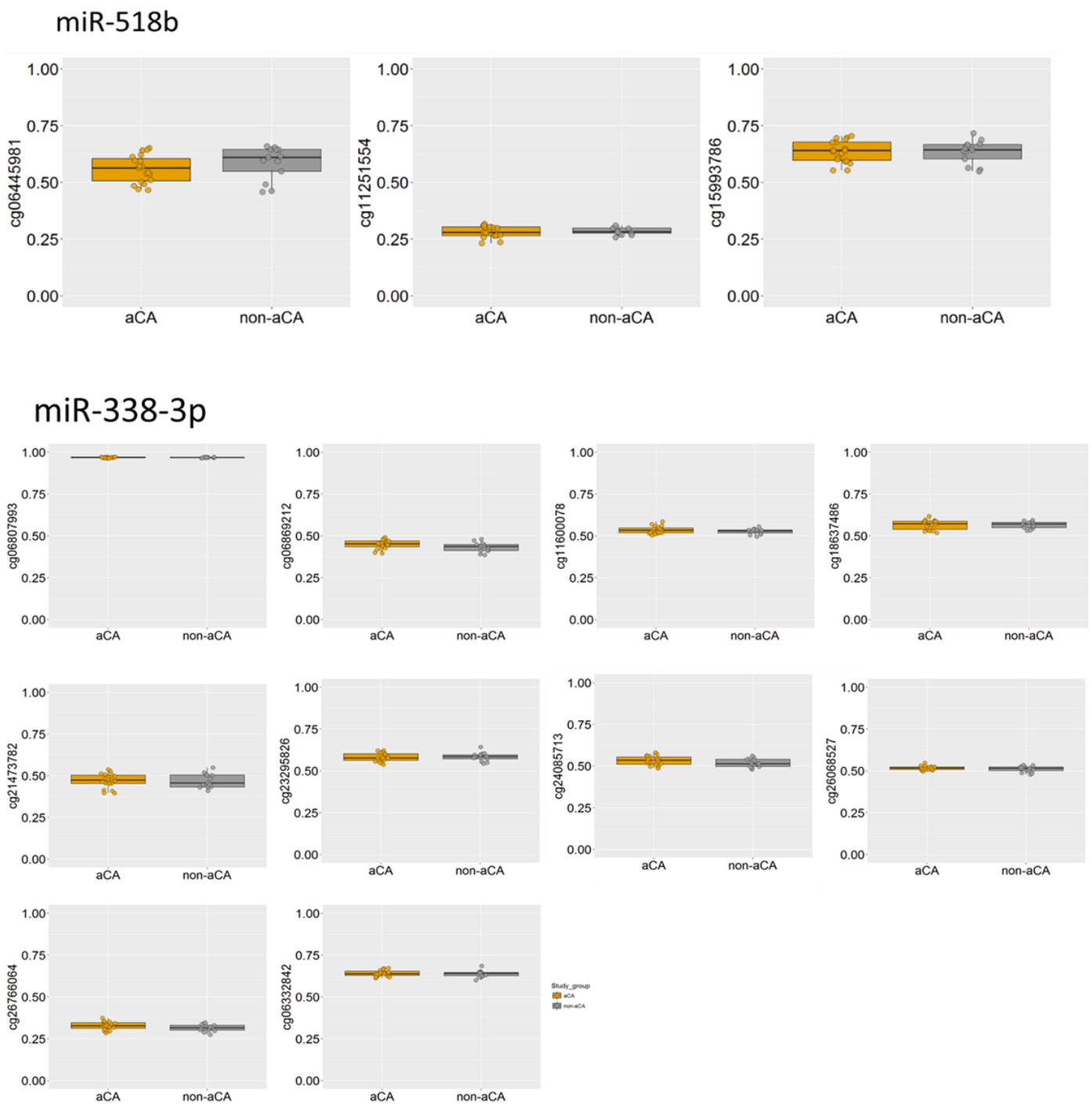

Supplementary Figure 5.5. CpG sites linked to miR-518b (3 CpGs) and miR-338-3p (11 CpGs) did not exhibit differential DNAme between aCA cases and non-aCA cases (Kruskal-Wallis test, p>0.05). The CpG sites were identified from the 850K array using Ilumina's annotation.

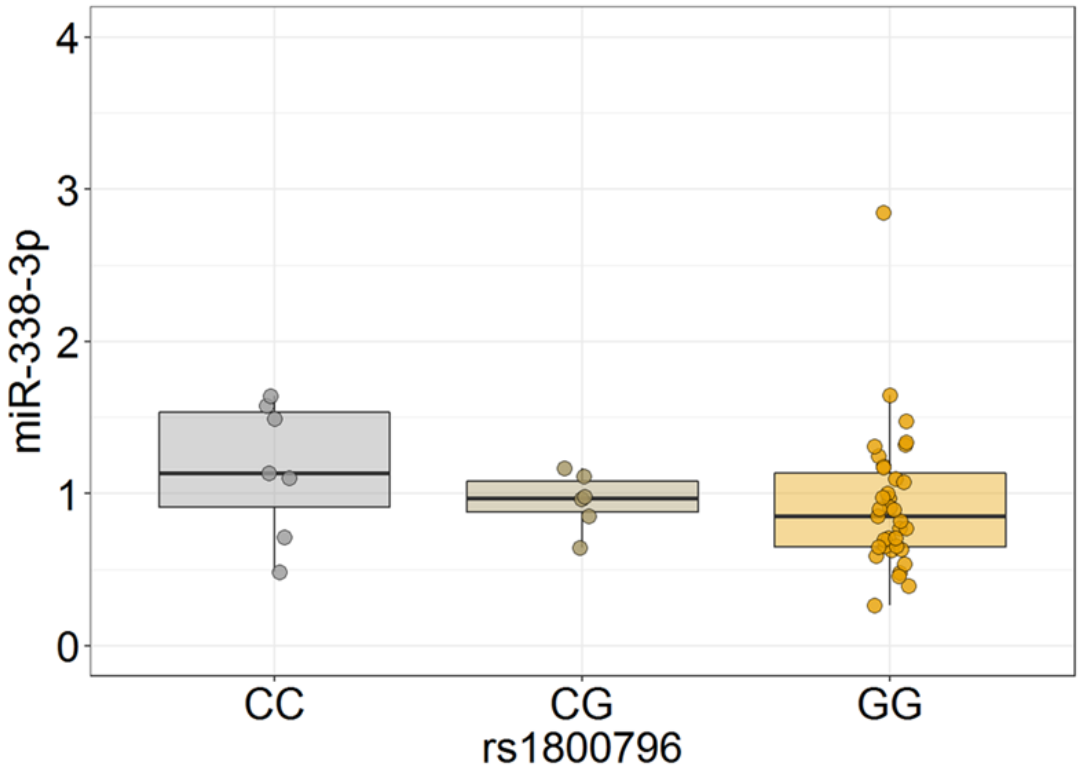

Supplementary Figure 5.6. miR-338-3p expression levels were also related to *Il6* genotype (rs1800796), where homozygous C individuals showed higher expression than homozygous G individuals, though not significant at $p<0.05$, Kruskal-Wallis test.

D.2 Supplementary tables

Supplementary Table 5.1. Gene targets identified by *TargetScan* and *miRDB* for miR-518b and miR-338-3p

miR-518b		**miR-338-3p**		
TSN	PVALB	DMRT2	ZBTB10	HCN1
ZNF282	DGKB	CBFB	ZDHHC18	PPP4R1
FBXO3	LGALSL	NOVA1	TTL	CCNT2
CPEB1	FKBP1A	PIP5KL1	CELSR2	ZBTB5
ZNF281	CHTOP	TAF1	HEXIM1	TSPYL4
TFE3	NTPCR	DCAF12	NOL4	MAPK1
ZNF608	C16orf87	WAPAL	HNF4G	SH3D19
RBM8A	ZBTB18	SEC61A2	SNX18	CPEB3
TEAD3	COPS4	MAFB	VAV3	TNRC6B
TP53INP1	WNK4	RAB14	YBX3	ZNF579
KCNK12	GNG12	ARPC1B	TBC1D8	C10orf54
RAP1B	THBS1	PTEN	PLA2G3	ARMCX3
NDUFA4	MTUS1	MAPK1IP1L	FRMD3	CNOT6
DPY19L1	SLC35G1	RNF114	AKAP12	SMTN
PLEKHH2	SLC30A9	NRP1	PCGF3	ADAM17
EGR1	SLC35F5	SLCO3A1	MECOM	KIAA1549L
HNRNPUL1	TRIM33	ESYT2	ATXN7L1	ZFHX4
TMEM71	RAB23	CHL1	SLK	ZADH2
ORC5	NNT	MYT1L	TBC1D15	SERINC5
LAPTM4B	ETS1	SEPT8	CDH1	SV2A
PRDX6	RAB30	CACNB4	TGOLN2	MAN2A1
SLCO4C1	VAMP3	B4GALT7	MSL2	RPH3A
TOLLIP	TERF2	KCND2	PPP1R16B	SRGAP3
LPIN1	KCNA4	FBXW7	C6orf222	SOX6
SYNRG	HMOX2	FAM120A	C1orf21	MYCBP2
HSPA12A	ARGLU1	MACROD2	C17orf75	LAMC1
C15orf54	LARP4	ATP10D	MAP2	TMEM255A
				GPR124
				TSR1

D.3 Supplementary methods

Supplementary Method 5.1. Selection of an appropriate endogenous control

Use of endogenous and exogenous controls is important to monitor and account for technical variation in relative expression analysis. Using a cohort of 57 placentas, we aimed to characterize aCA-associated miRNA changes and thus sought to evaluate two endogenous controls (miR92a, RNU48) that may be used to normalize our expression data. The six candidate miRNAs, two endogenous controls, and the exogenous control ath-miR-159a were detectable in the 57 placental samples; however their expression differed significantly with respect to their C_q values, ranging from 16.5 to 36.8 between samples. We used *NormFinder* to identify the optimal endogenous control, *Normfinder* is a bioinformatic tool that calculates stability as an "M" value, where lower "M" values suggest higher expression stability, by taking into account intra- and inter-group variability between user defined groups. *NormFinder* ranking showed that miR-92a (M=0.84) was a more stable endogenous control than RNU98 (M=1.34) in the cohort of 57 chorionic villus samples, and accordingly samples were normalized to miR-92a prior to downstream analysis.